

10-1-2007

# Erector Connector Meadow Burke Company In-Plane and Out-of-Plane Performance

Ian Hodgson

Clay Naito

F. Stokes

C. Bowman

Follow this and additional works at: <http://preserve.lehigh.edu/engr-civil-environmental-atlss-reports>

---

## Recommended Citation

Hodgson, Ian; Naito, Clay; Stokes, F.; and Bowman, C., "Erector Connector Meadow Burke Company In-Plane and Out-of-Plane Performance" (2007). ATLSS Reports. ATLSS report number 07-12.:  
<http://preserve.lehigh.edu/engr-civil-environmental-atlss-reports/99>

This Technical Report is brought to you for free and open access by the Civil and Environmental Engineering at Lehigh Preserve. It has been accepted for inclusion in ATLSS Reports by an authorized administrator of Lehigh Preserve. For more information, please contact [preserve@lehigh.edu](mailto:preserve@lehigh.edu).



**LEHIGH**  
UNIVERSITY

**ERECTOR CONNECTOR  
MEADOW BURKE COMPANY  
IN-PLANE AND OUT-OF-PLANE  
PERFORMANCE**

**FINAL REPORT**

**By**

**Ian C. Hodgson**

**Clay Naito, Ph.D**

**Frank Stokes**

**Carl Bowman**

**October 2007**

**ATLSS REPORT NO. 07-12**

**ATLSS is a National Center for Engineering Research  
on Advanced Technology for Large Structural Systems**

117 ATLSS Drive

Bethlehem, PA 18015-4729

Phone: (610)758-3525

Fax: (610)758-5902

[www.atlss.lehigh.edu](http://www.atlss.lehigh.edu)

Email: [inatl@lehigh.edu](mailto:inatl@lehigh.edu)

## Users of Erector Connector Reviewing Test Data

### Change to Erector Connector after Lehigh Testing

The following test results were performed using a weld plate 3.25 inches wide. To improve upon these initial results the width of the current weld plate was increased to 3.35 inches. This increase in width reduces the lateral movement before contact of the weld plate to the Type-A Erector Connector during horizontal shear loading.

If you have any questions concerning the Meadow Burke Erector Connector or the following test data, please contact us at (877) 518-7665.



Lance Osborne, PE  
Meadow Burke  
Engineering Manager  
Tampa Florida

## TABLE OF CONTENTS

---

Table of Contents.....	1
Abstract .....	2
Summary of Test Results.....	3
Background.....	4
Subassembly Details.....	4
Deformation Protocols.....	9
Monotonic In-plane Shear.....	9
Cyclic In-plane Shear.....	9
Monotonic In-plane Tension .....	9
Cyclic In-plane Tension .....	10
Monotonic In-plane Shear with Proportional In-plane Tension .....	11
Monotonic Out-of-plane Shear.....	12
Phase 1 Testing.....	15
Phase 2 Testing.....	15
Material Properties .....	18
Phase 1 – Test A1: Erector Connector under Monotonic Tension with No Shear Force.....	22
Phase 1 – Test A2: Erector Connector under Monotonic Shear Deformation with $\Delta T = 0$ .....	24
Phase 1 – Test A3: Erector Connector under Monotonic Shear Deformation w/ Tension $\Delta T = 0$ .....	26
Phase 1 – Test A4: Erector Connector Under Cyclic Shear Deformation w/ Tension $\Delta T = 0$ .....	28
Phase 1 – Test A5: Erector Connector Under Cyclic Shear Deformation w/ Tension $\Delta T = 0$ .....	31
Phase 1 – Test A6: Erector Connector Under Shear w/ Proportional Tension Deformation ( $\Delta V/\Delta T$ ) = 2.0.....	34
Phase 2 – Test Series 1 – Out-of-Plane Shear – Stepped Panel – “A” Connector .....	37
Phase 2 – Test Series 2 – Out-of-Plane Shear – 4” Uniform Panel – “B” Connector.....	38
Phase 2 – Test Series 3 – Out-of-Plane Shear – Stepped Panel – “B” Connector .....	39
Phase 2 – Test Series 4 – In-Plane Shear – Stepped Panel – “A” to “A” Connector Configuration.....	40
Phase 2 – Test Series 5 – In-Plane Shear –Stepped Panel – “A” to “B” Connector Configuration.....	44
Phase 2 – Test Series 6 – In-Plane Shear – Stepped Panel – “B” to “A” Connector Configuration.....	49
Phase 2 – Test Series 7 – In-Plane Tension – Stepped Panel – “A” to “A” Connector Configuration.....	53
Phase 2 – Test Series 8 – In-Plane Tension – Stepped Panel – “B” to “A” Connector Configuration.....	57
Phase 2 – Test Series 9 – In-Plane Shear/Tension –Stepped Panel – “B” to “A” Connector Configuration.....	61
Phase 2 – Test Series 10 - In-Plane Shear/Tension –Stepped Panel – “A” to “B” Connector Configuration.....	64
Phase 2 – Test Series 1-A – In-Plane Shear – Altus Panel – “A” to “B” Connector Configuration.....	68
Phase 2 – Test Series 2-A – Out-of-Plane Shear – Altus Panel – “A” Connector .....	73
Phase 2 – Test Series 3-A – Out-of-Plane Shear – Altus Panel – “B” Connector .....	75
Phase 2 – Test Series 4-A – In-Plane Tension – Altus Panel – “B” Connector.....	76

## **ABSTRACT**

---

This report summarizes both the in-plane and out-of-plane performance of the Erector Connector developed by Meadow Burke Company. The connector is intended for use as flange-to-flange connectors between precast double tee panels with 4-in. flanges. The testing proceeded in two phases. During Phase 1 testing, the connector was tested under monotonically increasing shear, monotonically increasing tension, cyclic shear, and shear with proportional tension. During Phase 2 testing, monotonically increasing shear, monotonically increasing tension, cyclic shear, cyclic tension, and shear with proportional tension were repeated. A number of panel geometries were tested including uniform 4 inch thick panels, 2 inch thick panels (representing the untopped condition), and 3 1/4" Altus panels. In addition, out-of-plane tests were performed. The resulting capacities and associated damage from both phases of testing are summarized in the report. This work was funded by Meadow Burke Co. and was conducted at the ATLSS Center at Lehigh University during 2006 and 2007.

## SUMMARY OF TEST RESULTS

The following table summarizes the results of the load testing. The results are presented in three groups, namely (1) typical configurations, (2) reference configurations; and (3) Altus configurations. For each test configuration, the average peak load is presented.

As noted in the table, tests were conducted on 4 inch thick panels, 2 inch thick panels, and 3.25 inch thick Altus panels. It is important to note that 2 inch thick panels were stepped to 4 inches to be accommodated in the test fixture. The connector was located on the 2 inch thick side. These tests are designed to represent a uniform 2 inch thick panel. Further details regarding the individual test series are presented in the body of this report. Connector configurations denoted “A-B” consist of single weld of the “A” connector to the “B” connector faceplate. Connector configurations denoted “B-A” consist of two welds; an additional weld of the “A” slug to the “A” faceplate is included.

	Load Dir	Connector Config.	Panel Thickness	Test Series	Loading Protocol	Avg. Peak Load (lb)
Typical configurations	In-plane Shear	A-B	4"	Phase 1 - A3	Monotonic	21,400
				Phase 1 - A4	Cyclic	19,200
	In-plane Shear	A-B	2"	Phase 2 - 5	Monotonic	13,600
					Cyclic	11,900
	Out-of-plane Shear	A	2"	Phase 2 - 1	Monotonic	2,040
			4"	Phase 2 - 2	Monotonic	6,810
			2"	Phase 2 - 3	Monotonic	2,840
	In-plane Tension	B-A	4"	Phase 1 - A1	Monotonic	3,600
In-plane Tension	B-A	2"	Phase 2 - 8	Monotonic	4,100	
				Cyclic	3,300	
Reference Configurations	In-plane Shear	B-A	4"	Phase 1 - A2	Monotonic	23,400
				Phase 1 - A5	Cyclic	17,600
	In-plane Shear	A-A	2"	Phase 2 - 4	Monotonic	10,700
					Cyclic	9,500
	In-plane Shear	B-A	2"	Phase 2 - 6	Monotonic	16,900
					Cyclic	9,600
	In-plane Tension	A-A	2"	Phase 2 - 7	Monotonic	6,500
					Cyclic	6,600
In-plane Shear/Tension	B-A	2"	Phase 2 - 9	Cyclic	10,200	
In-plane Shear/Tension	A-B	2"	Phase 2 - 10	Cyclic	11,500	
In-plane Shear/Tension	B-A	4"	Phase 1 - A6	Monotonic	15,200	
Altus	In-plane Shear	A-B	3.25" (Altus)	Phase 2 - 1A	Monotonic	15,900
					Cyclic	16,500
	Out-of-plane Shear	A	3.25" (Altus)	Phase 2 - 2A	Monotonic	4,530
		B	3.25" (Altus)	Phase 2 - 3A	Monotonic	4,820
In-plane Tension	B	3.25" (Altus)	Phase 2 - 4A	Monotonic	7,090	

## **BACKGROUND**

---

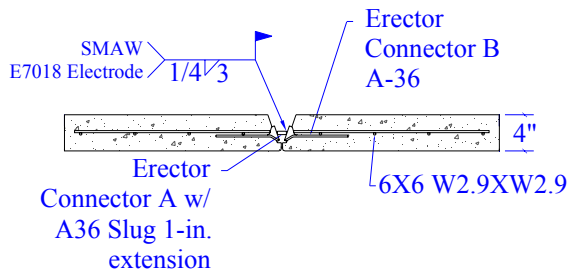
As a means of assessing the displacement capacity and structural stiffness of connections in precast diaphragms, an experimental study was conducted. A subassembly consisting of the connector and a portion of the surrounding diaphragm was developed. The subassemblies include a Type A connector and Type B connector embedded in standard 4-in. pretopped, 2-in. untopped, and 3.25-in thick Altus concrete panels. The Altus panels utilize carbon fiber “C-grid” reinforcement. All specimens were fabricated at full-scale. This report summarizes the experimental results of the Erector connector tested under displacement control in monotonic tension, monotonic shear, cyclic shear and combined shear with tension.

### **Subassembly Details**

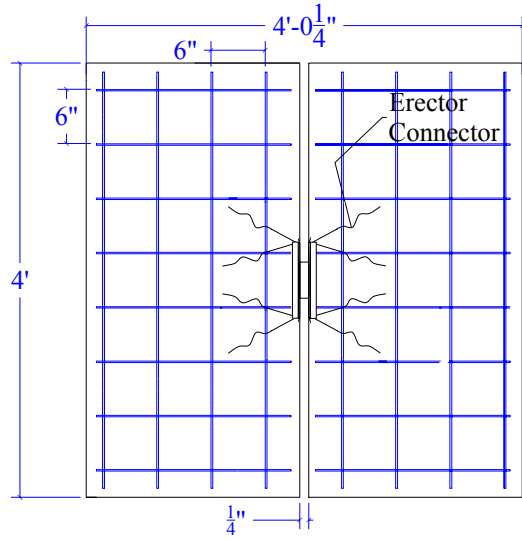
---

The subassembly was developed assuming that the connectors are spaced at 4 feet and embedded in a double tee panel with a 2ft distance from the DT web to the free flange face. The test specimens are fabricated from two panels 2ft wide and 4ft long (Figure 1). The panels are connected to form a 4ft square subassembly. Welded wire reinforcement (WWR) is included in each panel to meet ACI temperature and shrinkage reinforcement requirements. In addition to the WWR conventional reinforcement is used to maintain integrity during testing. The bars are placed at the periphery of the panel to minimize influence on the connector response. The connectors are shown in Figures 2, 3, 4, and 5. The supplemental reinforcement is illustrated in Figure 6.

The Erector Connector developed by the Meadow Burke Company is evaluated. The connector (Figures 2, 3, 4, and 5) is designed for placement in 4-in. double tee flanges. It consists of two connector types A and B. Connector type A (Figures 2 and 3) consists of a bent plate connector with four anchor legs, two oriented at 45-degrees and 2 and 90-degrees from the face plate. A slug is included with the connector which allows it to be pulled out once the DT members are in place. Connector type B (Figure 4) has a similar configuration to type A, but does not include the removable slug. A mockup of the two connectors is shown in Figure 5. Both connectors are fabricated from ASTM A36 steel and welded to the adjacent panel the embedded Type A ASTM A36 steel slug and a E7018 weld electrode. The welds were conducted at room temperature using a SMAW process according to AWS specifications. Variations on welding were used in some cases a weld was placed only at the connection B face and in other cases at both the B and A faces. Photographs of a 3.25” Altus Panel prior to concrete placement is presented in Figure 7.



**SIDE ELEVATION**



**TOP PLAN**

Figure 1: Specimen details – 4" uniform thickness



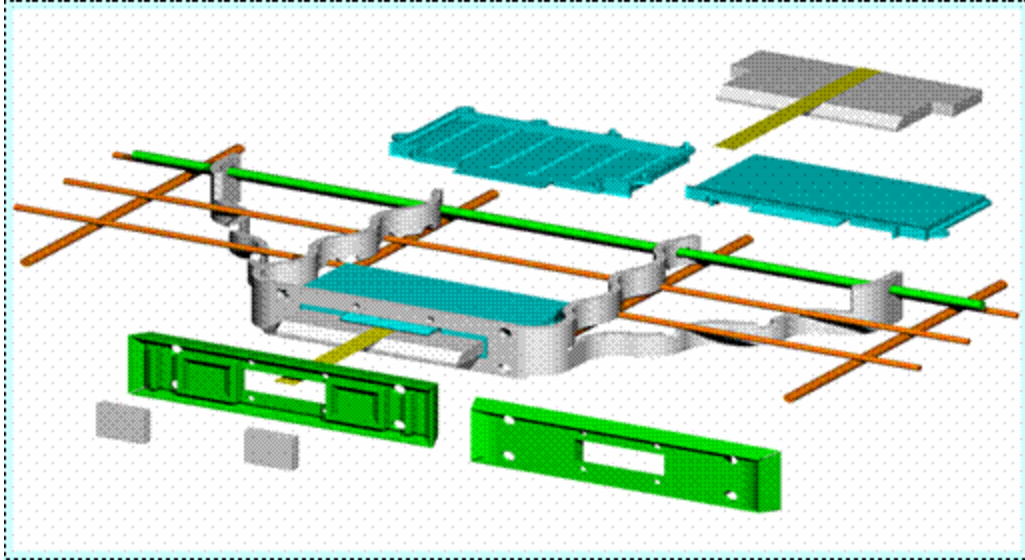


Figure 2: Type A erector connector schematic



Figure 3: Type A erector connector without slug



Figure 4: Type B erector connector

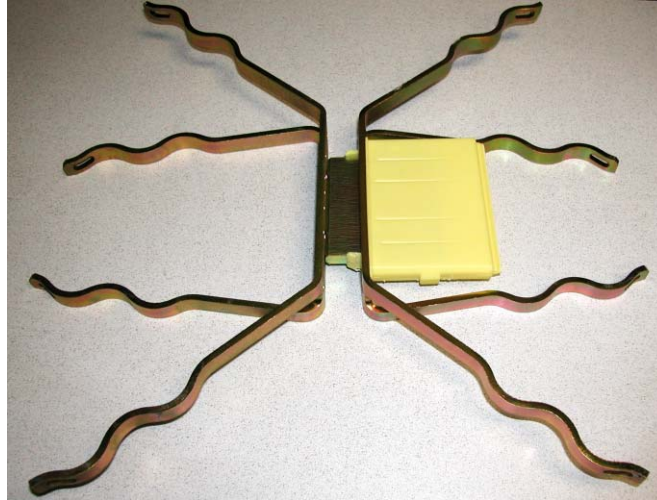


Figure 5: Connector A-B mockup

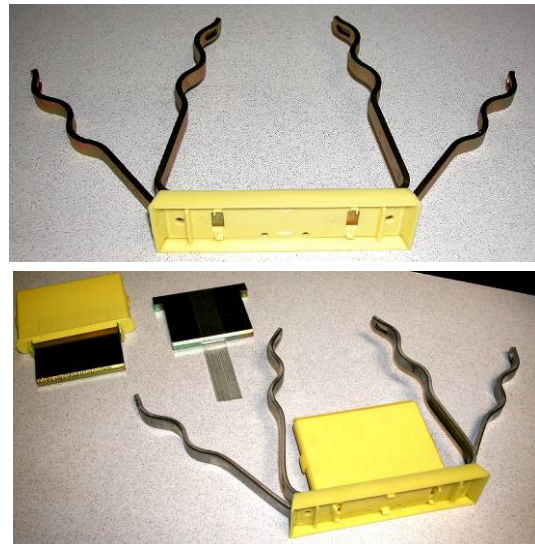
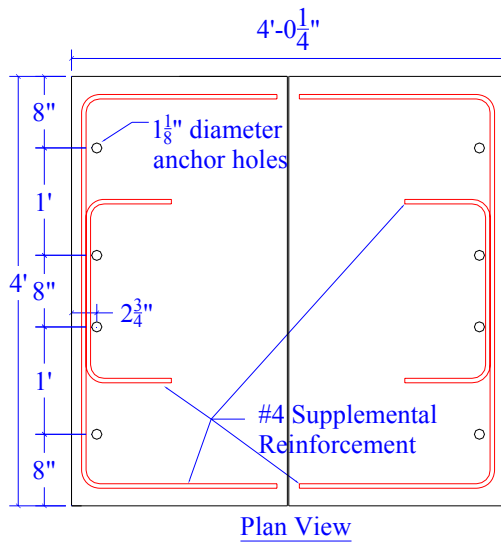


Figure 6: Supplemental reinforcement layout and construction details

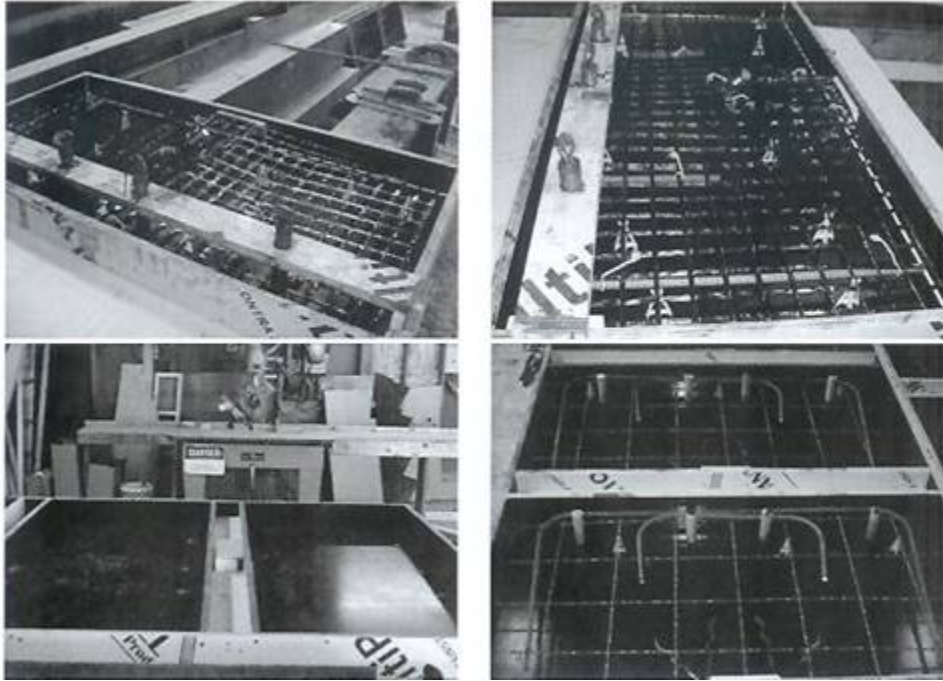


Figure 7: Photographs of 3.25" Altus panels prior to concrete placement

### ***Deformation Protocols***

The connector was evaluated under in-plane shear, tension, and combined shear with tension. All tests were conducted under quasi-static displacement control at a rate less than 0.05in/sec. The tests were continued until failure. Failure is defined as the point where the specimen capacity drops below 25% of the measured ultimate. Six displacement protocols have been developed to represent the spectrum of demands a local diaphragm connector could experience under lateral loading [Naito 2005]. All of these deformation protocols were used in the current study:

1. Monotonic In-plane Shear
2. Cyclic In-plane Shear
3. Monotonic In-plane Tension
4. Cyclic In-plane Tension
5. Monotonic In-plane Shear with Proportional In-plane Tension
6. Monotonic Out-of-plane Shear

#### ***Monotonic In-plane Shear***

The monotonic in-plane shear tests were conducted to evaluate the connector response under pure shear deformation. The original panel separation of was maintained through the test. The test represents the joint condition where the panels are shearing without any flexural opening or closing. The test thus provides an estimate of average connector yield, peak strength, and the deformation capacity. Monotonic shear protocol consists of three cycles to 0.01-in. to estimate initial stiffness and verify equipment operation. Afterwards, the specimens were loaded monotonically to failure (Figure 10).

#### ***Cyclic In-plane Shear***

Cyclic in-plane shear tests provide insight on the degradation of shear properties (i.e., stiffness and ultimate strength) under loading reversals. The loading protocol is based on the PRESSS program [Priestley 1992]. Three preliminary cycles to 0.01-in. are conducted to evaluate control and acquisition accuracy. The remaining protocol consisted of groups of three symmetric shear cycles at increasing deformation levels. Each level is based on a percentage of a reference deformation computed from the preceding monotonic test. The reference deformation represents the effective yield deformation of the connector. It is computed by taking the intercept of a horizontal line at the max load and a secant stiffness line at 75% of the max load (Figure inset). Three elastic levels of 0.25 $\Delta$ , 0.50 $\Delta$  and 0.75 $\Delta$  followed by inelastic cycles to 1.0 $\Delta$ , 1.5 $\Delta$ , 2.0 $\Delta$ , 3.0 $\Delta$ , 4.0 $\Delta$ , 6.0 $\Delta$ , 8.0 $\Delta$ , *etc...* were conducted. The loading protocol is illustrated in Figure 10.

#### ***Monotonic In-plane Tension***

In current diaphragm design, the flexural diaphragm tensile forces are assumed to be resisted by the chord reinforcement. The contribution of shear connectors to flexural resistance is commonly neglected. Previous research has shown that in many cases web connectors provide high tension stiffness. To quantify the relative tensile contribution of the web connectors and chord connectors, monotonic in-plane tension tests were conducted. The loading protocol consisted of three tension/compression deformations to 0.01-in. followed by a monotonically increasing tension deformation to failure (Figure 11). The test was paused at each 0.1-in. for observations.

A special test setup was used to test the Altus panel under in-plane tension. The self-reacting tension frame shown in Figure 8 consists of C6 channels and 4-in. tubes. The frame bears against the 2-ft. x 4 ft. x 3-1/2-in. thick Altus test slab through 4-in. wide plates positioned 38-1/4-in. apart. The tab of the loading plate was fillet welded on the top side to the Type B connector, as shown in Figure 9. The loading plate was pulled up via a threaded rod passing through a hydraulic jack and load cell. The loading mechanism sat on the C channels that react against the slab

through the 4-in. tubes. A hand pump was used to slowly increase the pressure and the resulting tension force to the B connector.

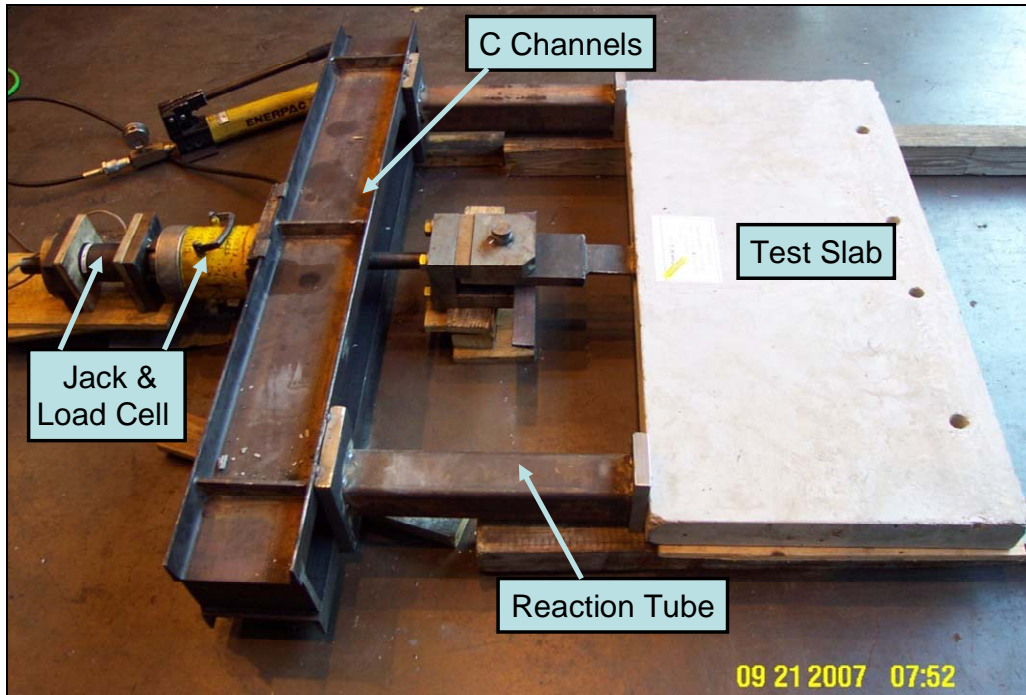


Figure 8: Altus slab in-plane tension test setup

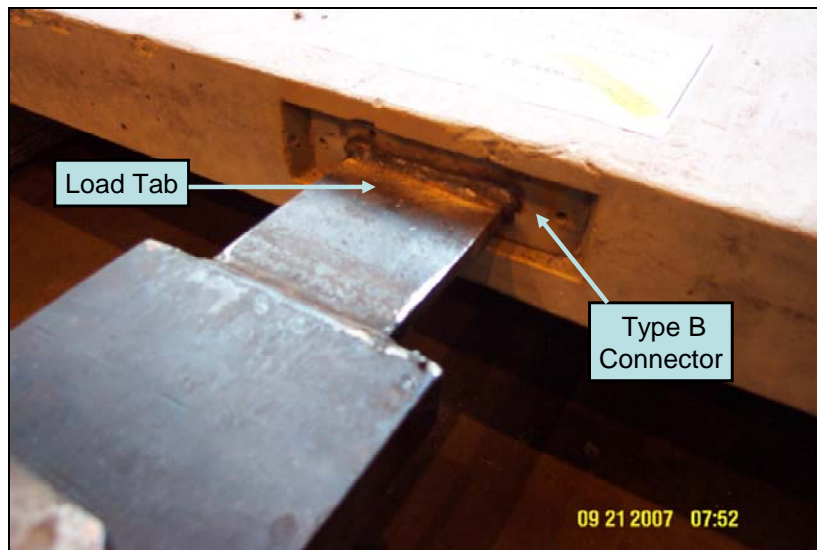


Figure 9: Load attachment plate welded to Type B Connector for in-plane tension test setup

### ***Cyclic In-plane Tension***

Cyclic in-plane tension tests provide insight on the degradation of tension properties (i.e., stiffness and ultimate strength) under loading reversals. The loading protocol is illustrated in Figure 11.



**Monotonic In-plane Shear with Proportional In-plane Tension:**

The monotonic in-plane shear with tension test consists of three cycles of 0.01-in. in shear and a proportional tension/compression deformation. The shear and tension deformations will be increased proportionally using the chosen constant shear-to-tension deformation ratio of 2.0. The test will be paused at each 0.1-in of shear deformation for observations. The test is performed with the initial joint opening maintained through the test.

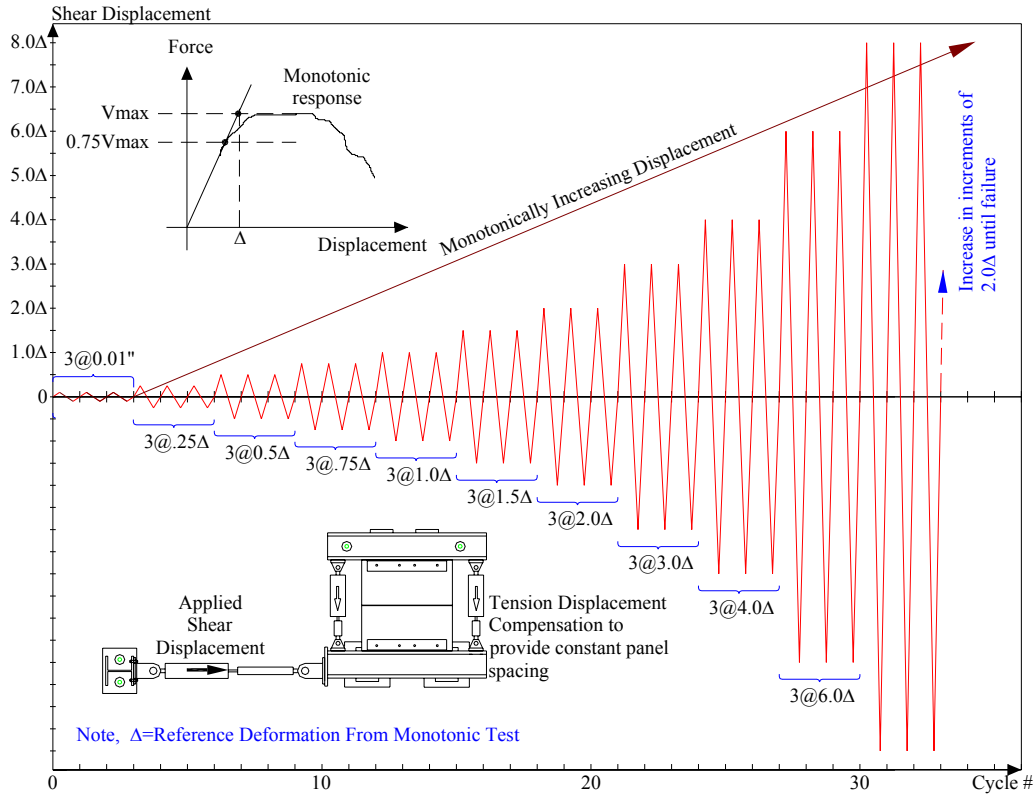


Figure 10: Shear loading protocol

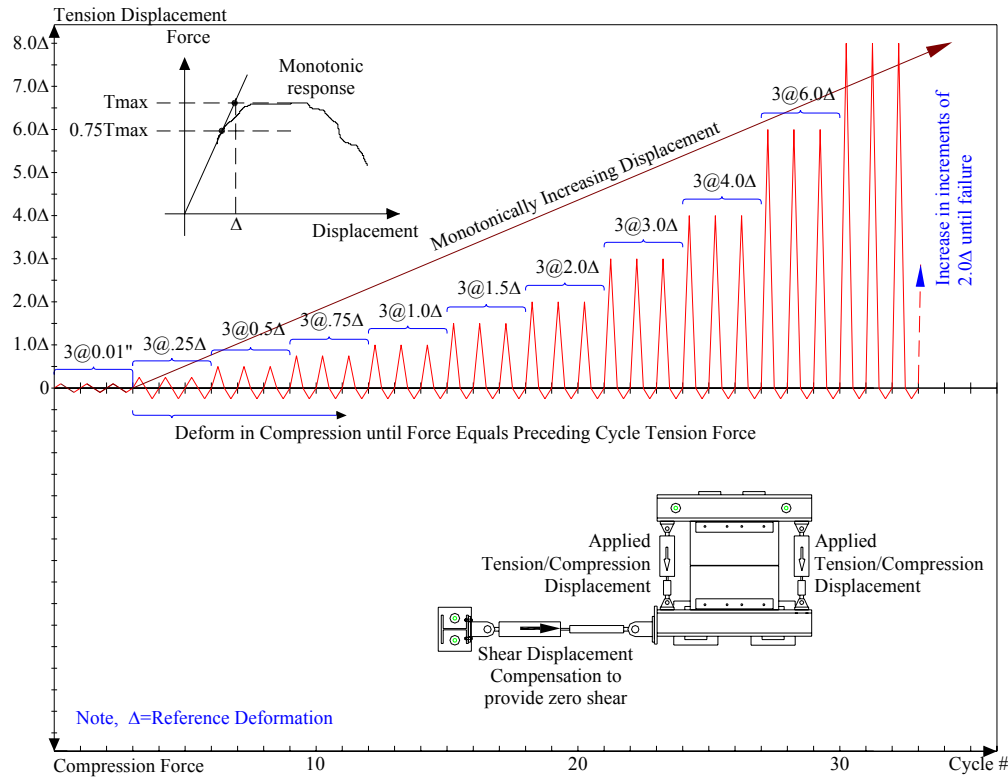


Figure 11: Tension/Compression protocol

**Monotonic Out-of-plane Shear:**

The monotonic out-of-plane shear tests were performed to quantify the behavior of the connector when the panels are subjected to out-of-plane loads. A self-reacting frame was used as shown in Figure 12. The test frame consists of W6 sections and C6 channels. The test slab was sandwiched between the W6 sections with the 6 inch flanges bearing on the outer 6 inches of the 48 inch slab width. Blocks and shims secured the non-uniform thickness panels (Figure 13).

Load was applied through a loading block attached to the slab. For Type A slabs, the slab tab was extended and welded to the front face of the loading block. For Type B slabs, a slug section was placed between the slab plate and the loading block. The slug was welded to both the loading block and the slab plate. The gap between the slab plate and loading block plate was kept between 1/4" and 3/8". Figure 14 shows an extended Type A tab welded to the loading block. The tab was pushed in and the loading block was positioned to obtain the 1/4" to 3/8" gap. The loading block was pulled up via a threaded rod passing through a hydraulic jack and load cell. The loading mechanism sat on the C channels that spanned across the W6 sections. Rotation of the loading block as it was pulled was restrained by a C channel on the opposite side of the block as the slab. Friction between the loading block and channel was minimized by a Teflon sheet affixed to the loading block. A hand pump was used to slowly increase the pressure and the resulting uplift force to the slab plate. The vertical displacement was measured using an LVDT. The load and displacement were recorded at one second intervals on a Campbell Scientific CR5000 data logger.

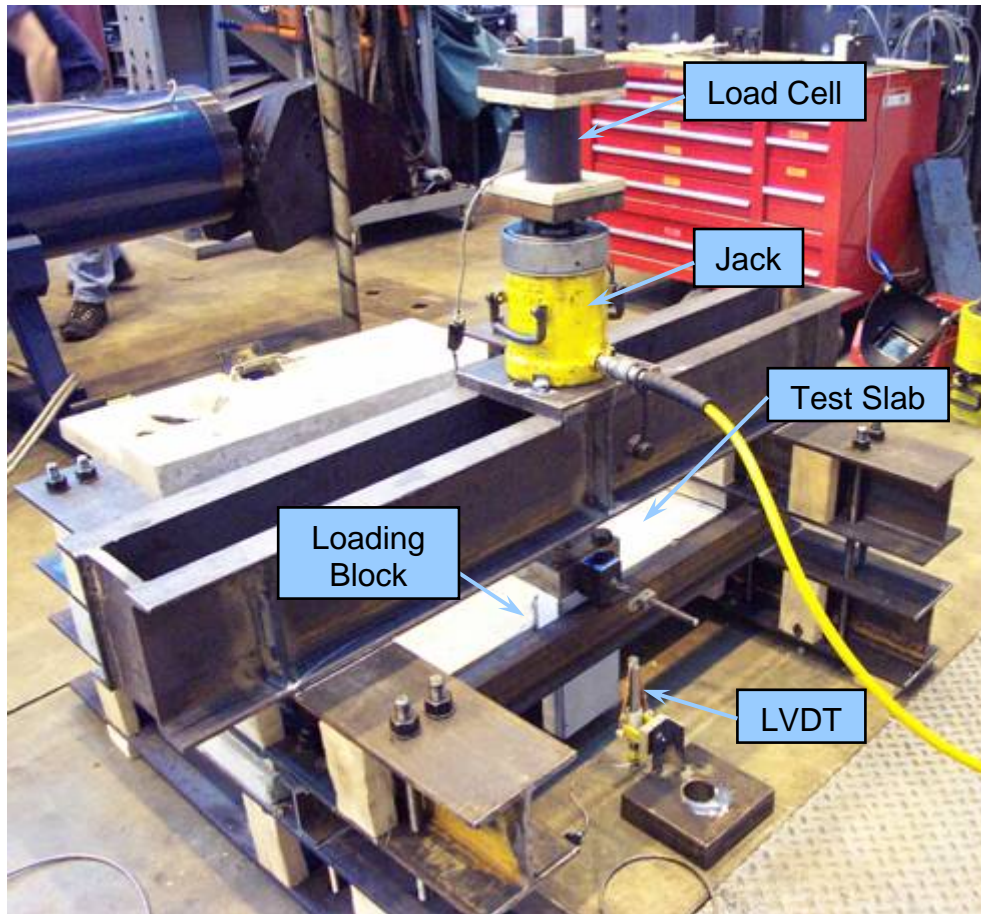


Figure 12: Setup for out-of-plane tests



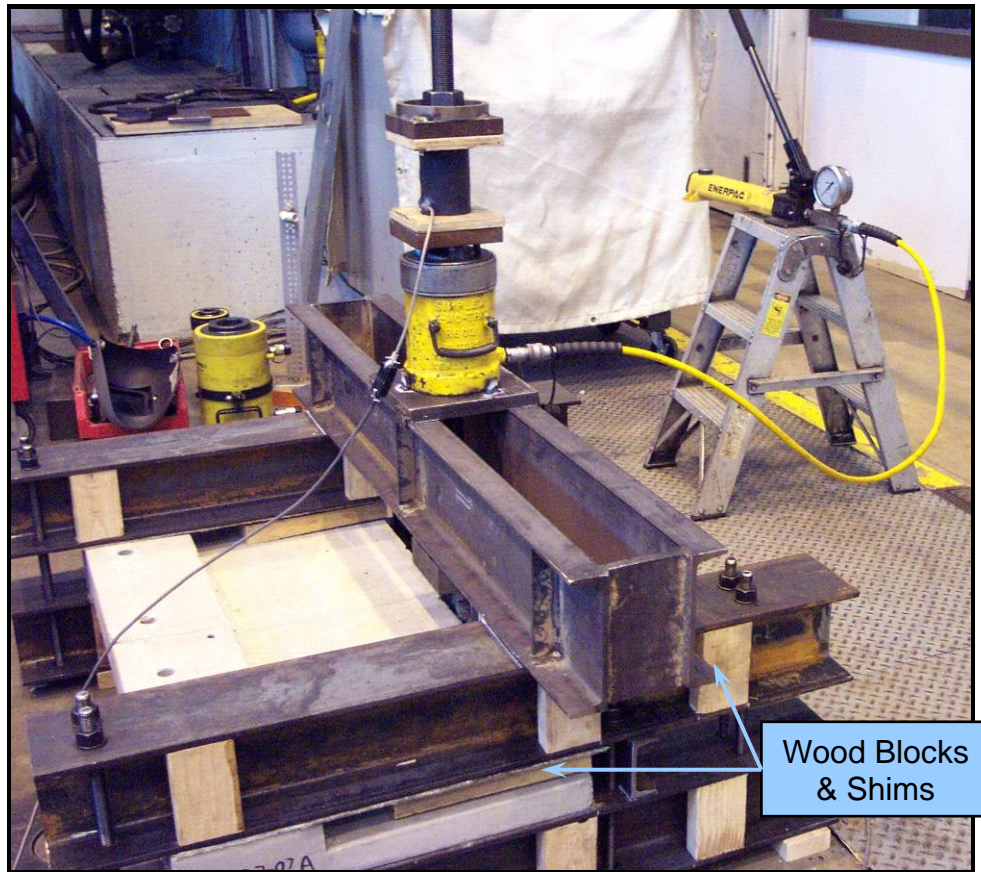


Figure 13: Out-of-plane test setup - side view showing wood blocks and shims securing reduced thickness region



Figure 14: Out-of-plane tests – detail showing a Type A tab welded to the loading block

## Phase 1 Testing

---

A total of six tests were performed on the connector during Phase 1. The Phase 1 tests were performed in late 2006. In each case one type A connector was welded to one Type B connector. In some cases one side was welded (termed an “A-B” connection) and in other cases both sides were welded (termed a “B-A” connection). For the single weld tests the embedded slug was pulled out of connector A and welded to connector B. For the double weld tests an additional weld was applied to connector A to secure the embedded slug to the faceplate of the connection. Each weld consisted of a 3in. long 1/4in. fillet weld. The test designations and the type of test are presented in Table 1.

Designation	Weld Configuration	Description
A1	Both sides welded (B-A)	Monotonic tension with no shear force
A2	Both sides welded (B-A)	Monotonic shear with no tension deformation
A3	One side welded (A-B)	Monotonic shear with no tension deformation
A4	One side welded (A-B)	Cyclic shear with no tension deformation
A5	Both sides welded (B-A)	Cyclic shear with no tension deformation
A6	Both sides welded (B-A)	Shear with proportional tension deformation ( $\Delta V/\Delta T = 2.0$ )

## Phase 2 Testing

---

A total of 62 tests were performed on the connector during Phase 2. The Phase 2 tests were performed between March and September 2007. A summary of the Phase 2 test matrix is presented in Table 2. As shown, a significantly larger number of specimens were included in Phase 2. Additionally, the Phase 2 incorporates additional variables not considered during Phase 1.

As shown in Table 2, there were 13 test series considered during Phase 2. There were multiple specimens tested in each test series. Within each test series, the loading direction, connector configuration, and panel geometry were held constant.

Three different panel geometries were tested:

1. Stepped Panel – This represents the untopped panel condition. This panel has a thickness of 2 inches from the connection edge through 16 inches from the opposite edge, where the thickness is stepped to 4 inches. No topping slab was added to these specimens.
2. Uniform 4 inch Thickness – This configuration is identical to Phase 1 specimens and represents the topped panel configuration.
3. Altus Panel – This is a 3.25 inch thick panel which utilizes carbon fiber “C-grid” reinforcement. No topping of this type of panel would be required in the field.

Three different connection configurations were considered in the test matrix, namely (1) A to A; (2) A to B (single weld; and (3) B to A (two welds).

Table 2 – Phase 2 Test Matrix					
Test Series	Load Direction	Connector Config.	Panel Size	Loading Protocol	Test ID
1	Out-of-plane Shear	A	Stepped Panel	Monotonic	MOP_A-1
				Monotonic	MOP_A-2
				Monotonic	MOP_A-3
				Monotonic	MOP_A-4
2	Out-of-plane Shear	B	4" Uniform Panel	Monotonic	MOP_B_4-1
				Monotonic	MOP_B_4-2
				Monotonic	MOP_B_4-3
				Monotonic	MOP_B_4-4
3	Out-of-plane Shear	B	Stepped Panel	Monotonic	MOP_B-1
				Monotonic	MOP_B-2
				Monotonic	MOP_B-3
				Monotonic	MOP_B-4
4	In-plane Shear	A-A	Stepped Panel	Monotonic	MV_AA-1
				Cyclic	CV_AA-1
				Cyclic	CV_AA-2
				Cyclic	CV_AA-3
				Cyclic	CV_AA-4
5	In-plane Shear	A-B	Stepped Panel	Monotonic	MV_AB-1
				Cyclic	CV_AB-1
				Cyclic	CV_AB-2
				Cyclic	CV_AB-3
				Cyclic	CV_AB-4
6	In-plane Shear	B-A	Stepped Panel	Monotonic	MV_BA-1
				Cyclic	CV_BA-1
				Cyclic	CV_BA-2
				Cyclic	CV_BA-3
				Cyclic	CV_BA-4
7	In-plane Tension	A-A	Stepped Panel	Monotonic	MT_AA-1
				Cyclic	CT_AA-1
				Cyclic	CT_AA-2
				Cyclic	CT_AA-3

Table 2 – Phase 2 Test Matrix cont'd					
Test Series	Load Direction	Connector Config.	Panel Size	Loading Protocol	Test ID
8	In-plane Tension	B-A	Stepped Panel	Monotonic	MT BA-1
				Cyclic	CT BA-1
				Cyclic	CT BA-2
				Cyclic	CT BA-3
				Cyclic	CT BA-4
9	In-plane Shear/Tension $\Delta V/\Delta T = 2.0$	B-A	Stepped Panel	Cyclic	CVT BA-1
				Cyclic	CVT BA-2
				Cyclic	CVT BA-3
10	In-plane Shear/Tension $\Delta V/\Delta T = 2.0$	A-B	Stepped Panel	Cyclic	CVT AB-1
				Cyclic	CVT AB-2
				Cyclic	CVT AB-3
				Cyclic	CVT AB-4
1-A	In-plane Shear	A-B	3.25"	Monotonic	MV AB ALTUS-1
				Cyclic	CV AB ALTUS-1
				Cyclic	CV AB ALTUS-2
				Cyclic	CV AB ALTUS-3
				Cyclic	CV AB ALTUS-4
2-A	Out-of-plane Shear	A	3.25"	Monotonic	MOP A ALTUS -1
				Monotonic	MOP A ALTUS -2
				Monotonic	MOP A ALTUS -3
				Monotonic	MOP A ALTUS -4
				Monotonic	MOP A ALTUS -5
3-A	Out-of-plane Shear	B	3.25"	Monotonic	MOP B ALTUS-1
				Monotonic	MOP B ALTUS-2
				Monotonic	MOP B ALTUS-3
				Monotonic	MOP B ALTUS-4
				Monotonic	MOP B ALTUS-5
4-A	In-plane Tension	B	3.25"	Monotonic	MT B ALTUS-1
				Monotonic	MT B ALTUS-2
				Monotonic	MT B ALTUS-3
				Monotonic	MT B ALTUS-4

## Material Properties

---

### *Phase 1*

The base 4-in. precast panels were fabricated using ready mix concrete with design 28-day strength of 5000 psi. The WWR used in the base panel met the requirements of ASTM A185 grade 65 steel. The connectors were furnished by Meadow Burke. Material data supplied with the connectors indicated that the Erector connector was fabricated from A-36 steel, plate properties were not available. The slugs used to connect the panels are included in the Type A connector and were fabricated A-36 steel. The measured concrete strengths and mill certified steel properties are presented in Table 3.

Table 3: Steel Material Properties				
Size	Reinforcement Usage	ASTM Grade	Yield Stress (ksi)	Ultimate Strength (ksi)
Embedded	Connector Slug	A36	36*	50*
Bent plate	Connector	A36	36*	50*
#4	Reinforcing Bars	A615	90*	106*
W2.9XW2.9 6X6	Precast Panel Mesh	A185 Gr.65	65.00*	107.0

\* Data unavailable, value assumed

**Phase 2**

Steel properties are assumed to be as presented in Table 3. Cylinders were tested from all mixes of concrete used for all test panels. The results are summarized below in Table 4a (out-of-plane shear tests), Table 4b (in-plane shear tests), Table 4c (in-plane tension tests), and Table 4d (combined in-plane shear/tension tests).

Table 4a - Out-of-Plane Tests Avg. 28 day strength	
Test ID	f <sub>c</sub> (ksi)
MOP_A-1	4.8
MOP_A-2	6.4
MOP_A-3	5.0
MOP_A-4	6.4
MOP_B_4-1	4.9
MOP_B_4-2	4.9
MOP_B_4-3	4.9
MOP_B_4-4	4.9
MOP_B-1	6.4
MOP_B-2	4.5
MOP_B-3	6.4
MOP_B-4	4.5
MOP_A_ALTUS -1	5.0
MOP_A_ALTUS -2	6.8
MOP_A_ALTUS -3	6.8
MOP_A_ALTUS -4	5.0
MOP_A_ALTUS -5	5.0
MOP_B_ALTUS-1	6.8
MOP_B_ALTUS-2	5.0
MOP_B_ALTUS-3	5.0
MOP_B_ALTUS-4	6.8
MOP_B_ALTUS-5	5.0

Table 4b - In-Plane Shear Tests				
Avg. 28 day strength				
Test ID	Panel 1	f <sub>c</sub> (ksi)	Panel 2	f <sub>c</sub> (ksi)
MV_AA-1	A	7.2	A	7.2
CV_AA-1	A	5.4	A	7.2
CV_AA-2	A	6.4	A	6.4
CV_AA-3	A	5.4	A	5.4
CV_AA-4	A	5.4	A	5.4
MV_AB-1	A	5.6	B	5.6
CV_AB-1	A	5.6	B	5.6
CV_AB-2	A	5.6	B	5.6
CV_AB-3	A	5.7	B	5.7
CV_AB-4	A	5.7	B	5.7
MV_BA-1	A	5.7	B	5.7
CV_BA-1	A	4.8	B	4.8
CV_BA-2	A	4.8	B	4.8
CV_BA-3	A	4.8	B	4.8
CV_BA-4	A	4.8	B	4.8
MV_AB_ALTUS-1	A	6.8	B	6.8
CV_AB_ALTUS-1	A	6.8	B	6.1
CV_AB_ALTUS-2	A	6.1	B	6.1
CV_AB_ALTUS-3	A	6.1	B	6.1
CV_AB_ALTUS	A	6.1	B	6.1

Table 4c - In-Plane Tension Tests				
Avg. 28 day strength				
Test ID	Panel 1	f <sub>c</sub> (ksi)	Panel 2	f <sub>c</sub> (ksi)
MT_AA-1	A	5.0	A	5.0
CT_AA-1	A	5.0	A	6.8
CT_AA-2	A	6.8	A	6.8
CT_AA-3	A	5.0	A	7.2
MT_BA-1	A	4.8	B	4.8
CT_BA-1	A	4.8	B	4.8
CT_BA-2	A	5.8	B	5.8
CT_BA-3	A	5.8	B	5.8
CT_BA-4	A	4.5	B	4.5
MT B ALTUS-1	B	5.7		
MT B ALTUS-2	B	5.7		
MT B ALTUS-3	B	5.7		
MT B ALTUS-4	B	5.6		

Table 4d - Combined In-Plane Shear/Tension Tests				
Avg. 28 day strength				
Test ID	Panel 1	f <sub>c</sub> (ksi)	Panel 2	f <sub>c</sub> (ksi)
CVT_BA-1	A	4.5	B	4.5
CVT_BA-2	A	4.5	B	5.4
CVT_BA-3	A	6.4	B	6.4
MVT_AB-1	A	6.4	B	6.4
MVT_AB-2	A	5.9	B	5.9
MVT_AB-3	A	5.9	B	5.9
MVT_AB-4	A	5.9	B	5.9



## PHASE 1 - TEST A1

### ERECTOR CONNECTOR UNDER MONOTONIC TENSION WITH NO SHEAR FORCE

The performance of the Erector connector subjected to monotonic tension is presented in this section. *The connector is welded on both side A and B.* The panel was subjected to tension displacement with the shear force unrestrained,  $F_v=0$ . Connector damage initiated with faceplate bending of connector A. This placed large tensile demand on the top faceplate of the Type A connector. This resulted in high tension demands on the thin section above the faceplate opening adjacent to the weld. This tension demand resulted in fracture of the face plate at each end of the weld at 0.62-in. and 1.22-in. of opening displacement. A third increase in strength occurred as the embedded plate tabs contacted the opening of connector A. The slug pulled out at approximately 2-in. of deformation. A complete loss in resistance occurred after pullout of the plate. The observed key events and the corresponding displacement level are presented in Table 5. The photos of the damage are presented in Figure 15 and Figure 16. The global force deformation response and backbone curve are presented in Table 6 and Figure 17.

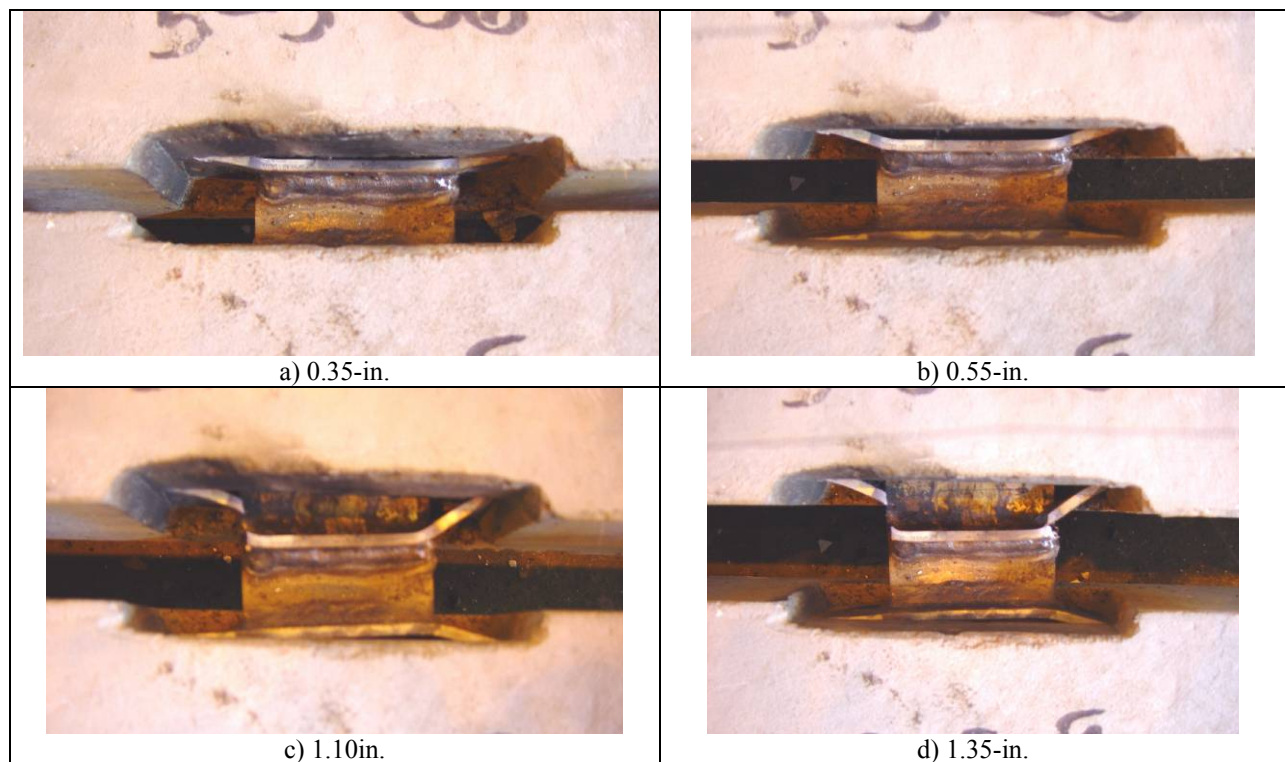


Figure 15: Damage state at various tensile openings

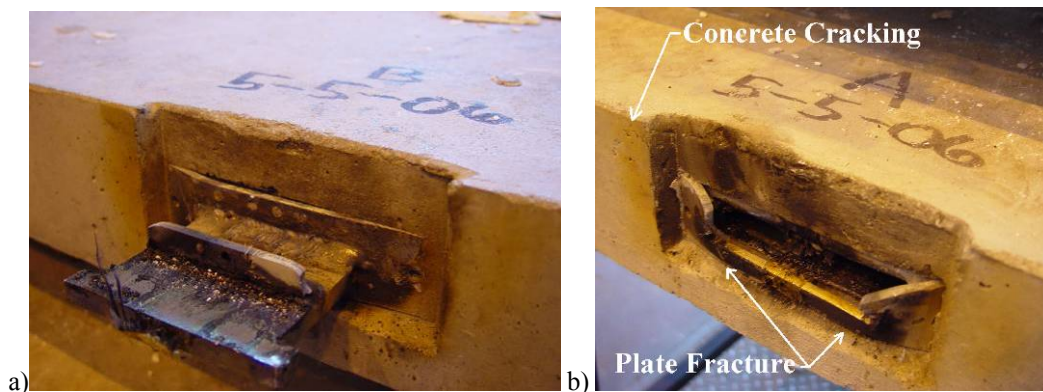


Figure 16: Damage at end of test a) Connector B, b) Connector A

Table 5: Key Test Observations (Monotonic Tension)		
Event #	Tensile $\Delta$ Step [in.]	Event Description
1	0.20	Face plate bending from connector A
2	0.85	Fracture of face plate of connector A near left side of weld
3	1.10-1.35	Fracture of face plate of connector A near right side of weld
4	2.1	Pullout of tab from box of connector A
5	3.10	Test Stopped

Table 6: Experimental Results Backbone Curve (Monotonic Tension)		
Event	Tensile Displacement [in.]	Tensile Force [kips]
Elastic Limit	0.104	1.80
-	0.145	2.28
-	0.177	2.44
Peak Load	0.518	3.59
-	0.624	3.50
-	0.668	1.40
End of test	2.35	0

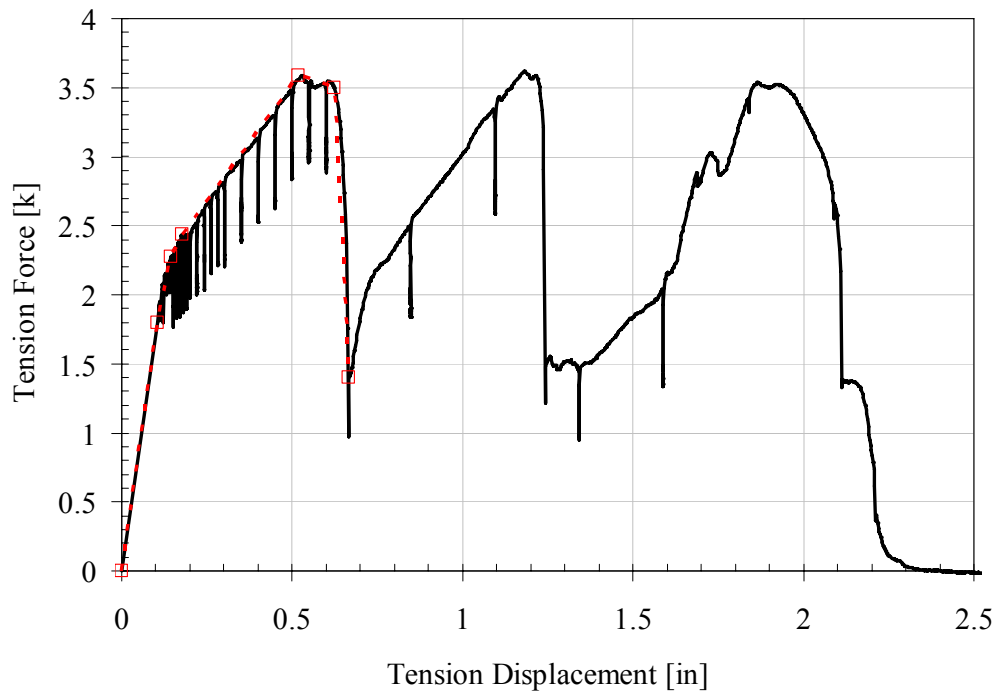


Figure 17: Force and axial displacement (Monotonic Tension)

## PHASE 1 - TEST A2

### ERECTOR CONNECTOR 1 UNDER MONOTONIC SHEAR DEFORMATION WITH $\Delta T = 0$

The performance of the Erector Connector subjected to monotonic shear is presented in this section. *The connector is welded on BOTH side A and B.* The panel was subjected to shear displacement with the tensile displacement restrained,  $\Delta T=0$ . Connector damage initiated with rotation of the front face plate of connector B which continued with additional shear deformation. Crushing and spalling occurred above the compression leg of connector A. This was followed by similar spalling damage over the compression leg of connector B. The amount of spalling increased on connection A. Fracture of connector A occurred on the tension leg. However even after the tension leg was lost the compression legs were capable of resisting shear through bearing of the embedded slug. The observed key events and the corresponding displacement level are presented in Table 7. The photos of the damage are presented in Figure 18. The global force deformation response and backbone curve are presented in Table 8 and Figure 19.

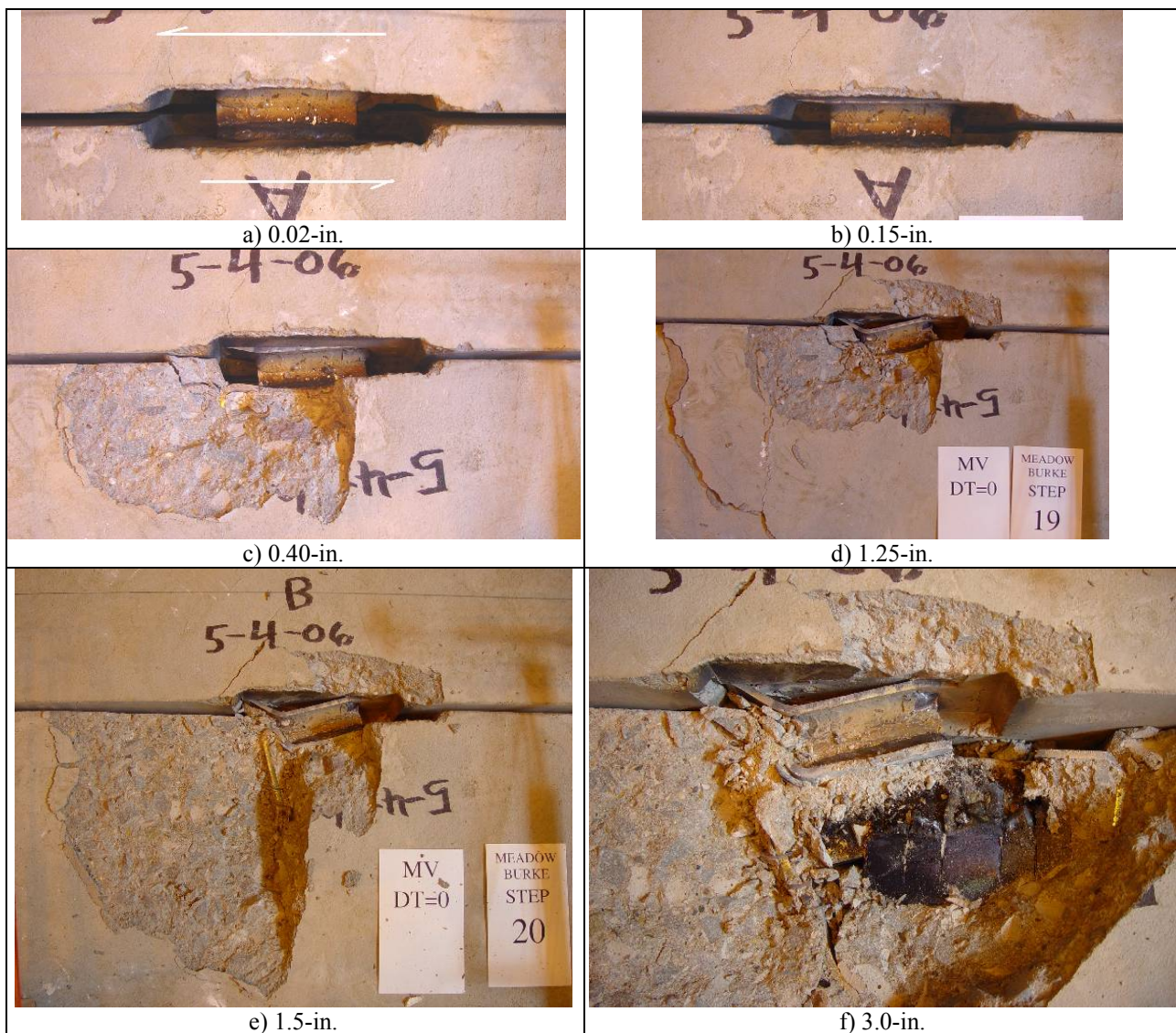


Figure 18: Damage state at increasing shear deformations



Table 7: Key Test Observations Erector Connector 2 Welds (Monotonic Shear)		
Event #	Shear $\Delta$ [in.]	Event Description
1	0.25	Cracking audible
2	0.30	Panel A compression leg cracking and associated spalling
3	1.00	Spalling over tension leg on panel B
4	1.25	Tension failure observed on connector A and compression pushout damage
5	1.50	Additional pushout of compression side panel A
6	2.50	Cracking over panel A tension side
7	3.00	Test Stopped

Table 8: Experimental Results Backbone Curve 2 Welds (Monotonic Shear)				
Step	Shear force – Shear deformation		Axial force – Shear deformation	
	Shear Force	Shear Displacement	Shear Displacement	Axial Force
	11.88	0.09	11.88	-3.01
First Peak	20.24	0.26	20.24	-6.88
	14.64	0.41	14.64	-5.09
	23.07	1.06	23.07	-10.81
Secondary Peak	23.42	1.19	23.42	-11.28
	5.47	1.47	5.47	-2.13
Failure of Connector	10.87	3.00	10.87	-2.33

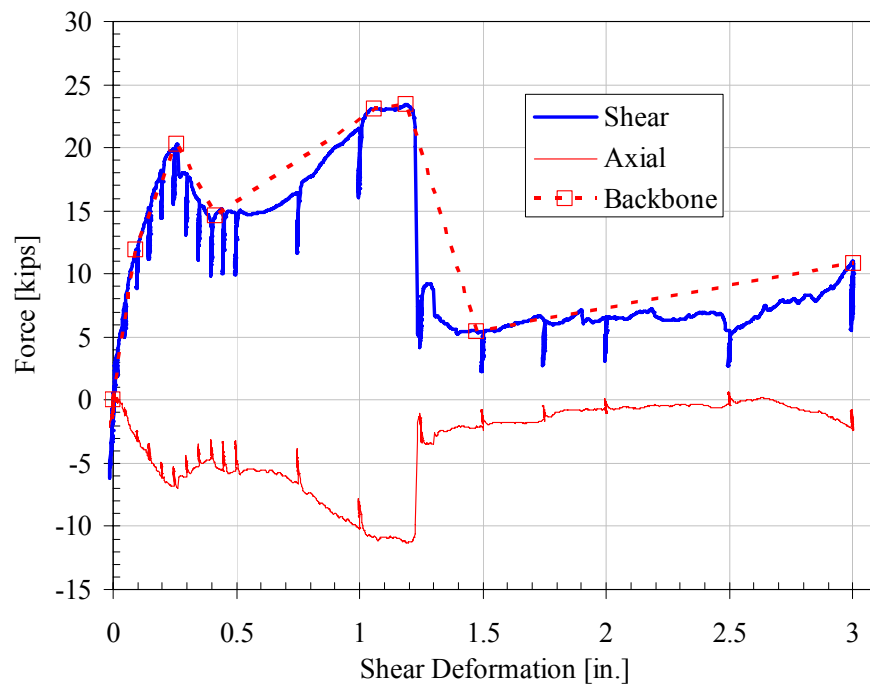


Figure 19: Force and shear displacement (monotonic shear w/ 2 welds)

## PHASE 1 - TEST A3

### ERECTOR CONNECTOR 2 MONOTONIC SHEAR DEFORMATION W/ TENSION $\Delta T = 0$

The performance of the Erector Connector subjected to monotonic shear is presented in this section. *The connector is welded on side B only.* The panel was subjected to a monotonic shear displacement with the tensile displacement restrained,  $\Delta T=0$ . The connector exhibited an initial shear resistance from the tension leg of connector B. This was followed by bearing of the embedded slug on the faceplate of connector A which produced a splitting crack above the compression connector leg. Fracture of the tension leg of connection B followed resulting in a loss in load carrying capacity. Fracture of the tension leg of connector B progressed slowly resulting in maintenance of shear resistance. After the faceplate was fully fractured shear was maintained through bearing of the slug. The observed key events and the corresponding displacement level are presented in Table 9. The photos of the damage are presented in Figure 20. The global force deformation response and backbone curve are presented in Table 10, and Figure 21.

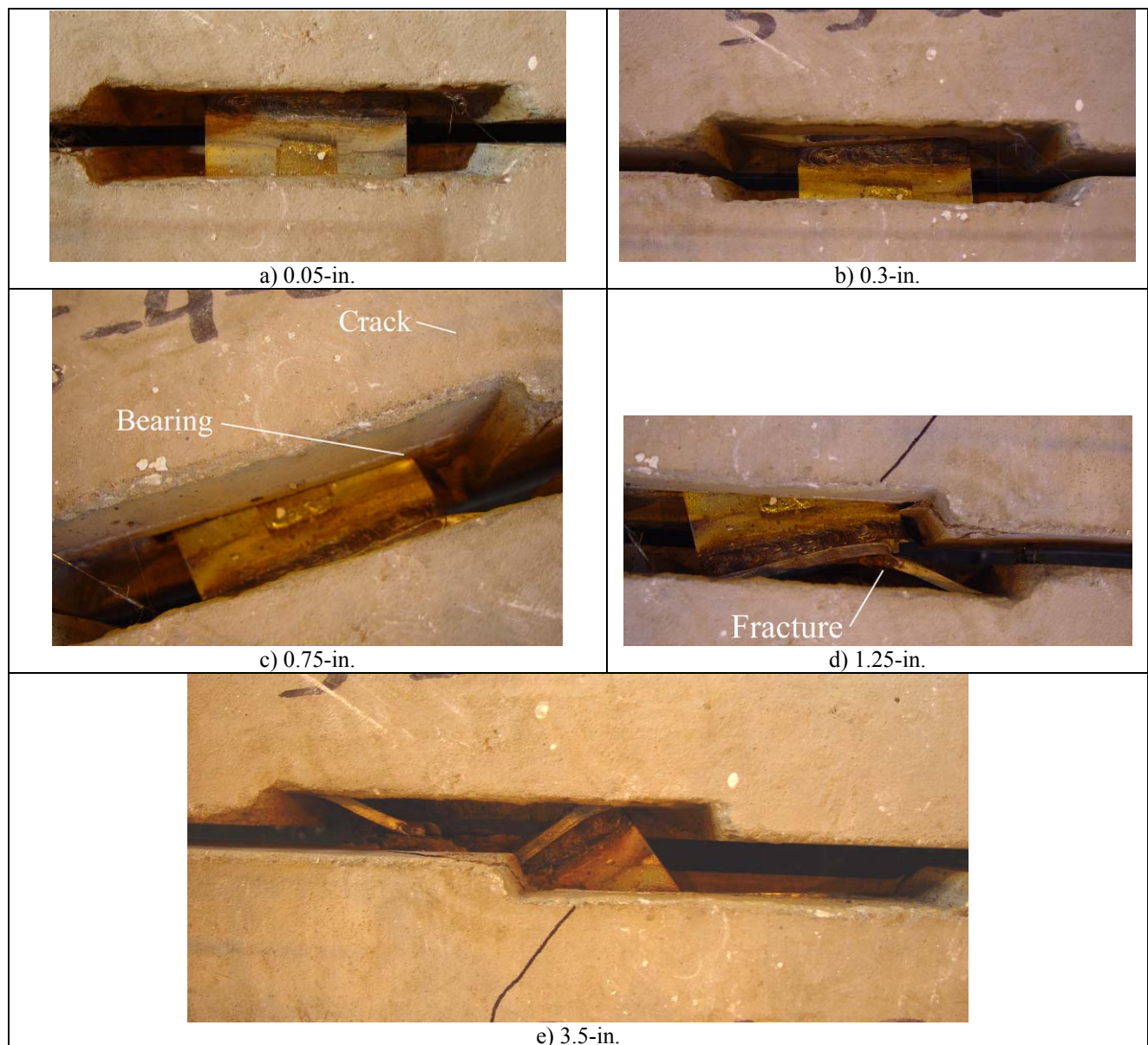


Figure 20: Damage state at increasing shear deformations

Table 9: Key Test Observations Erector Connector - 1 Weld (Monotonic Shear)			
Event #	Shear $\Delta$ [in.]	Tension $\Delta$ [in.]	Event Description
1	0.30	0.00	Noticeable bending of faceplate on panel B
2	0.75	0.01	Bearing of slug on panel A, yielding of faceplate on panel B
3	1.00	0.01	Concrete cracking around faceplate on panel A
4	1.25	0.02	Initiation of fracture of tension side of faceplate on panel B
5	1.75	0.04	Spalling on underside of panel A
6	2.00	0.05	Bearing of panel A faceplate on panel B
7	3.00	0.11	Complete fracture of faceplate on panel B

Table 10: Experimental Results Backbone Curve Erector Connector - 1 Weld (Monotonic Shear)			
Step	Shear Displacement [in.]	Shear Force [kips]	Axial Force [kips]
	0.143	6.38	-1.25
	0.337	11.92	-3.65
Max Load	0.838	21.43	-9.80
	1.128	8.68	-4.60
	1.395	10.46	-5.76
	1.828	5.97	-2.89
End of Test	4.233	4.61	-2.91

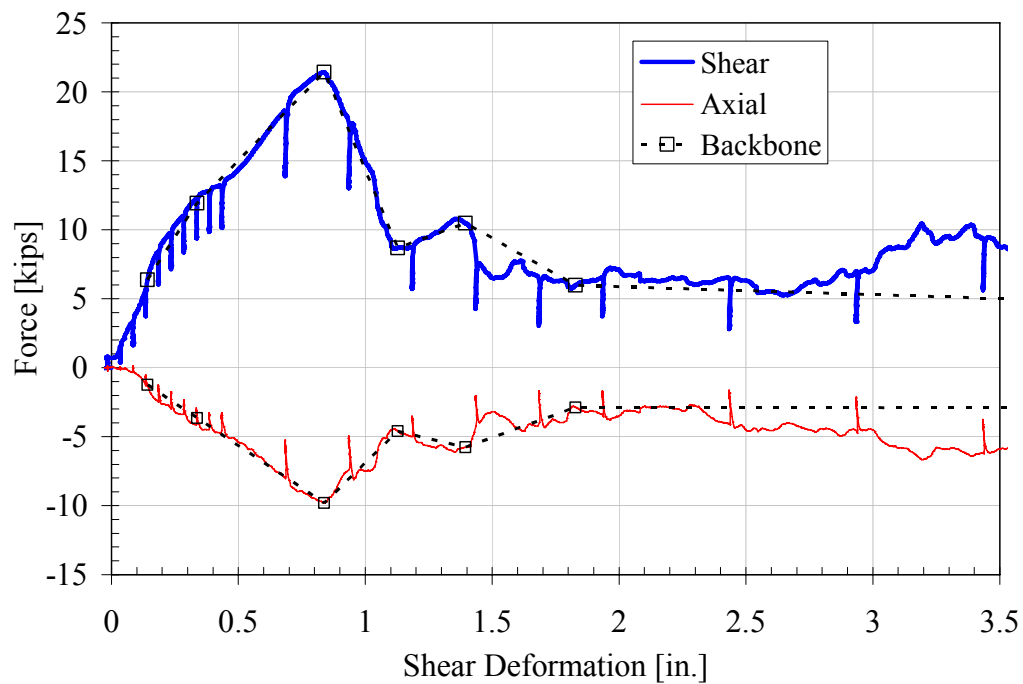


Figure 21: Shear force and displacement (monotonic shear w/ 1 weld)

## PHASE 1 - TEST A4

### ERECTOR CONNECTOR UNDER CYCLIC SHEAR DEFORMATION W/ TENSION $\Delta T = 0$

The performance of the Erector Connector subjected to cyclic shear is presented in this section. *The connector is welded on side B only.* The panel was subjected to a cyclic shear displacement with the tensile displacement restrained,  $\Delta T=0$ . Shear deformation resulted in tension demand on one leg of connector B and of the slug bearing on connection A. This produced rotation of the faceplate of connection B. Load reversal caused the faceplate to rotate in the opposite direction and produce tension on the opposite leg. The cyclic loading produced yielding in tension followed by buckling in compression. The repeated cyclic compression and tension resulted in fracture of the faceplate of connector B on either side of the slug. In addition, the bearing action of the slug within connector A produced cracking below the connector. The observed key events and the corresponding displacement level are presented in Table 11. The photos of the damage are presented in Figure 22. The global force deformation response and backbone curve are presented in Table 12, Figure 23 and Figure 24.

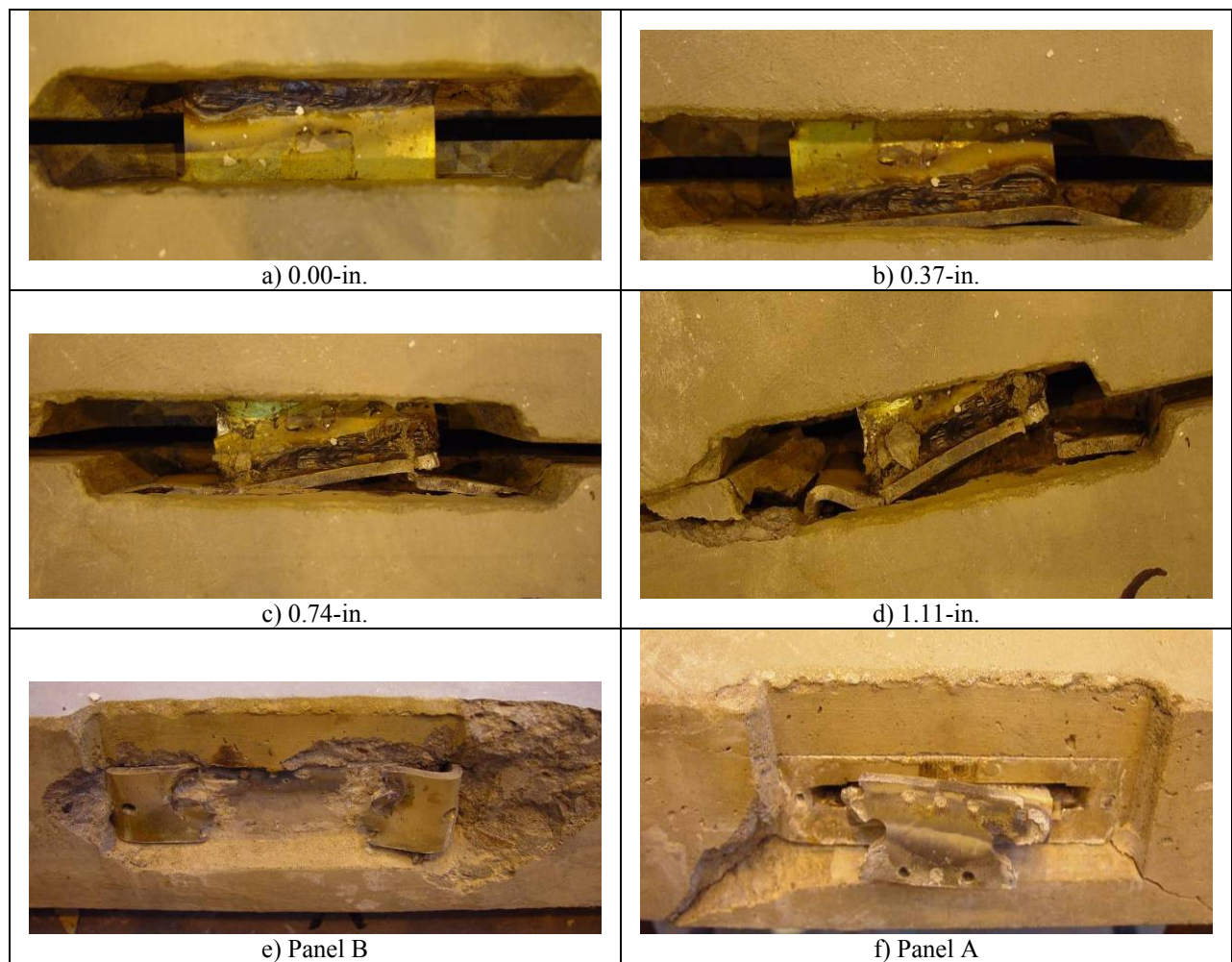


Figure 22: Damage states cyclic shear with 1 weld

Table 11: Key Test Observations Erector Connector – 1 Weld (Cyclic Shear)			
Event #	Shear $\Delta$ [in.]	Tension $\Delta$ [in.]	Event Description
1	0.555	0	Spalling on connector B
2	-0.74	0	Fracture on connector B
3	1.11	0	Through fracture on connector B
4	-1.11	0	90% fracture on other side of connector B
5	-1.48	0	Complete fracture of connector B
6	1.48	0	Test Stopped

Table 12: Experimental Results Backbone Curve Erector Connector – 1 Weld (Cyclic Shear)		
Event	Shear Displacement [in.]	Shear Force [kips]
	0.855	17.07
Positive Peak	0.736	19.18
	0.555	16.01
	0.370	12.93
	0.276	10.79
	0.183	8.14
	0.088	2.28
Zero	0.000	-0.18
	-0.097	-1.08
	-0.191	-5.93
	-0.284	-9.10
	-0.377	-10.90
	-0.565	-13.73
	-0.739	-14.96
Negative Peak	-1.076	-16.08

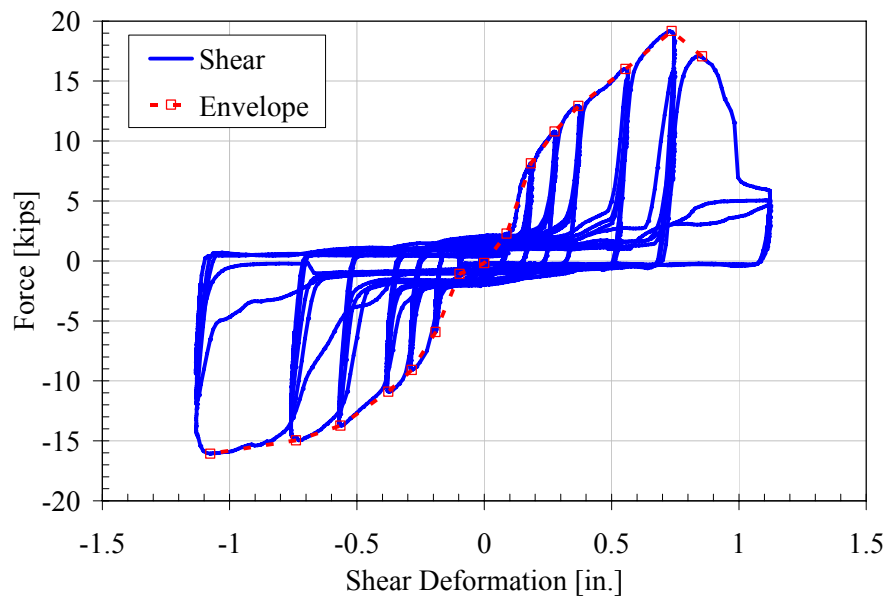


Figure 23: Force and shear displacement cyclic shear with 1 weld



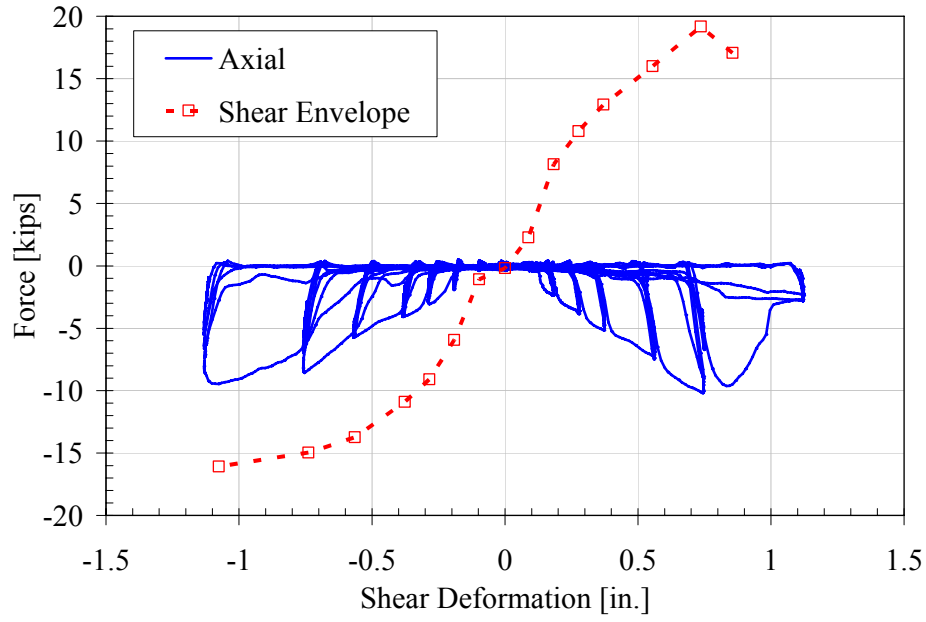
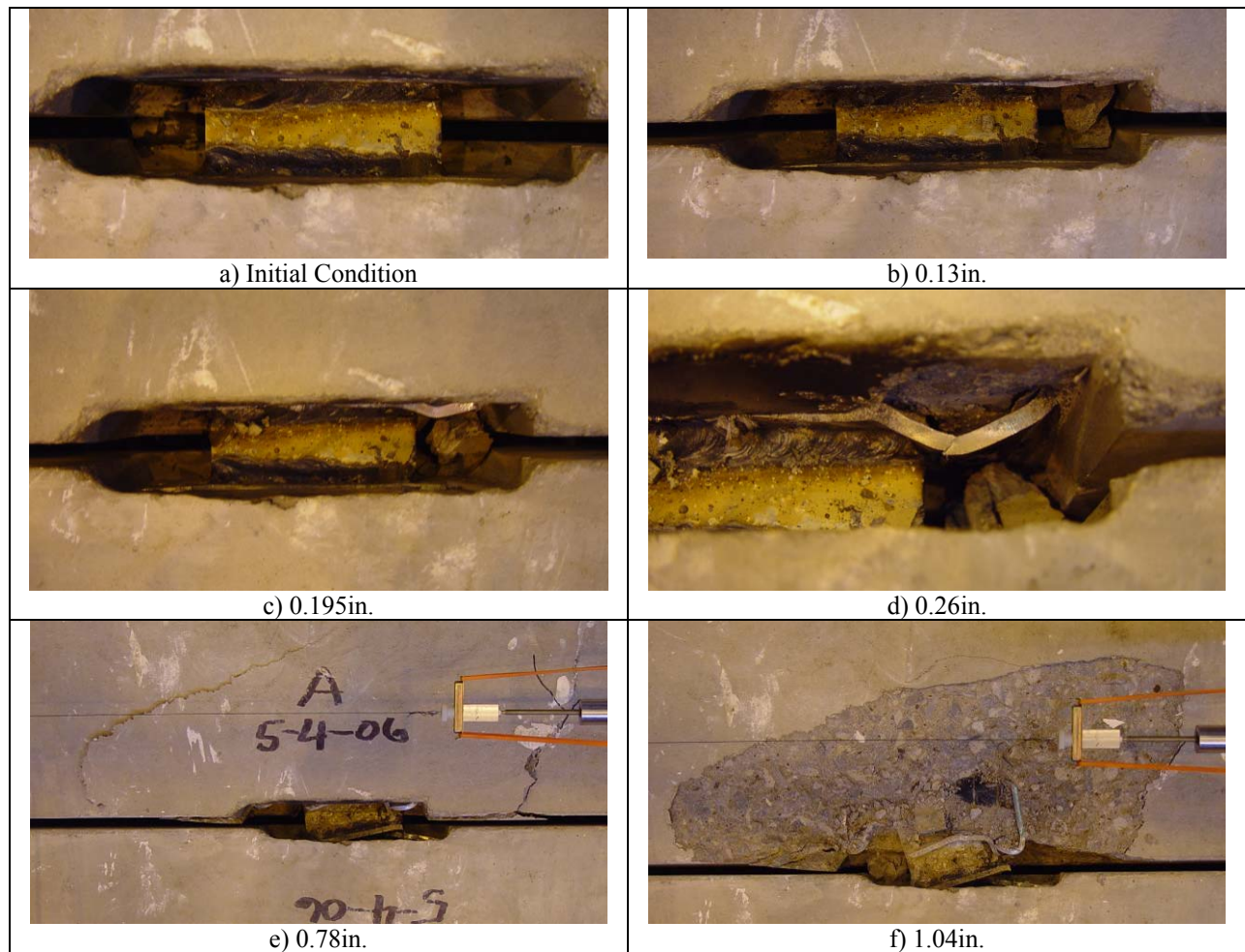


Figure 24: Axial force and shear displacement cyclic shear with 1 weld

## PHASE 1 - TEST A5

### ERECTOR CONNECTOR UNDER CYCLIC SHEAR DEFORMATION W/ TENSION $\Delta T = 0$

The performance of the Erector Connector subjected to cyclic shear is presented in this section. *The connector is welded on BOTH sides A and B.* The panel was subjected to a cyclic shear displacement with the tensile displacement restrained,  $\Delta T=0$ . Shear deformation resulted in tension demand on diagonally opposing legs of the connectors. This produced a rotation of the faceplates of the connection. Load reversal caused the connectors to rotate in the opposite direction and produce tension on the opposite legs. The cyclic loading produced yielding in tension followed by buckling in compression. This produced fracture of the faceplates on both connection A and B. This was followed by spalling above connection A. The observed key events and the corresponding displacement level are presented in Table 13. The photos of the damage are presented in Figure 25. The global force deformation response and backbone curve are presented in Table 14, Figure 26 and Figure 27.



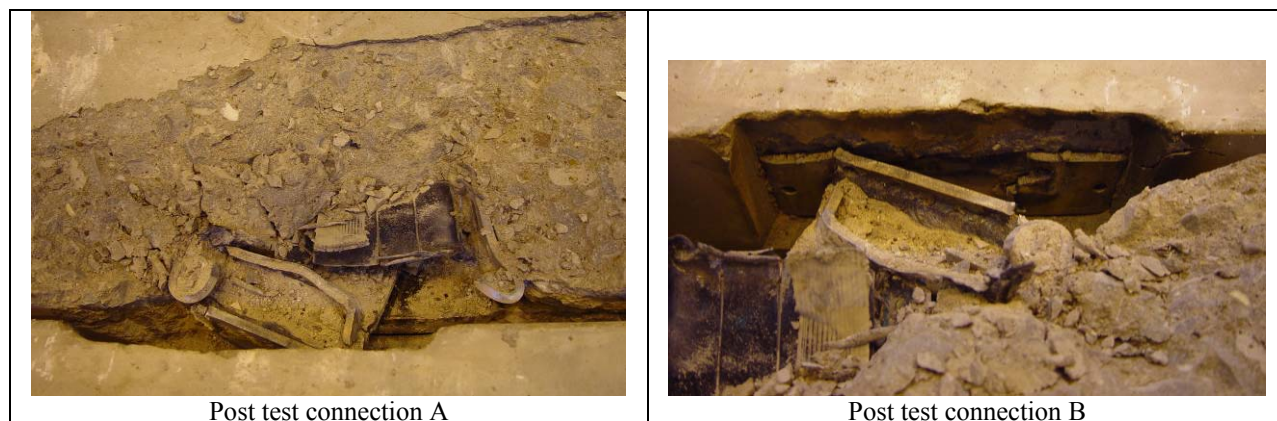


Figure 25: Damage states cyclic shear both sides welded

Event #	Shear $\Delta$ [in.]	Tension $\Delta$ [in.]	Event Description
1	0.033	0.000	Concrete cracking audible
2	0.098	0.000	Noticeable bending of faceplate on panel A
3	-0.130	0.000	Fracture on faceplate of panel A
4	0.130	0.000	Concrete spalling around faceplate on panel A
5	0.195	0.000	Spalling around faceplate on panel B
7	0.260	0.001	Fracture of faceplate on panel A
8	0.390	0.002	Additional spalling on panel A and faceplate bending
9	-0.520	0.003	Bending of faceplate on panel B
10	-0.520	0.003	Cracking on top of panel A
11	-0.780	0.007	Fracture of faceplate on panel B
12	1.040	0.013	Large spall on panel A
13	-1.300	0.021	Additional spalling
14	-1.560	0.030	End of test

Event	Shear Deformation [in.]	Shear Force [kip]	Axial Force [kip]
	0.027	7.48	-1.82
	0.058	9.06	-2.71
First Peak	0.092	9.80	-3.04
	0.122	9.09	-2.77
	0.190	5.62	-1.06
	0.257	8.14	-2.73
	0.387	12.66	-5.06
	0.524	15.51	-7.39
Positive Peak	0.710	16.73	-9.07
	1.051	9.87	-4.72
	1.279	3.96	-3.57
	1.575	8.77	-7.28
Negative Peak	-0.503	-17.64	-10.16

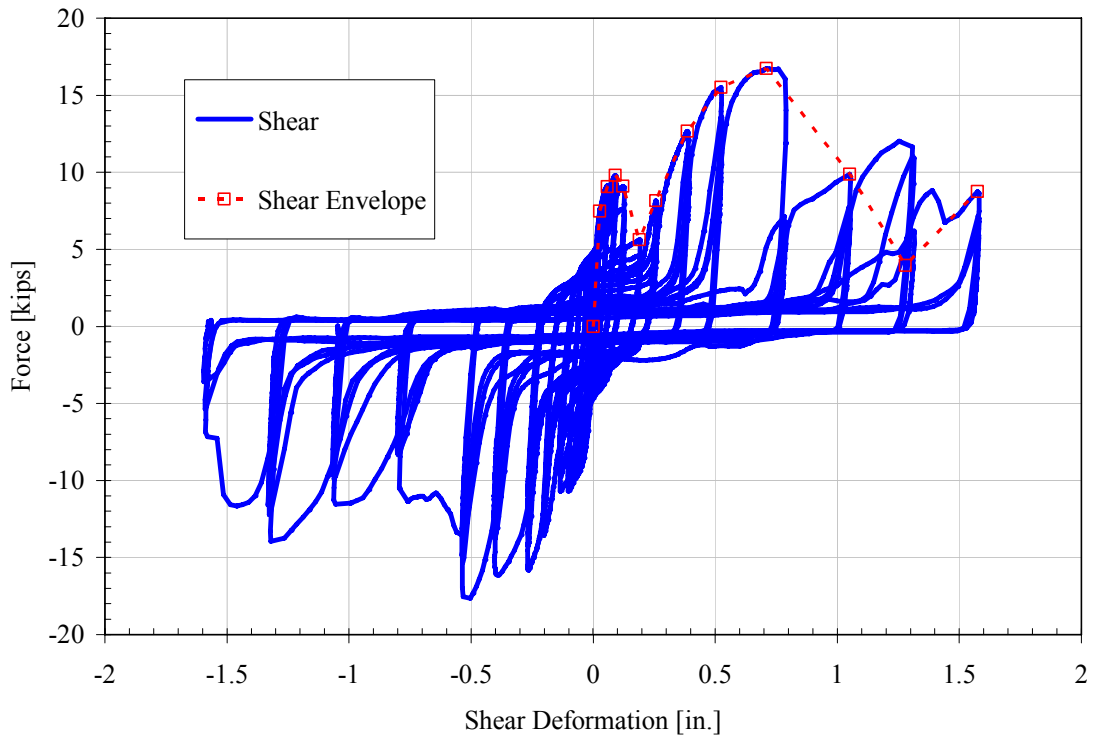


Figure 26: Force and shear displacement CV both sides welded

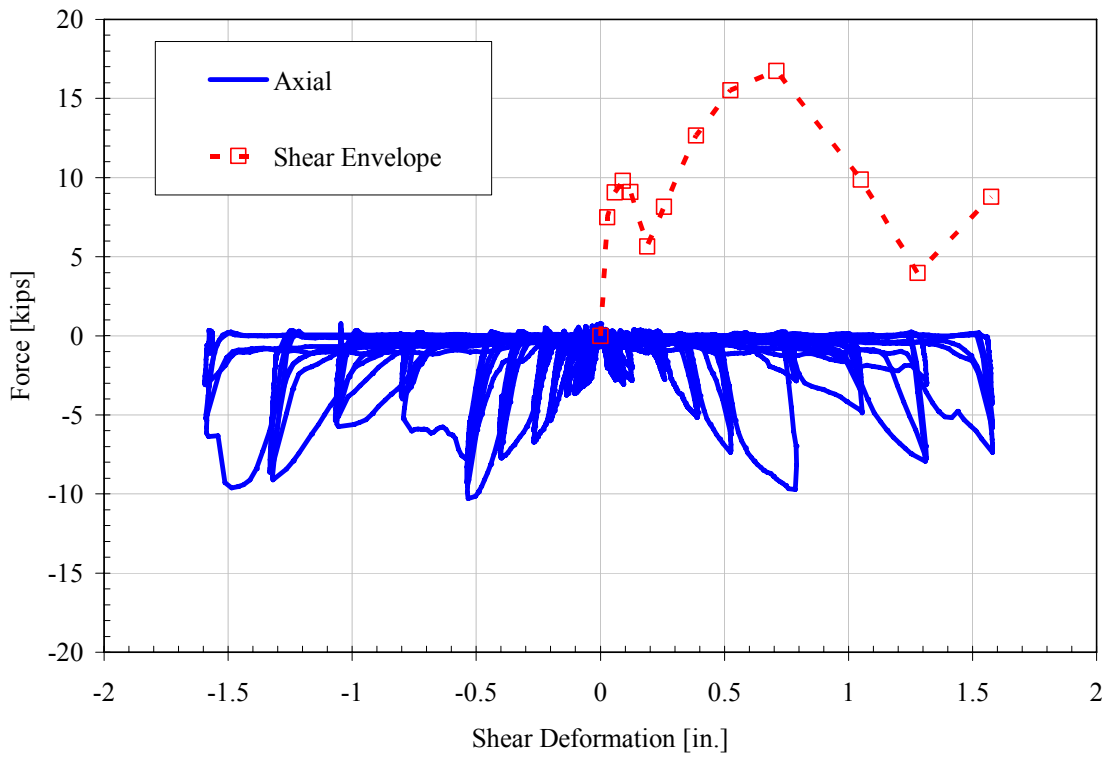


Figure 27: Axial force and shear displacement CV both sides welded



**PHASE 1 - TEST A6**

**ERECTOR CONNECTOR UNDER SHEAR W/ PROPORTIONAL TENSION DEFORMATION ( $\Delta V/\Delta T = 2.0$ )**

The performance of the Erector Connector subjected to shear with proportional tension is presented in this section. Shear deformation was applied at twice the tension deformation. *The connector is welded on BOTH sides A and B.* The concrete damage was focused on the panel with Type A connector, however connector fractures occurred on both side A and B. Fracture of connector A occurred first adjacent to the end of the left weld this was followed by fracture of connector B at the adjacent to the right side of the weld. This mechanism formed due to the tension force developed in these two legs as a result of the shear and opening. Once the tension legs were lost the shear was still supported through a compression strut through the opposing legs of the connector. The observed key events and the corresponding displacement level are presented in Table 15. The photos of the damage are presented in Figure 28. The global force deformation response and backbone curve are presented in Table 16, Figure 29 and Figure 30.

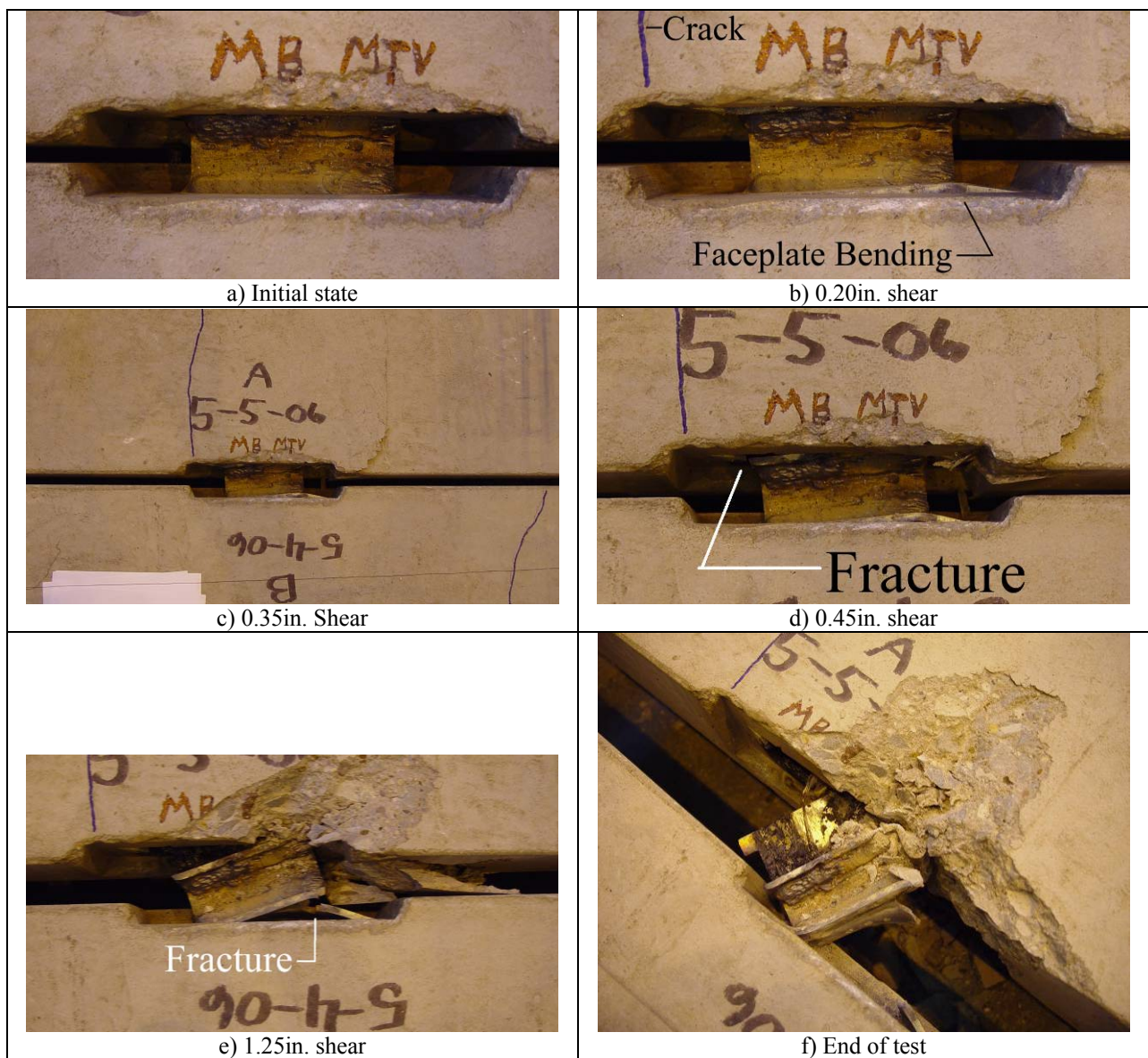


Figure 28: Damage states

Table 15: Key Test Observations Erector Connector – 2 Welds ( $\Delta V/\Delta T=2.0$ )

Event #	Shear $\Delta$ [in.]	Tension $\Delta$ [in.]	Event Description
1	0.0000	0.0000	Hairline cracks on panel B
2	0.1000	0.0501	Crack formation on left side of panel A
3	0.1500	0.0753	Noticeable bending of faceplates on both panels
4	0.2500	0.1258	Cracking on panel A above right leg of connector
5	0.3000	0.1511	Additional cracking on panel A above right leg of connector
6	0.4500	0.2275	Fracture of left side of faceplate on panel A
7	1.0000	0.5123	Initial fracture of right side of faceplate on panel B
8	1.7500	0.9128	Spalling on panel A
9	2.0000	1.0494	Complete fracture of right side of faceplate on panel B
10	4.5000	2.4992	End of test

Table 16: Experimental Results Backbone Curve Erector Connector – 2 Welds ( $\Delta V/\Delta T=2.0$ )

Event	Shear Deformation [in.]	Shear Force [kip]	Axial Force [kip]
-	0.102	9.83	1.59
First peak	0.215	13.91	2.20
-	0.361	10.50	1.87
-	0.831	13.99	8.32
Max Load	1.32	15.20	11.26
-	1.58	13.84	10.47
-	1.86	9.66	8.86
-	3.65	1.98	2.00

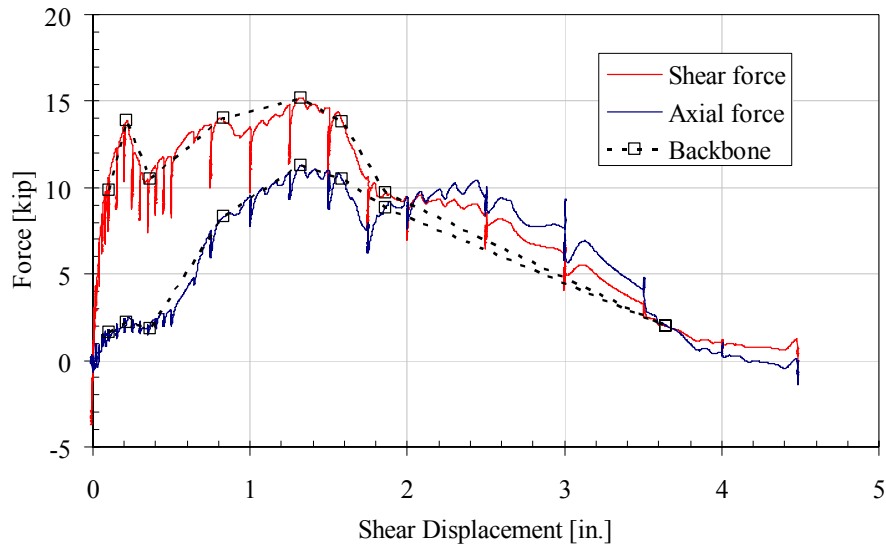


Figure 29: Force and shear displacement MTV

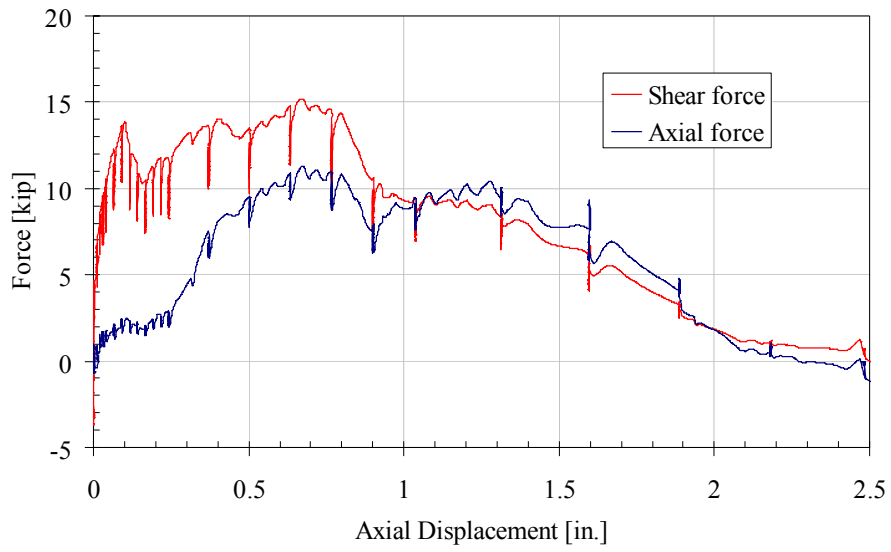


Figure 30: Force and axial displacement MTV

## PHASE 2 - TEST SERIES 1

### OUT-OF-PLANE SHEAR – STEPPED PANEL – “A” CONNECTOR

During Test Series 1, stepped panels were loaded out of plane, where the panel was connected to the loading fixture via an “A” connector. Four specimens were tested under monotonically increasing out-of-plane shear. A plot containing the measured out-of-plane shear versus displacement relationship for the four panels is shown in Figure 31. The behavior of the panels is different in that maximum load was reached at very different points in the loading history. For example, specimen MOP\_A-4 reaches its peak load at nearly 1 inch of displacement, while specimen MOP\_A-3 reaches its peak load at approximately 0.15 inches.

As load was increased, cracks formed on the slab upper surface. The load at which the first crack appeared was noted (see Table 17). The slab continued to accept increasing loads beyond the initial cracking load. As additional cracks appeared, they were marked and noted. Maximum loads for each specimen are presented in Table 17.

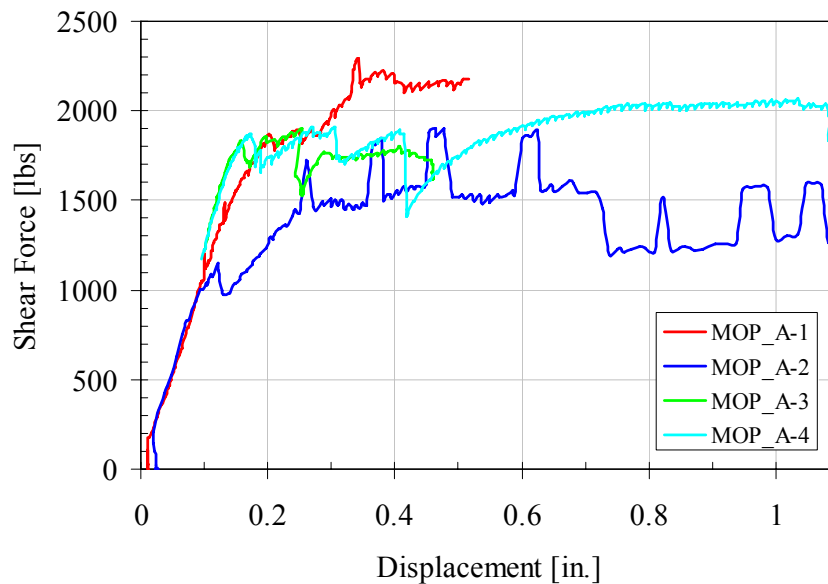


Figure 31: Test Series 1 – Out-of-plane load versus displacement stepped panel with “A” connector

Table 17: Test Series 1 Maximum Load and Load at First Crack			
Specimen	Max Load (lbs)	$\Delta$ @ Max Load (in)	Load at 1st Crack (lbs)
MOP_A-1	2,290	0.34	1,865
MOP_A-2	1,906	0.46	1,725
MOP_A-3	1,899	0.25	1,834
MOP_A-4	2,072	1.03	1,869
<i>Average =</i>	<i>2,042</i>	<i>0.52</i>	<i>1,823</i>
<i>Standard. dev. =</i>	<i>183.9</i>	<i>0.35</i>	<i>67.3</i>



**PHASE 2 - TEST SERIES 2**  
**OUT-OF-PLANE SHEAR – 4” UNIFORM PANEL – “B” CONNECTOR**

During Test Series 2, panels with a uniform thickness of 4 inches were loaded out of plane, where the panel was connected to the loading fixture via a “B” connector. Four specimens were tested under monotonically increasing out-of-plane shear. A plot containing the measured out-of-plane shear versus displacement relationship for the four panels is shown in Figure 32. It can be seen that the behavior of the four specimens was comparable.

As load was increased, cracks formed on the slab upper surface. The load at which the first crack appeared was noted (see Table 18). The slab continued to accept increasing loads beyond the initial cracking load. As additional cracks appeared, they were marked and noted. Maximum loads for each specimen are presented in Table 18.

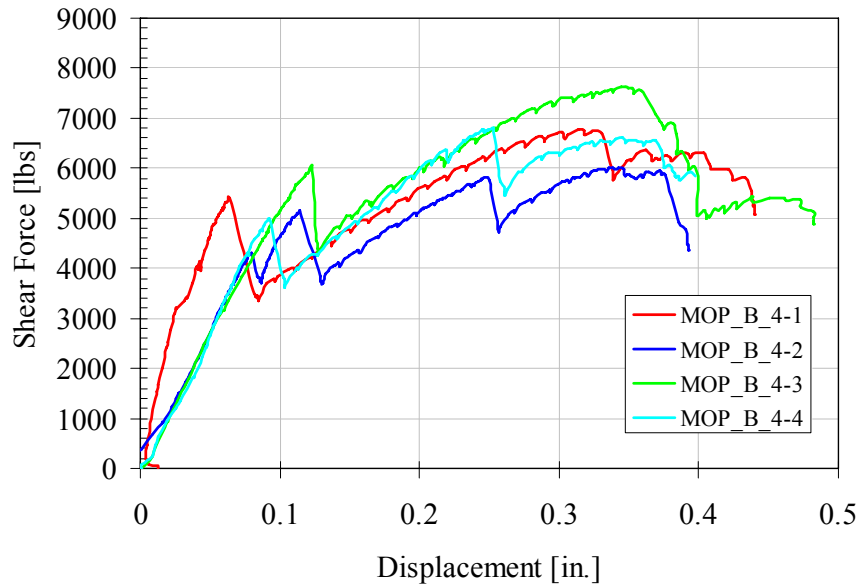


Figure 32: Test Series 1 – Out-of-plane load versus displacement panel with 4” uniform thickness with “B” connector

Table 18: Test Series 2 Maximum Load and Load at First Crack			
Specimen	Max Load (lbs)	Δ @ Max Load (in)	Load at 1st Crack (lbs)
MOP_B_4-1	6,781	0.31	5,416
MOP_B_4-2	6,011	0.34	4,307
MOP_B_4-3	7,633	0.34	6,056
MOP_B_4-4	6,794	0.25	4,992
<i>Average =</i>	<i>6,805</i>	<i>0.31</i>	<i>5,193</i>
<i>Standard. dev. =</i>	<i>662.8</i>	<i>0.04</i>	<i>734.8</i>

**PHASE 2 - TEST SERIES 3**  
**OUT-OF-PLANE SHEAR – STEPPED PANEL – “B” CONNECTOR**

During Test Series 3, stepped panels were loaded out of plane, where the panel was connected to the loading fixture via a “B” connector. Four specimens were tested under monotonically increasing out-of-plane shear. A plot containing the measured out-of-plane shear versus displacement relationship for the four panels is shown in Figure 33. The behavior of the panels is similar however the maximum loads levels are somewhat different.

As load was increased, cracks formed on the slab upper surface. The load at which the first crack appeared was noted (see Table 19). The slab continued to accept increasing loads beyond the initial cracking load. As additional cracks appeared, they were marked and noted. Maximum loads for each specimen are presented in Table 19.

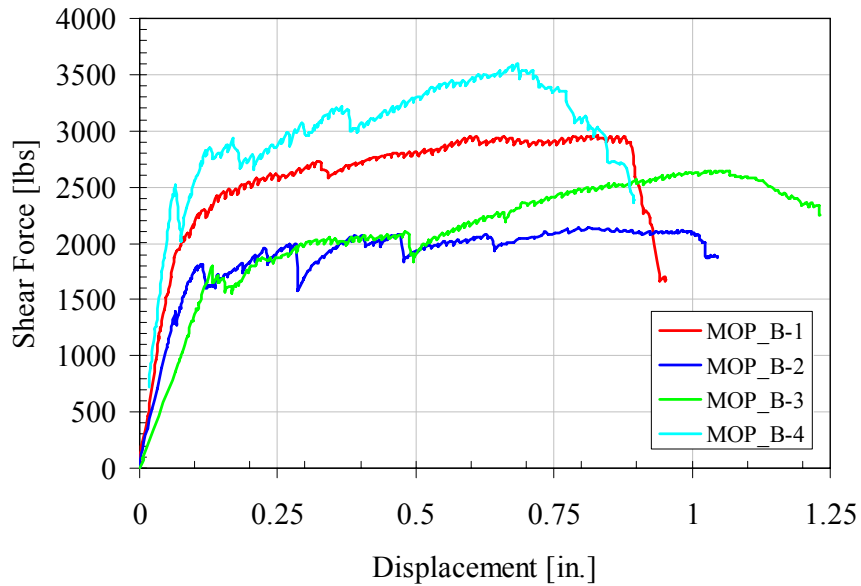


Figure 33: Test Series 1 – Out-of-plane load versus displacement stepped panel with “B” connector

Table 19: Test Series 3 Maximum Load and Load at First Crack			
Specimen	Max Load (lbs)	$\Delta$ (@ Max Load (in)	Load at 1st Crack (lbs)
MOP_B_4-1	2,956	0.83	2,061
MOP_B_4-2	2,139	0.81	1,814
MOP_B_4-3	2,648	1.06	1,793
MOP_B_4-4	3,598	0.69	2,510
<i>Average =</i>	<i>2,835</i>	<i>0.85</i>	<i>2,045</i>
<i>Standard. dev. =</i>	<i>609.7</i>	<i>0.15</i>	<i>333.3</i>

## PHASE 2 - TEST SERIES 4

### IN-PLANE SHEAR – STEPPED PANEL – “A” TO “A” CONNECTOR CONFIGURATION

The in-plane shear behavior of the connector was investigated in Test Series 4. In this test series, five specimens were tested. Each specimen consisted of two stepped panels with an “A-A” connector configuration. The first specimen, MV\_AA-1, was tested under monotonically increasing shear load while tensile deformations were restrained. Figure 34 contains a photograph of the condition of the A-A connector at a shear load of 10.5 kips. It can be seen that there is significant rotation of the connector in the pocket. The load versus displacement curve is shown in Figure 35.



Figure 34: Specimen MV\_AA-1 - condition of A-A connector at a shear load of 10.5 kips showing spalling of concrete

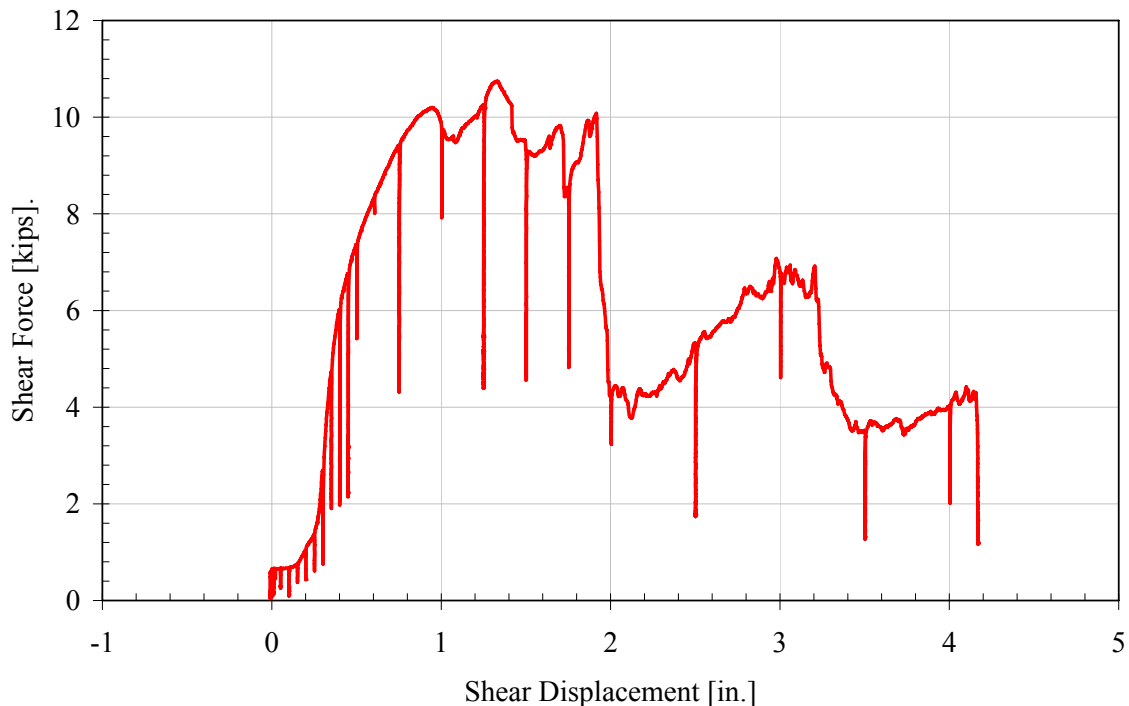


Figure 35: Monotonic shear test MV\_AA-1 - shear load versus shear displacement

Four cyclic shear tests were performed (tests CV\_AA-1 through CV\_AA-4). The behavior of the four specimens was similar. Figure 36 shows the spalling failure specimen CV\_AA-1 at a load of 9.2 kips (displacement of 2.3 inches). This type of failure was typical of all specimens. Figure 37 through 40 contain the load versus displacement relationship for the four specimens. Finally Table 20 contains the peak load and displacements for all specimens.

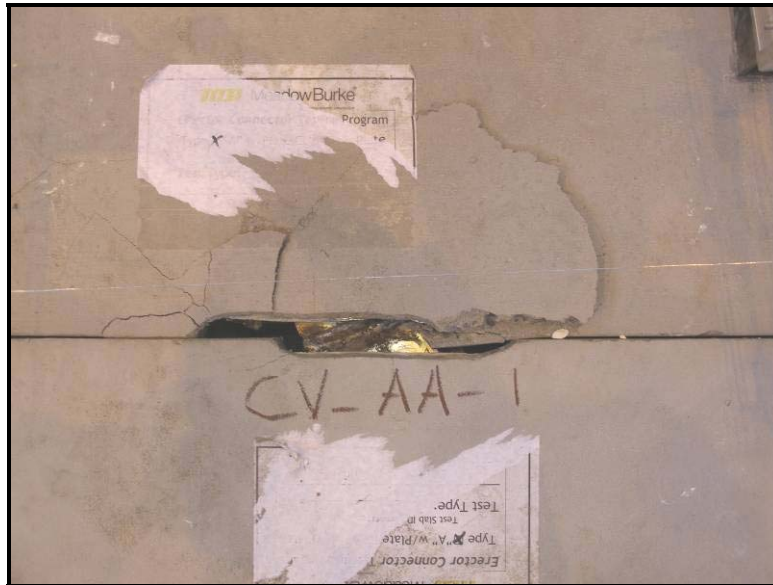


Figure 36 – Specimen CV\_AA-1 - spalling of top surface of panel at a load of 9.2 kips

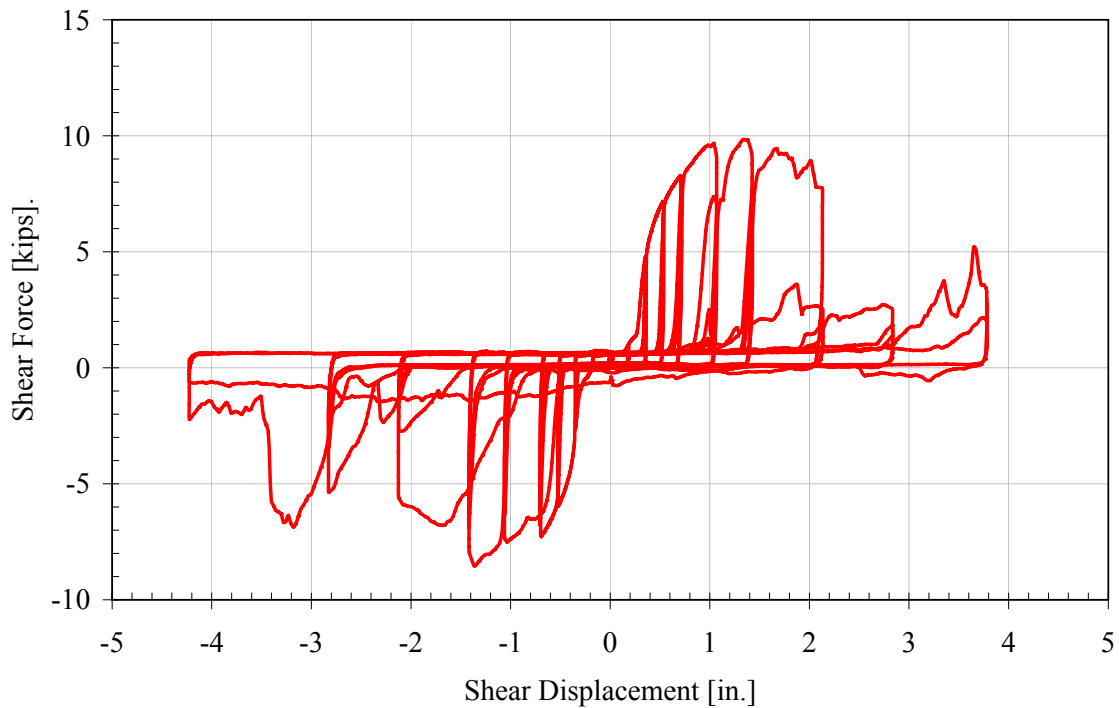


Figure 37: Cyclic shear test CV\_AA-1 - shear load versus shear displacement

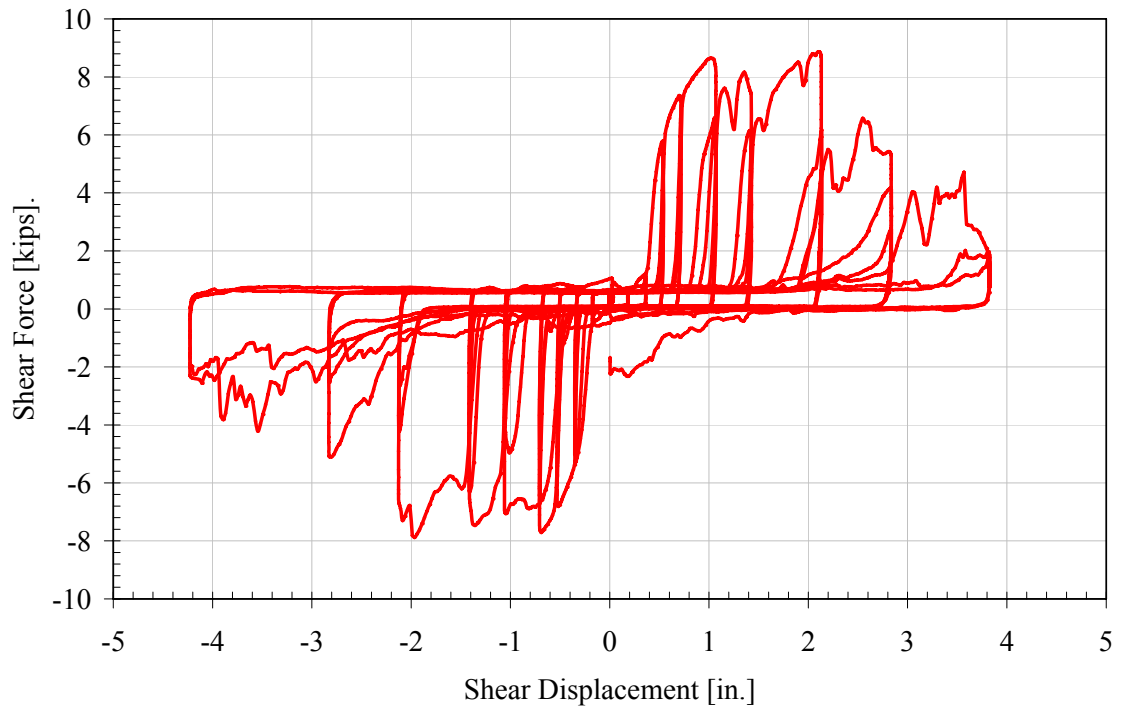


Figure 38: Cyclic shear test CV\_AA-2 - shear load versus shear displacement

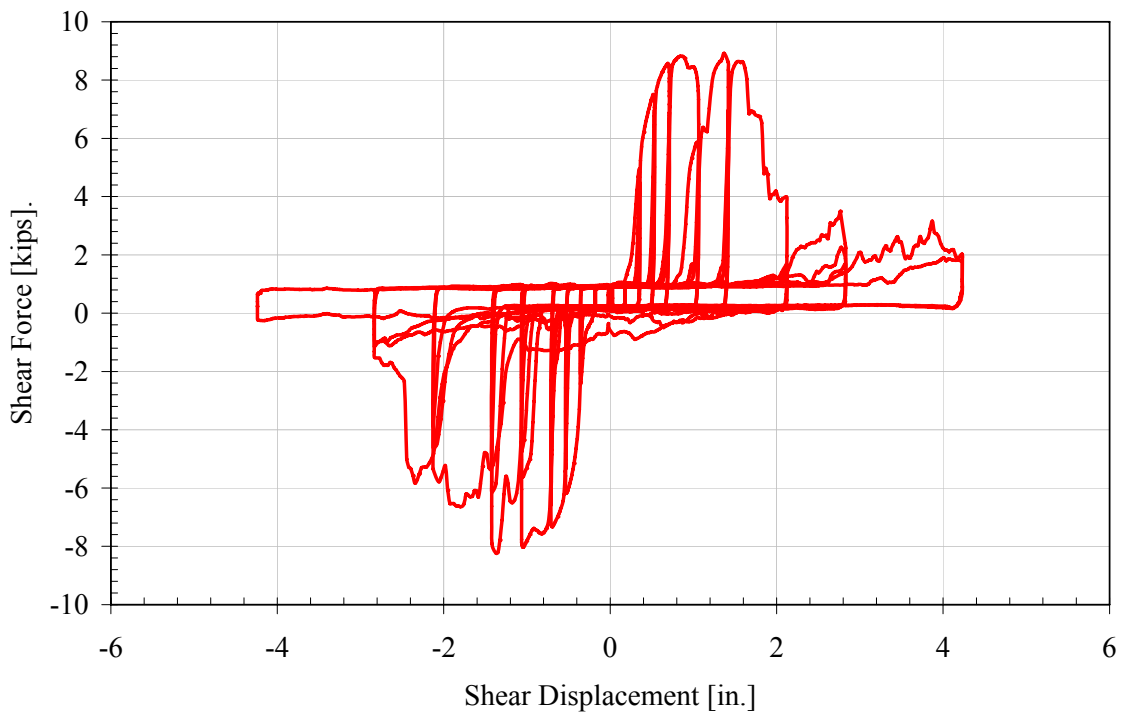


Figure 39: Cyclic shear test CV\_AA-3 - shear load versus shear displacement

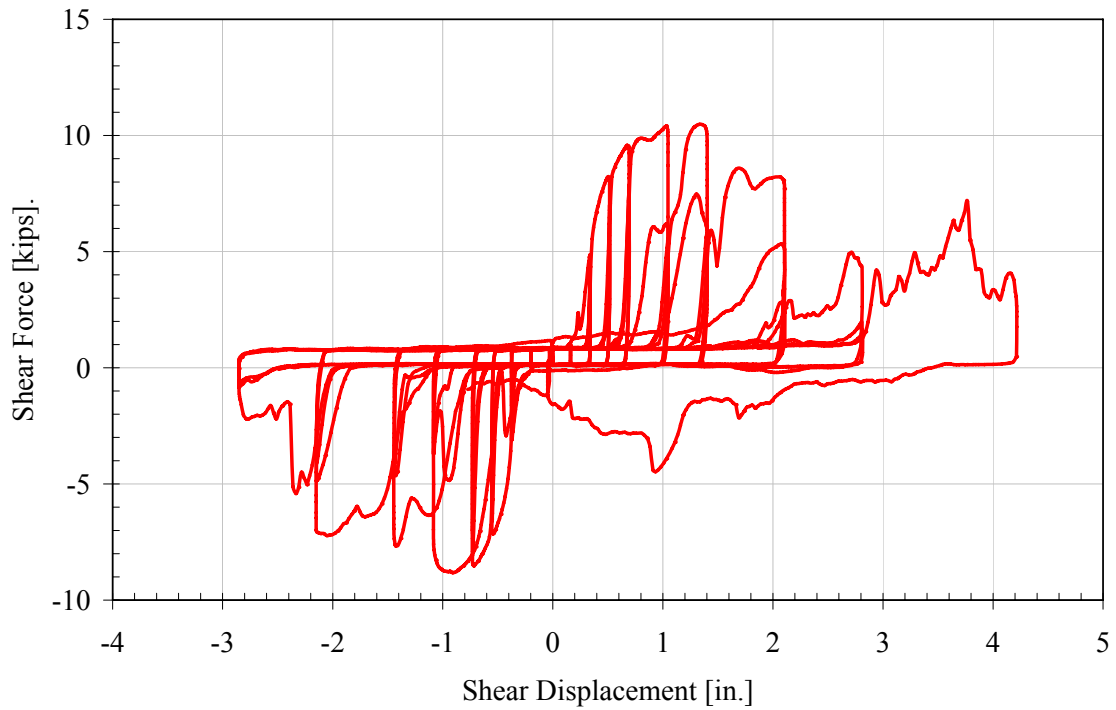


Figure 40: Cyclic shear test CV\_AA-4 - shear load versus shear displacement

Table 20: Test Series 4 Maximum Load and Displacement		
Specimen	Max Load (kips)	$\Delta$ @ Max Load (in)
MV AA-1	10.7	1.3
CV AA-1	9.8	1.3
CV AA-2	8.9	2.1
CV AA-3	8.9	1.4
CV AA-4	10.5	1.3
<i>Average*</i> =	9.5	
<i>Standard. dev*</i> =	0.78	

\*for cyclic tests only

## PHASE 2 - TEST SERIES 5

### IN-PLANE SHEAR – STEPPED PANEL – “A” TO “B” CONNECTOR CONFIGURATION

The in-plane shear behavior of the connector was further investigated in Test Series 5. In this test series, five specimens were tested. Each specimen consisted of two stepped panels with an “A-B” connector configuration. The first specimen, MV\_AB-1, was tested under monotonically increasing shear load while tensile deformations were restrained. Figure 41 contains a photograph of the condition of the A-B connector at a shear load of 12.0 kips. It can be seen that there is significant deformation of the connection faceplates. The load versus displacement curve is shown in Figure 42.

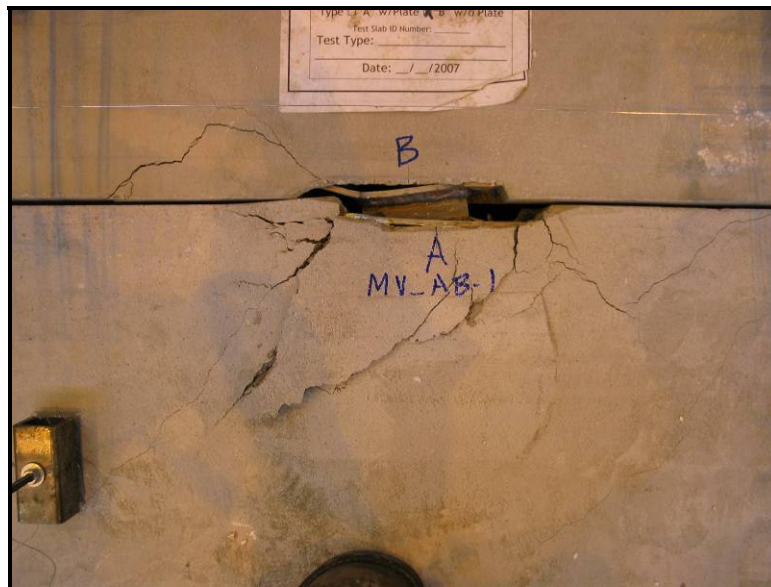


Figure 41: Specimen MV\_AB-1 - condition of A-B connector at a shear load of 12.0 kips showing spalling of concrete



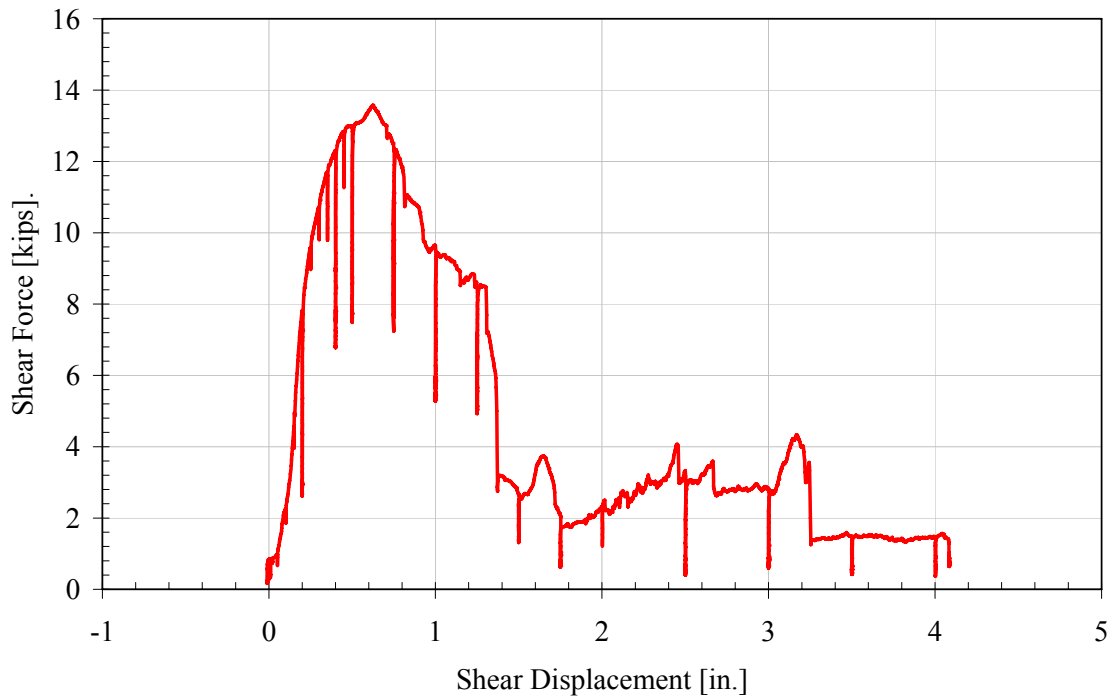


Figure 42: Monotonic shear test MV\_AB-1 - shear load versus shear displacement

Four cyclic shear tests were performed (tests CV\_AB-1 through CV\_AB-4). The behavior of the four specimens was generally similar. Figure 43 shows the onset of spalling in specimen CV\_AA-1 at a load of 8.9 kips (displacement of 1.2 inches). This type of behavior was typical of all specimens. Figure 44 through 47 contain the load versus displacement relationship for the four specimens. Finally Table 21 contains the peak load and displacements for all specimens. It can be seen that the peak displacements are lower than the specimens of Test Series 4 most likely due to the fact that the A to B connection has increased stiffness.



Figure 43: Specimen CV\_AB-1 - spalling of top surface of panel at a load of 8.9 kips

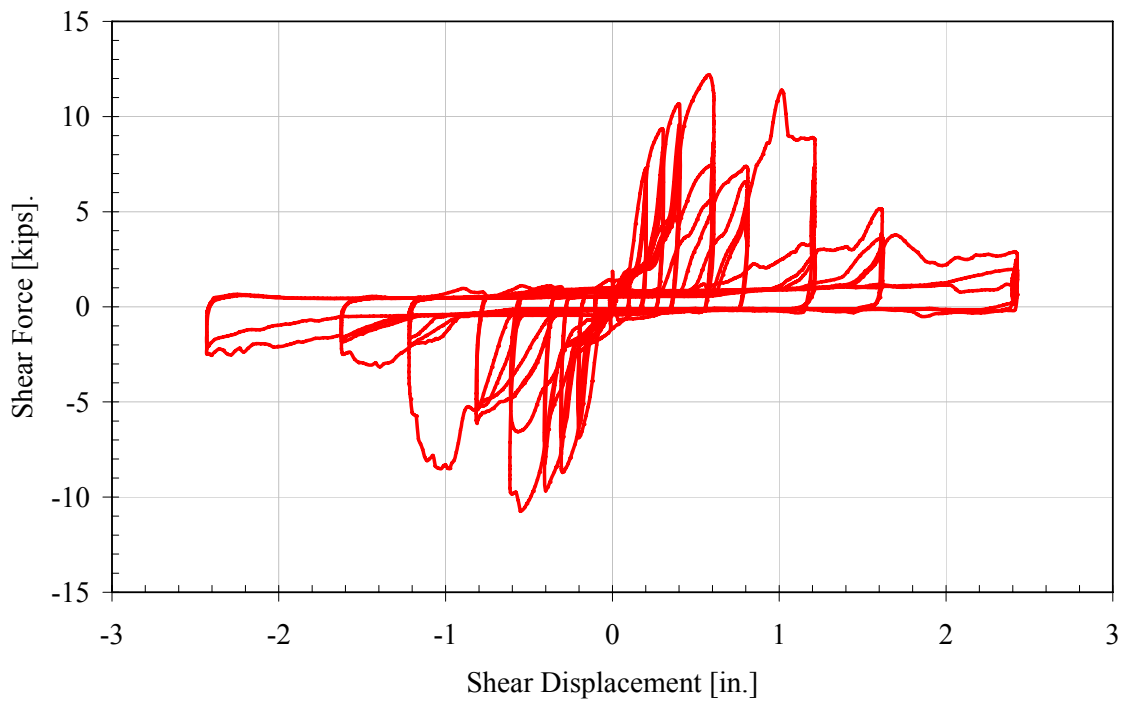


Figure 44: Cyclic shear test CV\_AB-1 - shear load versus shear displacement

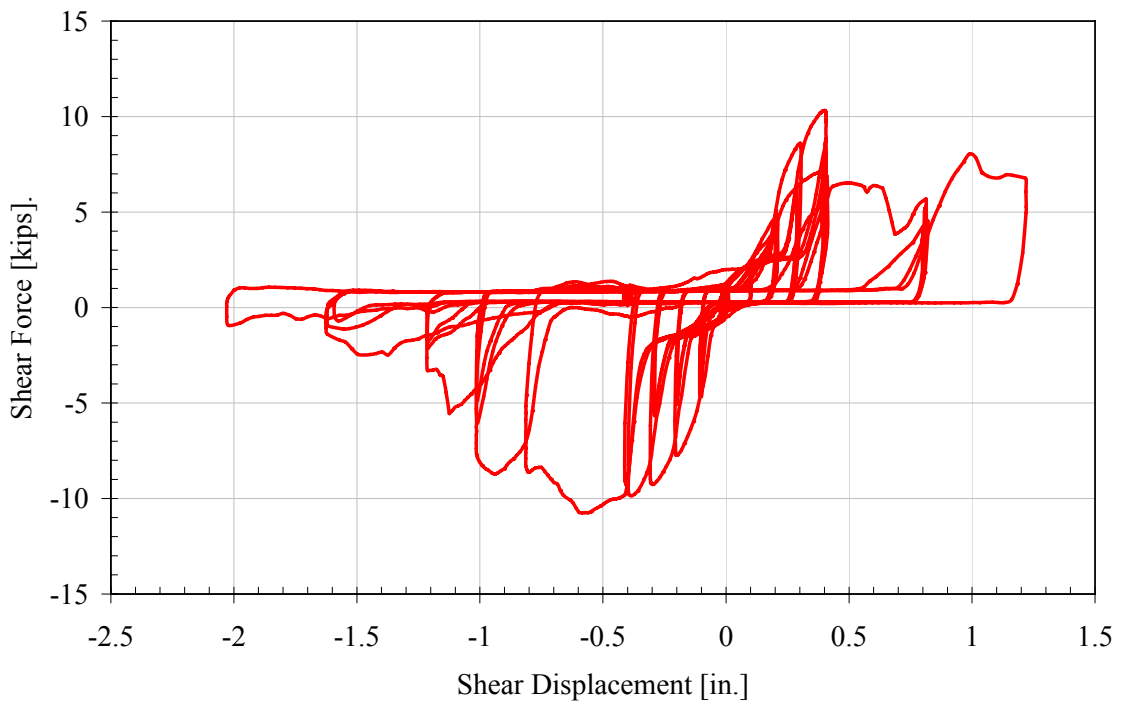


Figure 45: Cyclic shear test CV\_AB-2 - shear load versus shear displacement

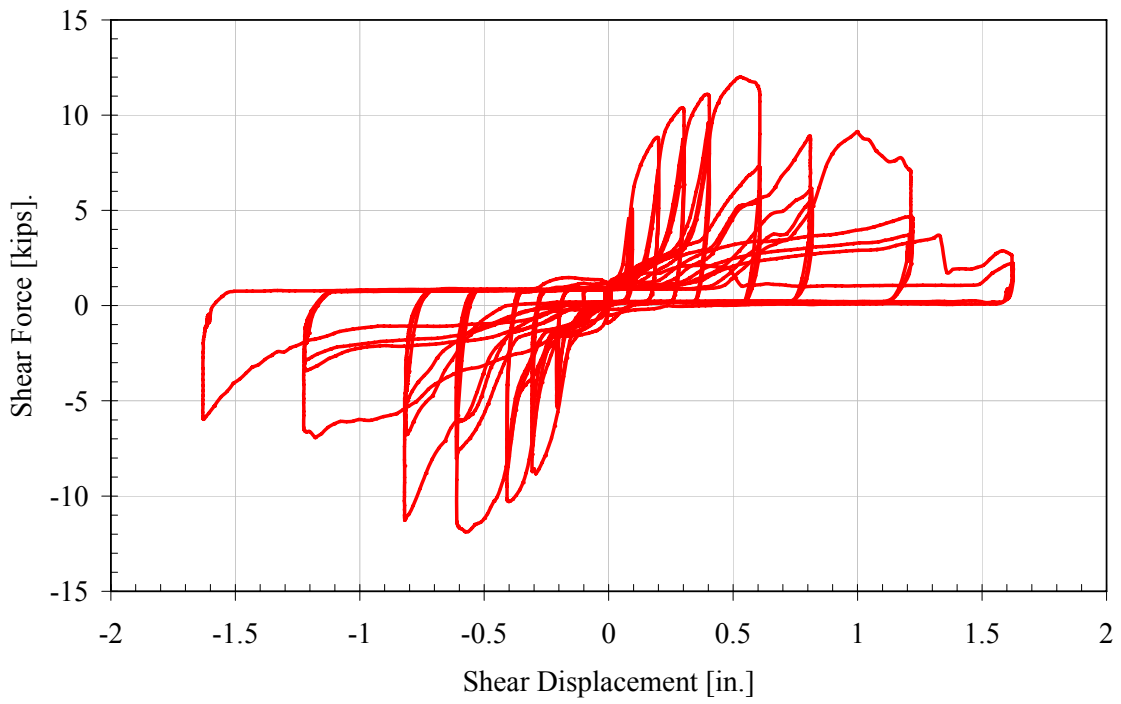


Figure 46: Cyclic shear test CV\_AB-3 - shear load versus shear displacement

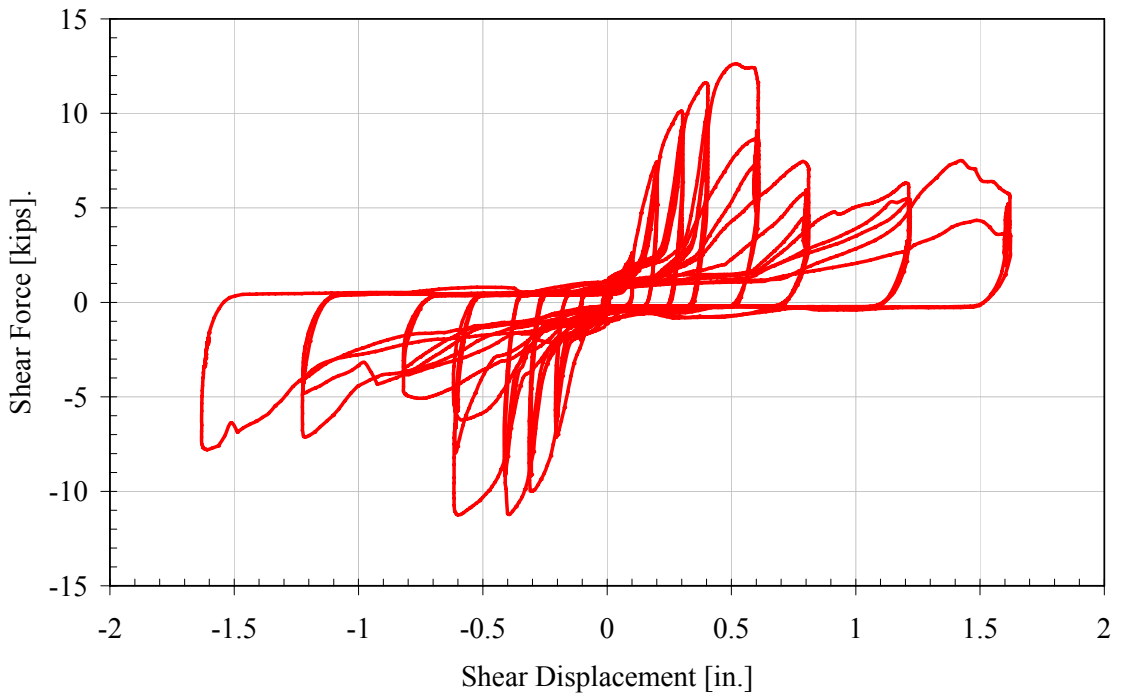


Figure 47: Cyclic shear test CV\_AB-4 - shear load versus shear displacement

Table 21: Test Series 5 Maximum Load and Displacement		
Specimen	Max Load (kips)	$\Delta$ @ Max Load (in)
MV AB-1	13.6	0.62
CV AB-1	12.2	0.58
CV AB-2	10.8	0.58
CV AB-3	12.0	0.53
CV AB-4	12.6	0.52
<i>Average*</i> =	<i>11.9</i>	<i>0.6</i>
<i>Standard. dev*</i> =	<i>0.80</i>	<i>0.03</i>

*\* for cyclic tests only*

## PHASE 2 - TEST SERIES 6

### IN-PLANE SHEAR – STEPPED PANEL – “B” TO “A” CONNECTOR CONFIGURATION

The in-plane shear behavior of the connector was further investigated in Test Series 6. In this test series, five specimens were tested. Each specimen consisted of two stepped panels with an “B-A” connector configuration. The first specimen, MV\_BA-1, was tested under monotonically increasing shear load while tensile deformations were restrained. Figure 48 contains a photograph of the condition of the B-A connector at a shear load of 15.2 kips. The load versus displacement curve is shown in Figure 49. It can be seen that the connector in the “B-A” configuration has a higher shear capacity than the “A-A” or “A-B” configurations.



Figure 48: Specimen MV\_BA-1 - condition of A-B connector at a shear load of 15.2 kips showing spalling of concrete

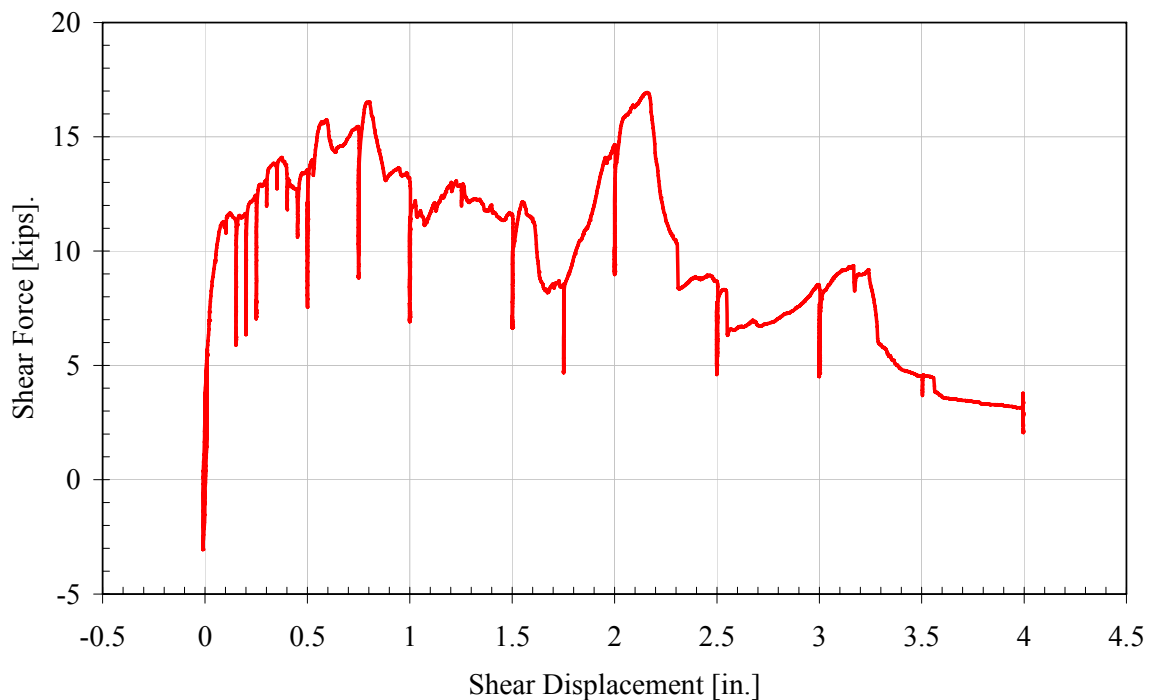


Figure 49: Monotonic shear test MV\_BA-1 - shear load versus shear displacement

Four cyclic shear tests were performed (tests CV\_BA-1 through CV\_BA-4). The behavior of the four specimens was generally similar. Figure 50 shows the onset of spalling in specimen CV\_BA-1 at a load of 2.2 kips (displacement of 0.225 inches). This type of behavior was typical of all specimens. Figure 51 through 54 contain the load versus displacement relationship for the four specimens. Note that the integrity of the data collected during test CV\_BA-1 (see Figure 42) was compromised and is therefore incomplete as shown. Finally Table 22 contains the peak load and displacements for all specimens. It can be seen that the peak displacements are lower than the specimens of Test Series 4 most likely due to the fact that the A to B connection has increased stiffness.



Figure 50: Specimen CV\_BA-4 - spalling of top surface of panel at a load of 2.2 kips (displacement of 0.225 inches)

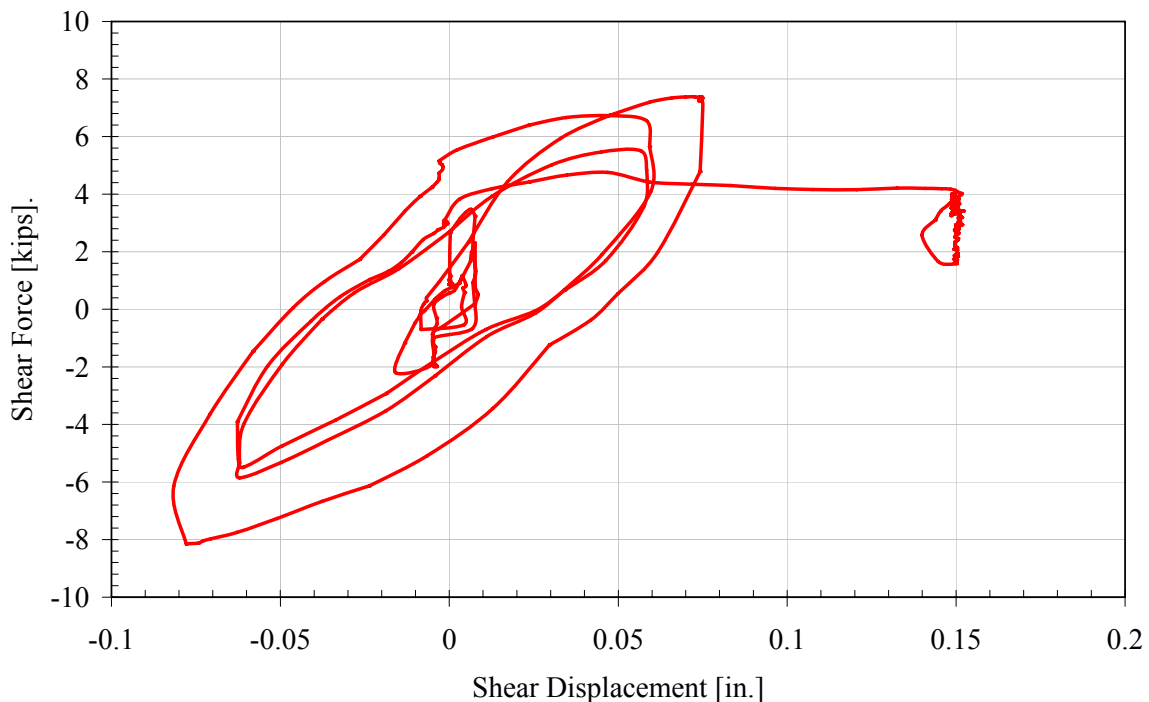


Figure 51: Cyclic shear test CV\_BA-1 - shear load versus shear displacement

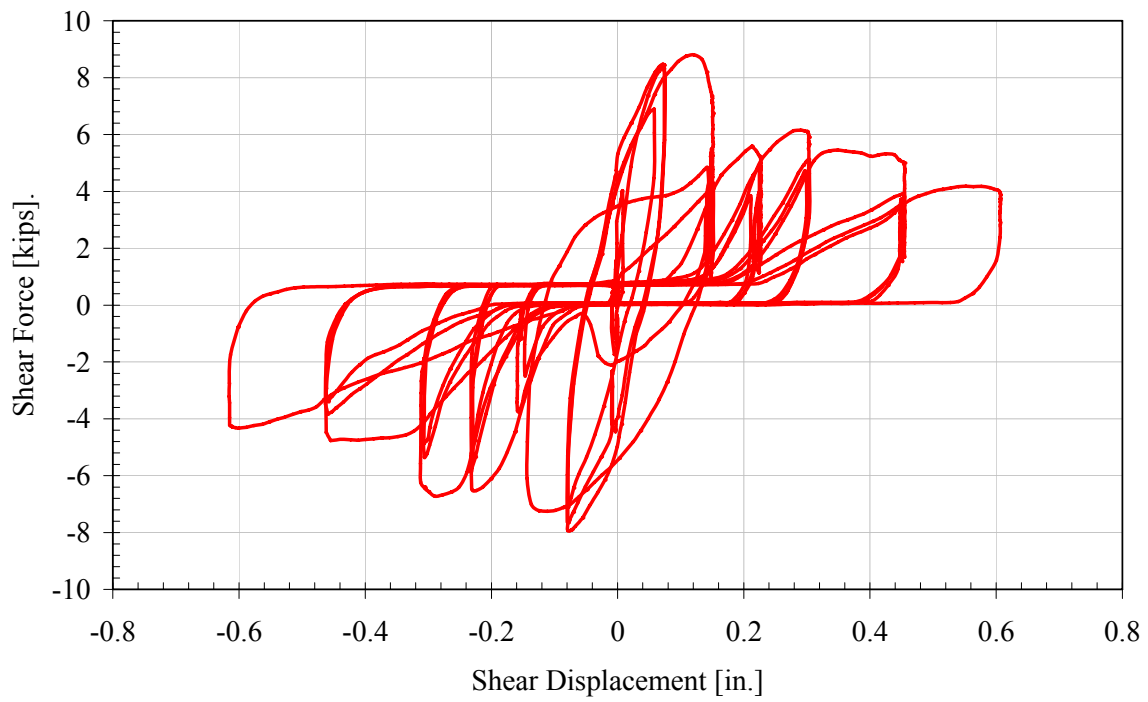


Figure 52: Cyclic shear test CV\_BA-2 - shear load versus shear displacement

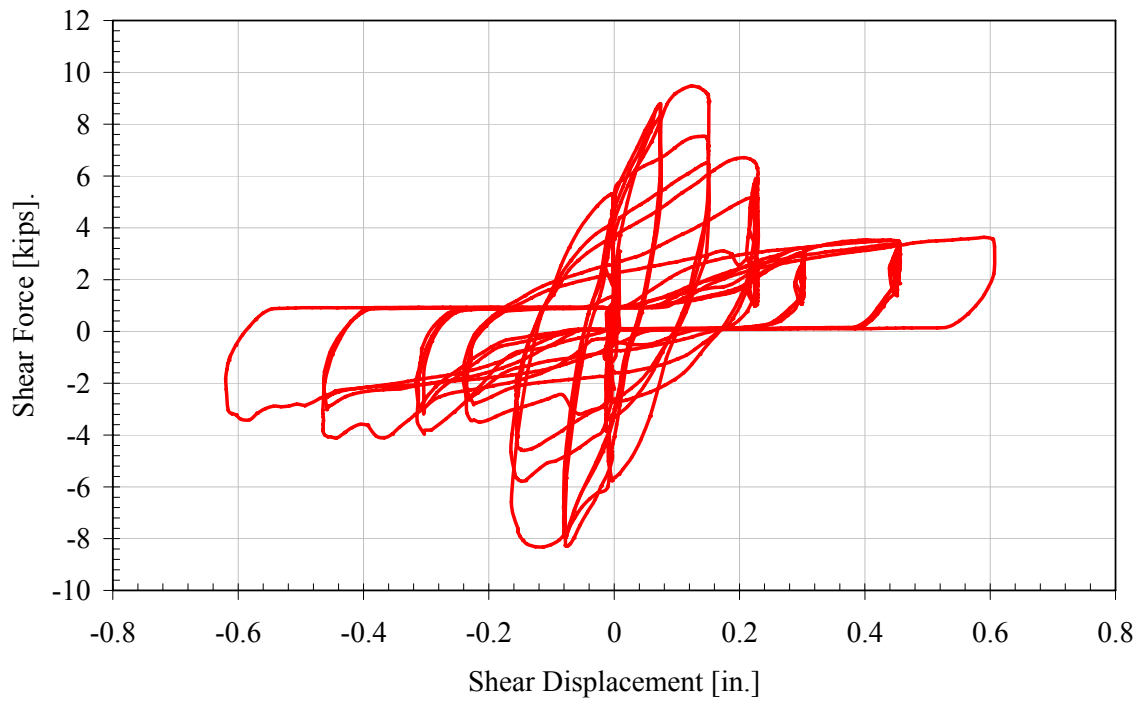


Figure 53: Cyclic shear test CV\_BA-3 - shear load versus shear displacement



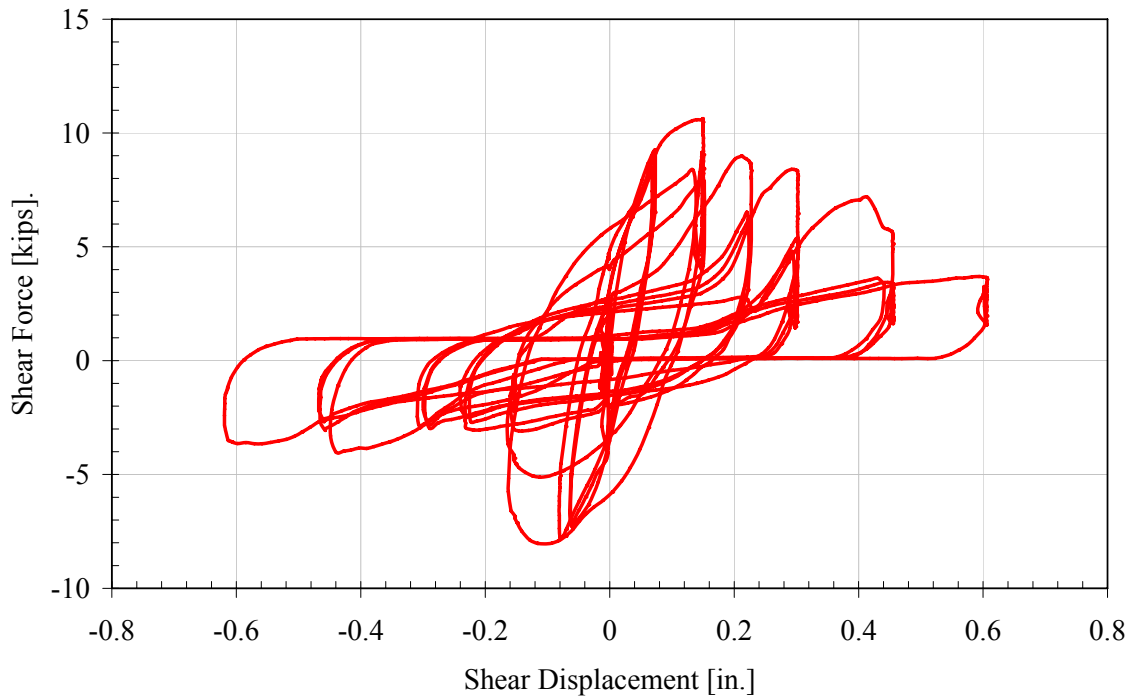


Figure 54: Cyclic shear test CV\_BA-4 - shear load versus shear displacement

Table 22: Test Series 6 Maximum Load and Displacement		
Specimen	Max Load (kips)	$\Delta$ @ Max Load (in)
MV BA-1	16.9	2.16
CV BA-1	8.1	0.08
CV BA-2	8.8	0.12
CV BA-3	9.5	0.12
CV BA-4	10.6	0.15
<i>Average** =</i>	<i>9.6</i>	<i>0.1</i>
<i>Standard. dev** =</i>	<i>0.92</i>	<i>0.03</i>

*\*data incomplete*

*\*\*for cyclic tests 2 through 4 only*

## PHASE 2 - TEST SERIES 7

### IN-PLANE TENSION – STEPPED PANEL – “A” TO “A” CONNECTOR CONFIGURATION

The in-plane tensile behavior of the connector was investigated in Test Series 7. In this test series, four specimens were tested. Each specimen consisted of two stepped panels with an “A-A” connector configuration. The first specimen, MT\_AA-1, was tested under monotonically increasing tension load while shear deformations were unrestrained. The load versus displacement curve is shown in Figure 55. It can be seen that during the initial portion of the test, there was increasing displacement without load. This results from the extension of the connector without bearing. Only nominal friction loads are acting. Once the connector begins to bear, the load increases (starting at a displacement of approximately 0.4 inches in the Figure 55).

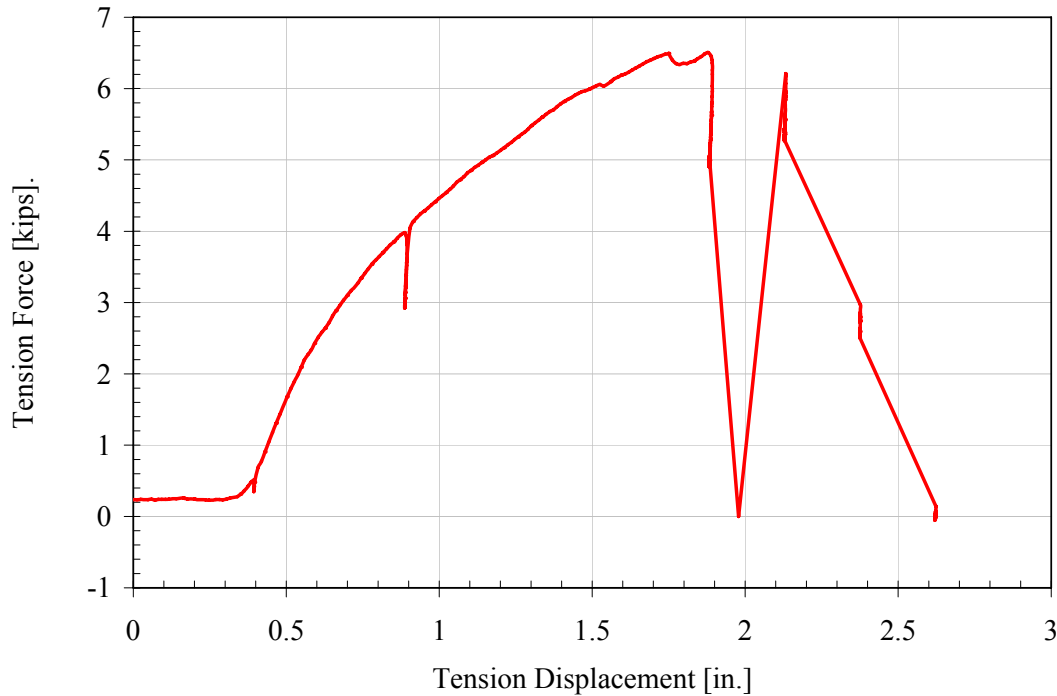


Figure 55: Monotonic tension test MT\_AA-1 - tension load versus tension displacement

Three cyclic tension tests were performed (tests CT\_AA-1 through CT\_AA-3). The behavior of the three specimens was generally similar. Similar to the monotonic test, during the initial small cycles, there is no bearing of the connector and therefore only nominal friction forces resist the imposed deformations. Once bearing occurs (at approximately 0.25, 1.25, and 0.25 inches for tests CT\_AA-1, CT\_AA-2, CT\_AA-3, respectively) the load increases. Figure 56 shows the onset of spalling in specimen CV\_BA-1 at a load of 2.2 kips (displacement of 0.225 inches). This type of behavior was typical of all specimens. Figure 57 through 59 contain the load versus displacement relationship for the three specimens. Finally Table 23 contains the peak load and displacements for all specimens. Peak displacements shown are the difference between the maximum imposed displacement and the displacement at the onset of bearing (i.e., where tension loads increased above the friction threshold).



Figure 56: Specimen CT\_AA-2 – after fracture of connector at a displacement of 3.6 inches

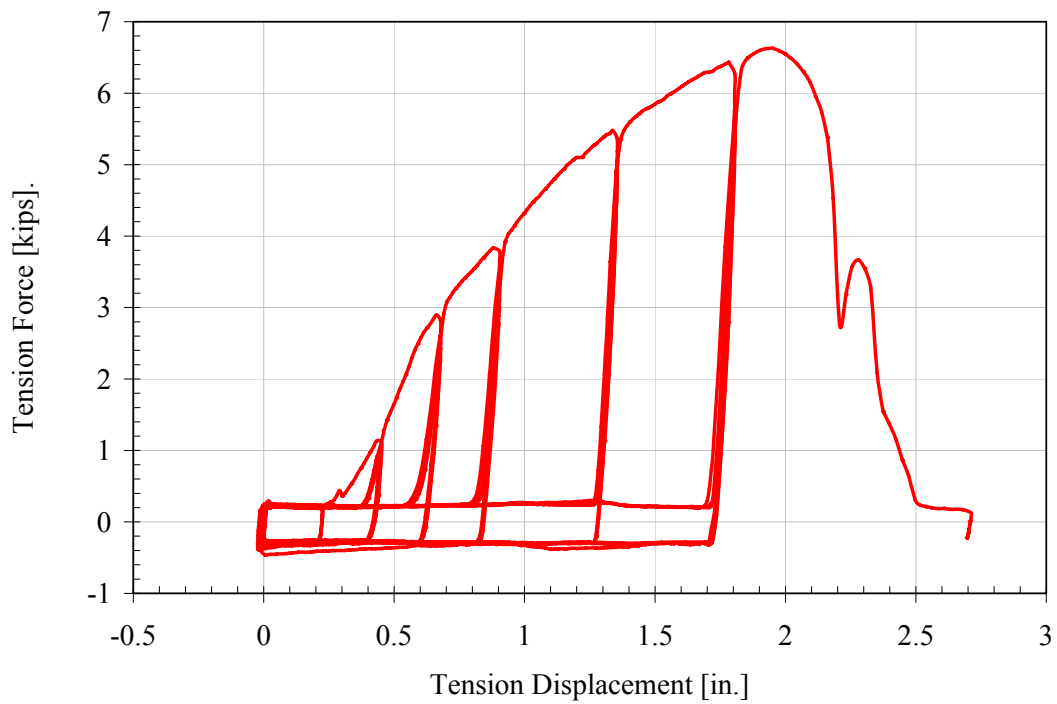


Figure 57: Cyclic shear test CT\_AA-1 - tension load versus tension displacement

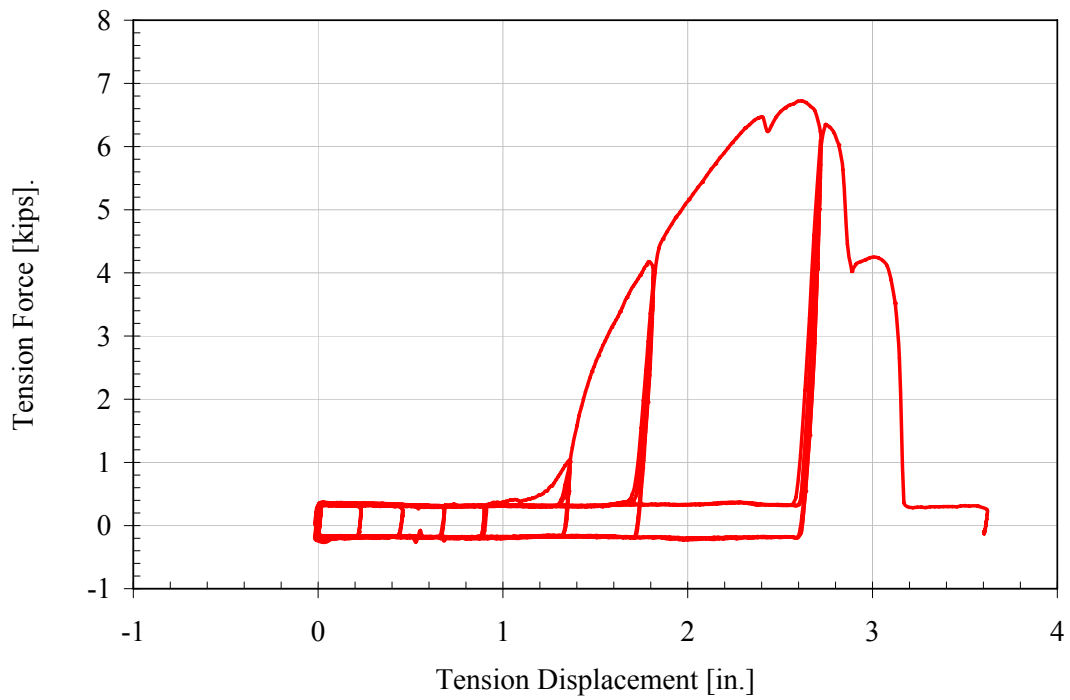


Figure 58: Cyclic shear test CT\_AA-2 - tension load versus tension displacement

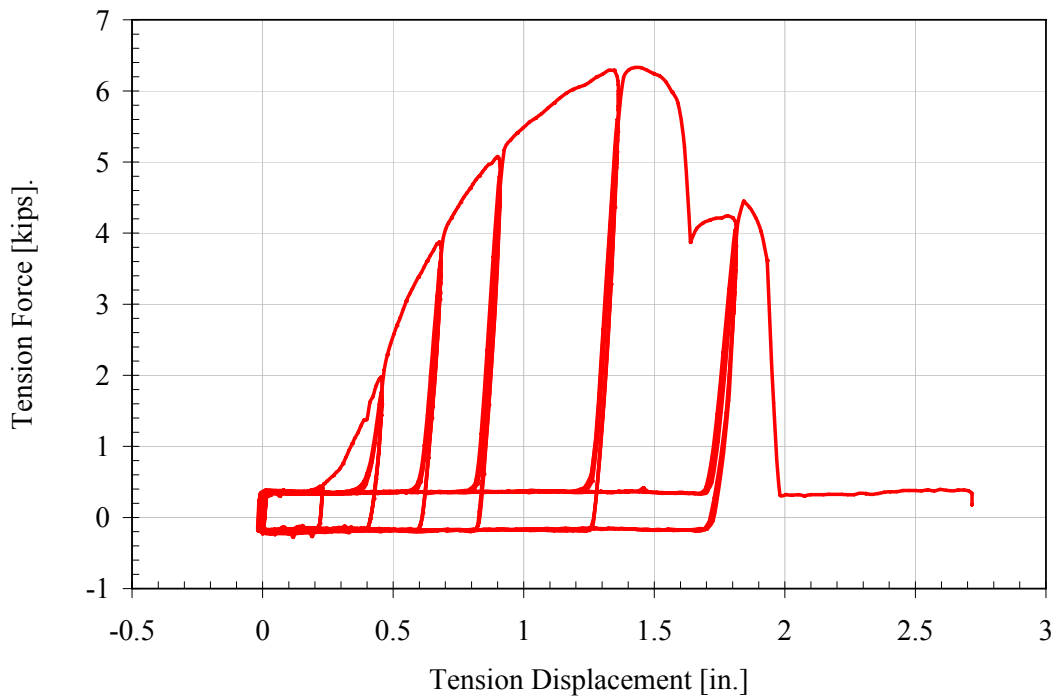


Figure 59: Cyclic shear test CT\_AA-3 - tension load versus tension displacement

Table 23: Test Series 7 Maximum Load and Displacement		
Specimen	Max Load (kips)	$\Delta$ @ Max Load (in)*
MT AA-1	6.5	1.5
CT AA-1	6.6	1.7
CT AA-2	6.7	1.7
CT AA-3	6.3	1.2
<i>Average** =</i>	<i>6.6</i>	<i>1.5</i>
<i>Standard. dev** =</i>	<i>0.20</i>	<i>0.30</i>

*\*Max. displacement is displacement from onset of bearing.*

*\*\*for cyclic tests only*

*\*Max. displacement is displacement from onset of bearing.*

## PHASE 2 - TEST SERIES 8

### IN-PLANE TENSION – STEPPED PANEL – “B” TO “A” CONNECTOR CONFIGURATION

The in-plane tensile behavior of the connector was further investigated in Test Series 8. In this test series, five specimens were tested. Each specimen consisted of two stepped panels with an “B-A” connector configuration. The first specimen, MT\_BA-1, was tested under monotonically increasing tension load while shear deformations were unrestrained. The load versus displacement curve is shown in Figure 60. The results from the extension of the connector without bearing. Only nominal friction loads are acting.

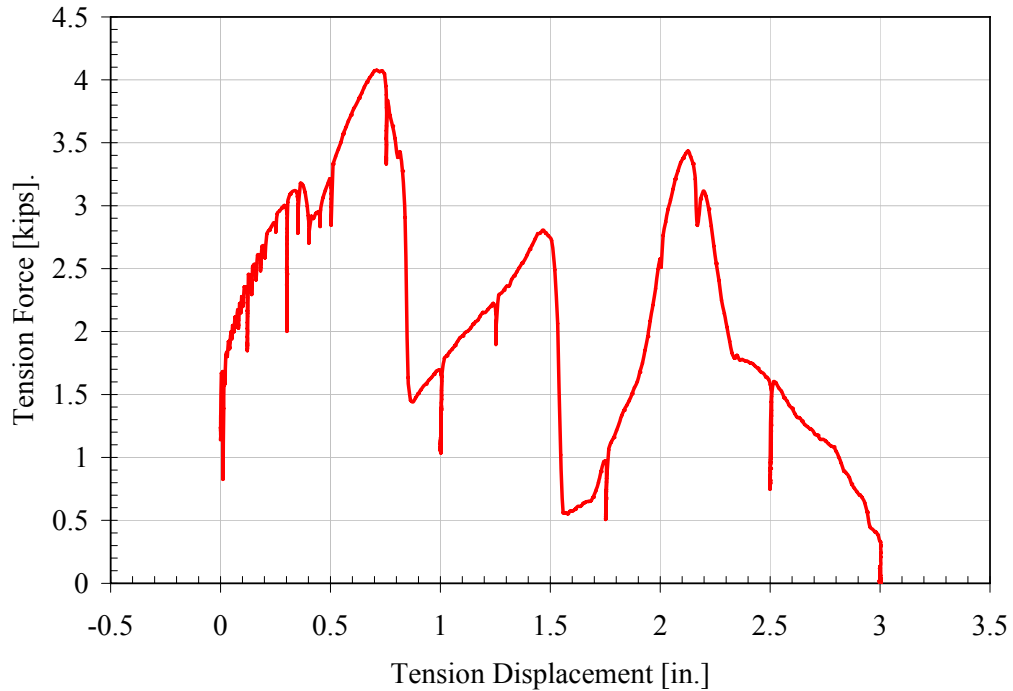


Figure 60: Monotonic tension test MT\_BA-1 - tension load versus tension displacement

Four cyclic tension tests were performed (tests CT\_BA-1 through CT\_BA-4). The behavior of the four specimens was generally similar. Figure 61 shows the connection after a complete fracture of the “A” connector. This type of behavior was typical of all specimens. Figure 62 through 65 contain the load versus displacement relationship for the four specimens. Finally Table 24 contains the peak load and displacements for all specimens.

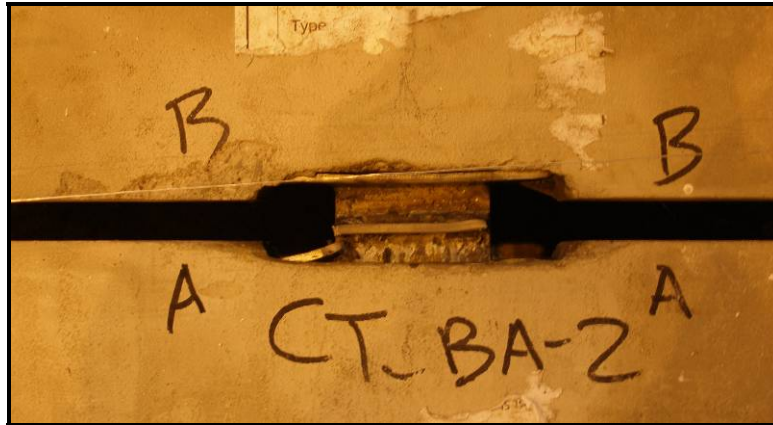


Figure 61: Specimen CT\_AA-2 – after fracture of “A” connector at a displacement of 0.74 inches

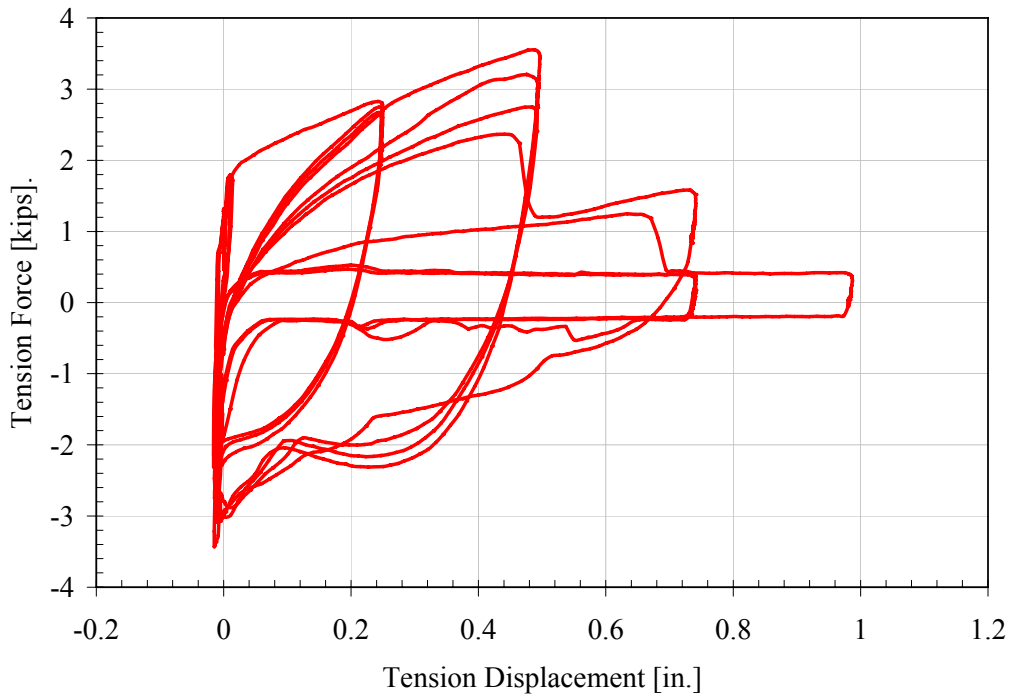


Figure 62: Cyclic shear test CT\_BA-1 - tension load versus tension displacement



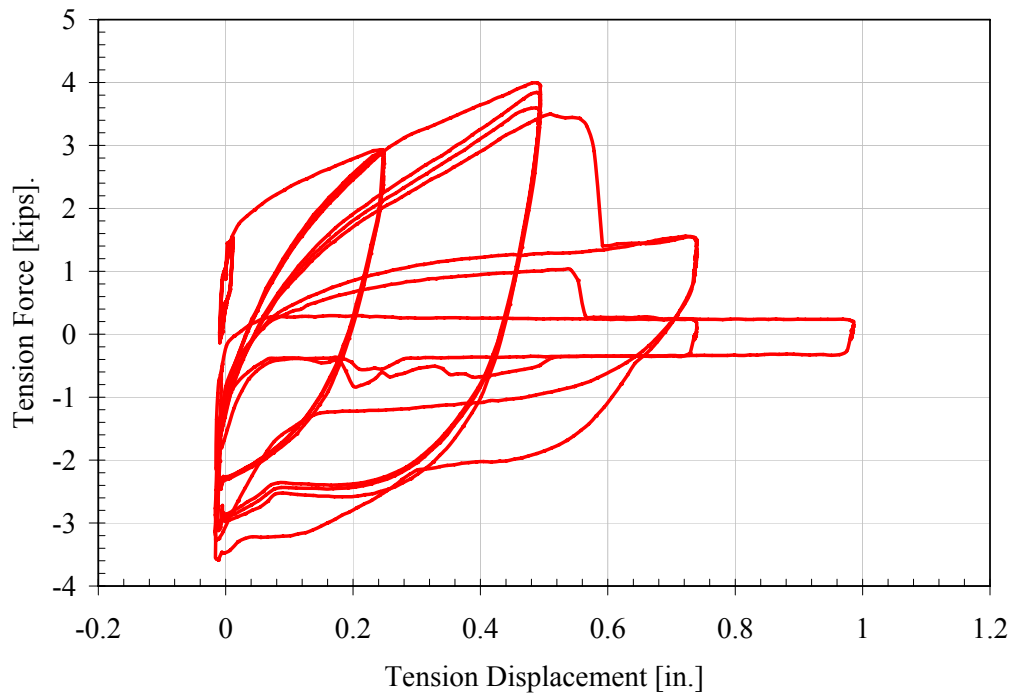


Figure 63: Cyclic shear test CT\_BA-2 - tension load versus tension displacement

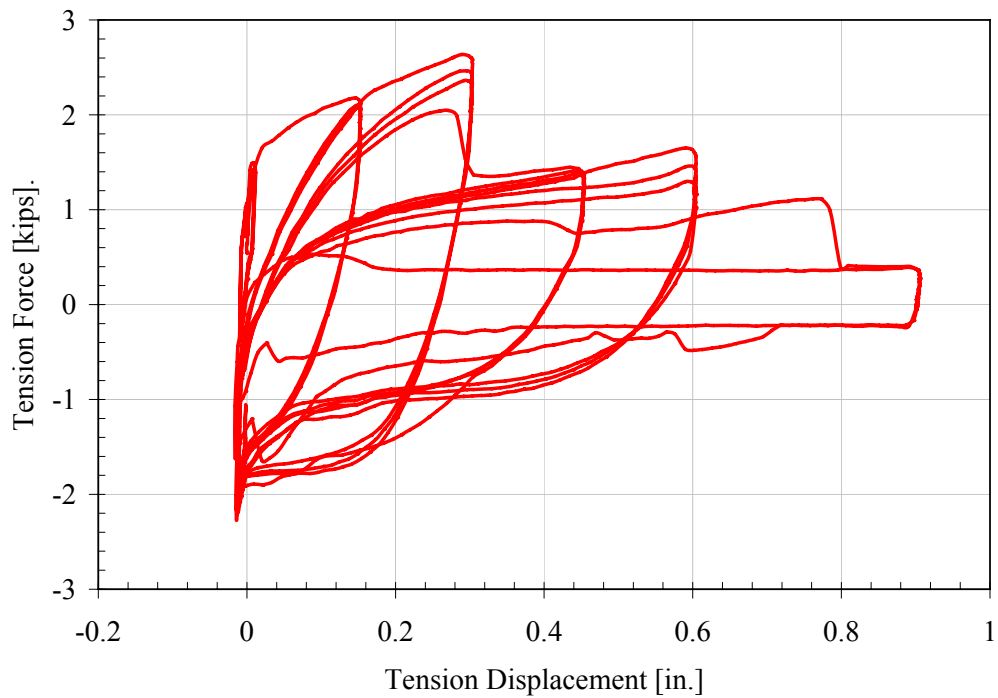


Figure 64: Cyclic shear test CT\_BA-3 - tension load versus tension displacement

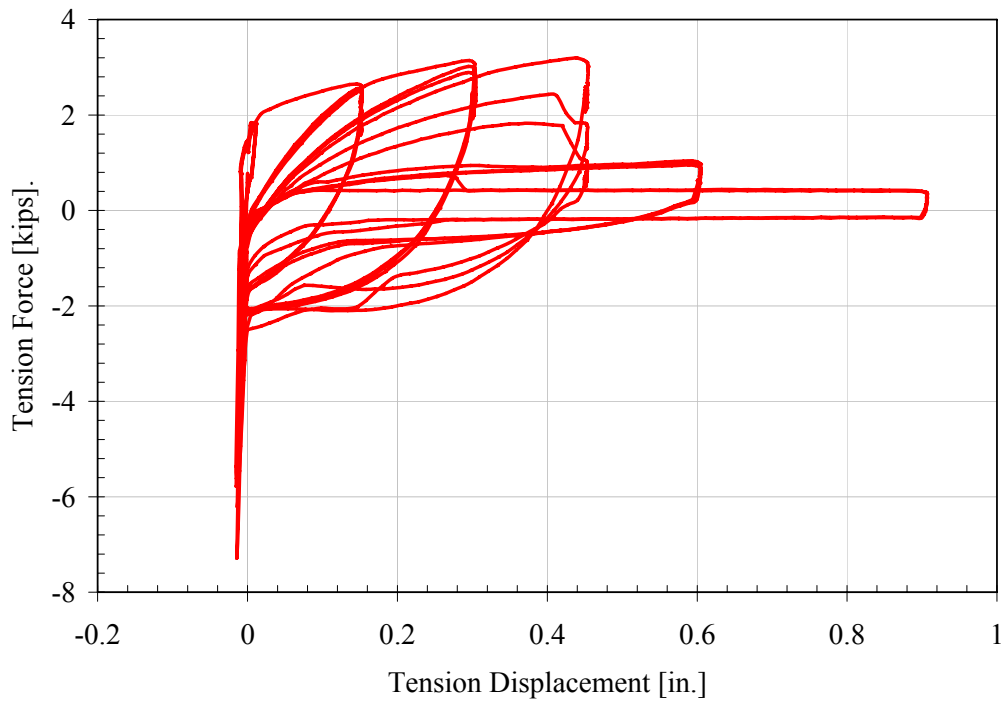


Figure 65: Cyclic shear test CT\_BA-4 - tension load versus tension displacement

Table 24: Test Series 8 Maximum Load and Displacement		
Specimen	Max Load (kips)	$\Delta$ @ Max Load (in)
MT BA-1	4.1	0.71
CT BA-1	3.6	0.49
CT BA-2	4.0	0.49
CT BA-3	2.6	0.29
CT BA-4	3.2	0.44
<i>Average*</i> =	3.3	0.4
<i>Standard. dev*</i> =	0.57	0.09

*\*for cyclic tests only*

## PHASE 2 - TEST SERIES 9

### IN-PLANE SHEAR/TENSION – STEPPED PANEL – “B” TO “A” CONNECTOR CONFIGURATION

The in-plane behavior under combined shear and tension of the connector was investigated in Test Series 9. In this test series, three specimens were tested. Each specimen consisted of two stepped panels with an “B-A” connector configuration. Each specimen (CVT\_BA-1 through CVT\_BA-3) was tested under cyclic shear with proportional tension. The shear deformation commands were twice the tension deformation commands. The behavior of the three specimens was generally similar, however specimen CVT\_BA-2 had increased load-carrying capacity. Figure 66 shows the specimen CVT\_BA-2 under a shear load of 4.1 kips and tension load of -1.0 kips. Spalling and cracking of the top panel surface is evident in the photograph. This type of behavior was typical of all specimens. Figure 67 through 69 contain the load versus displacement relationship for the four specimens. Note that the shear and tension loads are plotted separately versus the shear displacement. Finally Table 25 contains the peak load (tension and shear) and displacements for all specimens.



Figure 66: Specimen CVT\_BA-2 – cracking and spalling of top surface at a shear load of 4.1 kips and a tension load of -1.0 kips (shear displacement of 0.3 inches)

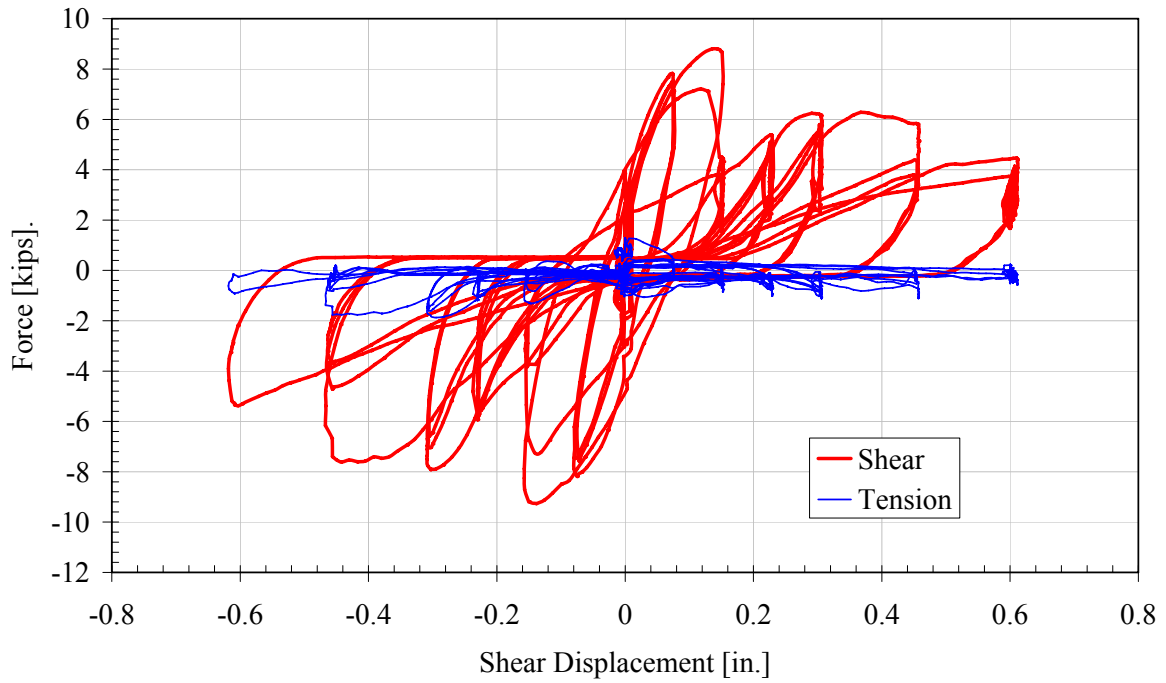


Figure 67: Cyclic combined shear/tension test CVT\_BA-1 – shear and tension load versus shear displacement

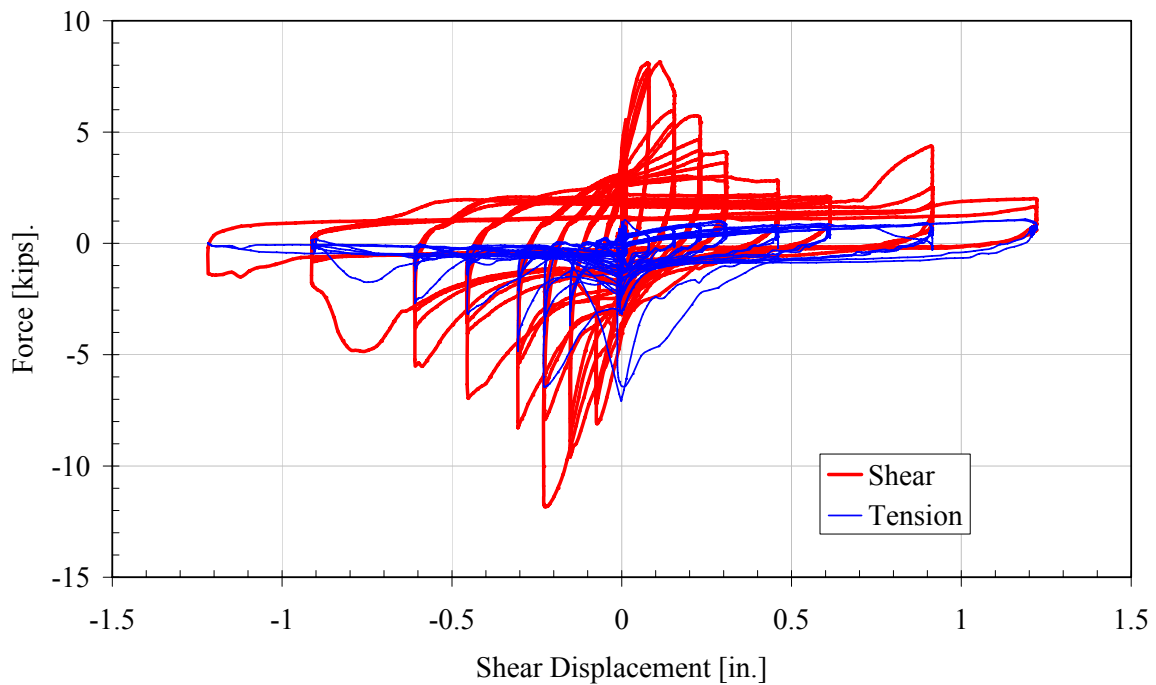


Figure 68: Cyclic combined shear/tension test CVT\_BA-2 – shear and tension load versus shear displacement

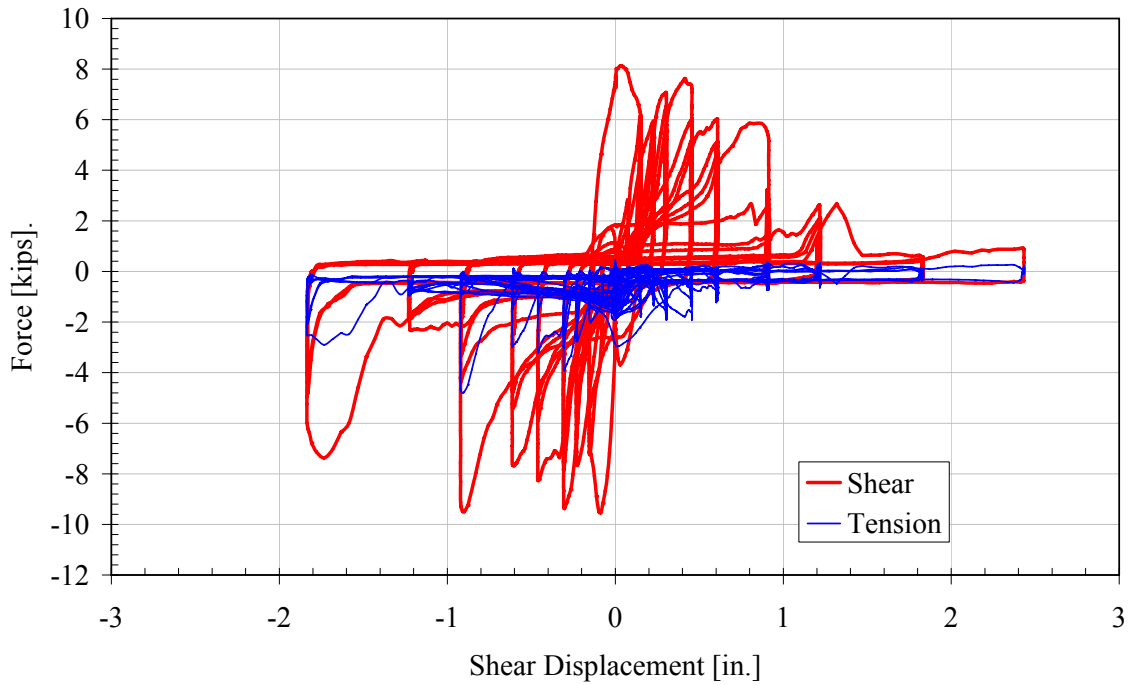


Figure 69: Cyclic combined shear/tension test CVT\_BA-3 – shear and tension load versus shear displacement

Table 25: Test Series 9 Maximum Load and Displacement			
Specimen	Max Shear (kips)	$\Delta$ @ Max Shear (in)	Max Tension (kips)
CVT BA-1	9.3	0.14	1.9
CVT BA-2	11.9	0.22	7.1
CVT BA-3	9.5	0.09	4.8
<i>Average =</i>	<i>10.2</i>	<i>0.1</i>	<i>4.6</i>
<i>Standard. dev. =</i>	<i>1.42</i>	<i>0.07</i>	<i>2.61</i>

## PHASE 2 - TEST SERIES 10

### IN-PLANE SHEAR/TENSION – STEPPED PANEL – “A” TO “B” CONNECTOR CONFIGURATION

---

The in-plane behavior under combined shear and tension of the connector was further investigated in Test Series 10. In this test series, four specimens were tested. Each specimen consisted of two stepped panels with an “A-B” connector configuration. Each specimen (CVT\_AB-1 through CVT\_AB-4) was tested under cyclic shear with proportional tension. The shear deformation commands were twice the tension deformation commands. The behavior of the four specimens was generally similar, however, the post-yield behavior was slightly different. Figure 70 shows the specimen CVT\_AB-3 under a shear load of 8.6 kips and tension load of 1.0 kips. The face plate is severely deformed. This type of behavior was typical of all specimens. Figure 71 through 74 contain the load versus displacement relationship for the four specimens. Note that the shear and tension loads are plotted separately versus the shear displacement. Finally Table 25 contains the peak load (tension and shear) and displacements for all specimens.



Figure 70: Specimen CVT\_AB-3 – deformation of the “B” connector face plate at a shear load of 4.1 kips and a tension load of 1.1 kips (shear displacement of 0.3 inches)

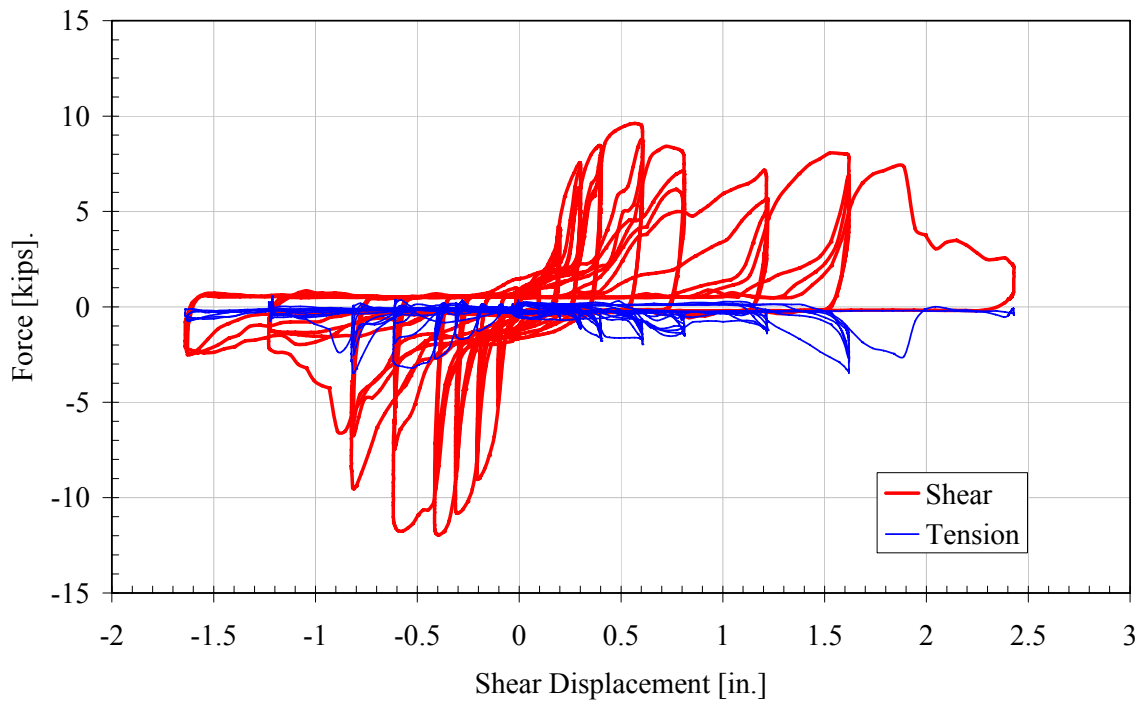


Figure 71: Cyclic combined shear/tension test CVT\_AB-1 – shear and tension load versus shear displacement

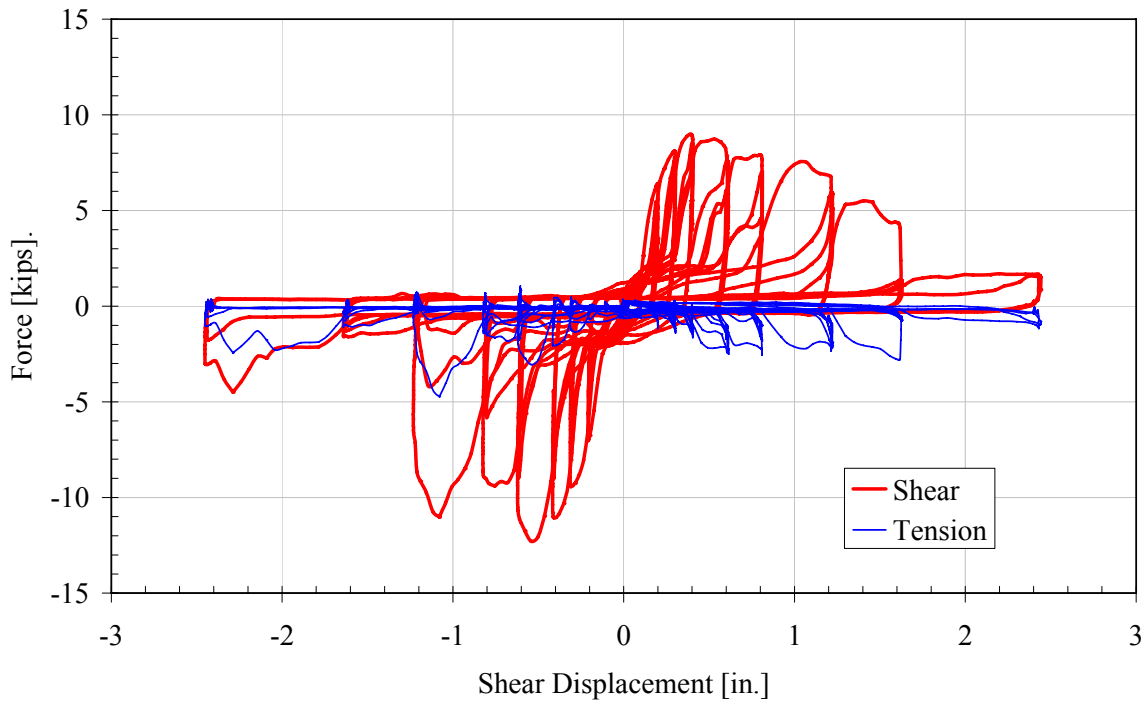


Figure 72: Cyclic combined shear/tension test CVT\_AB-2 – shear and tension load versus shear displacement



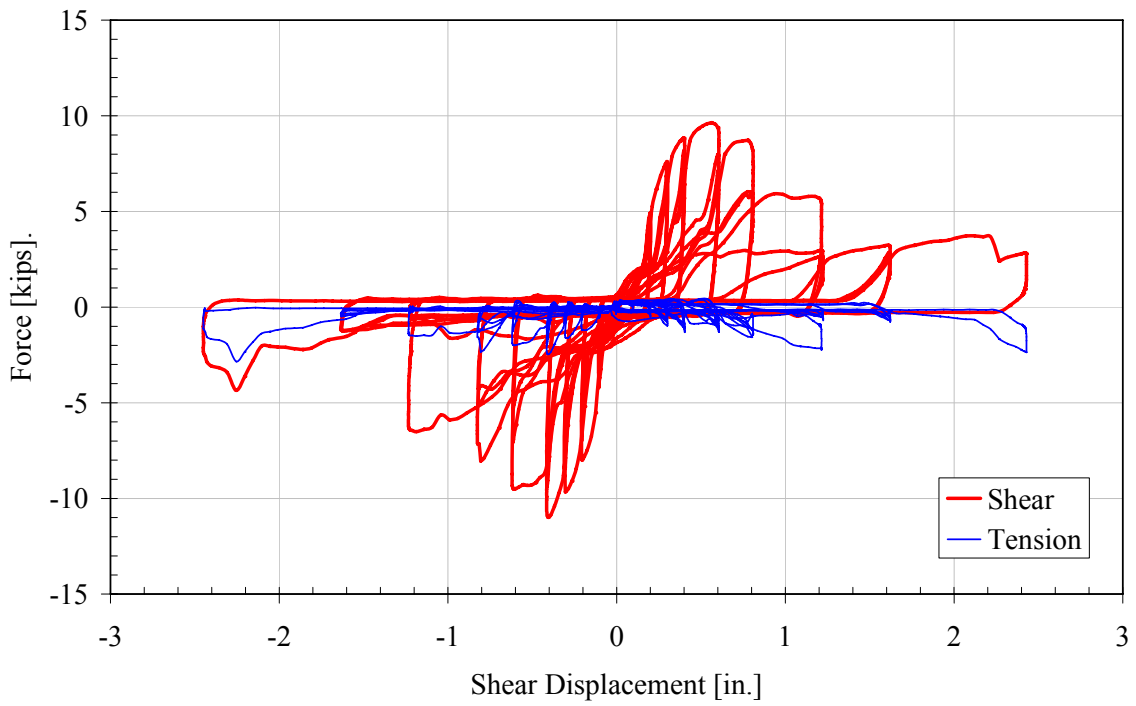


Figure 73: Cyclic combined shear/tension test CVT\_AB-3 – shear and tension load versus shear displacement

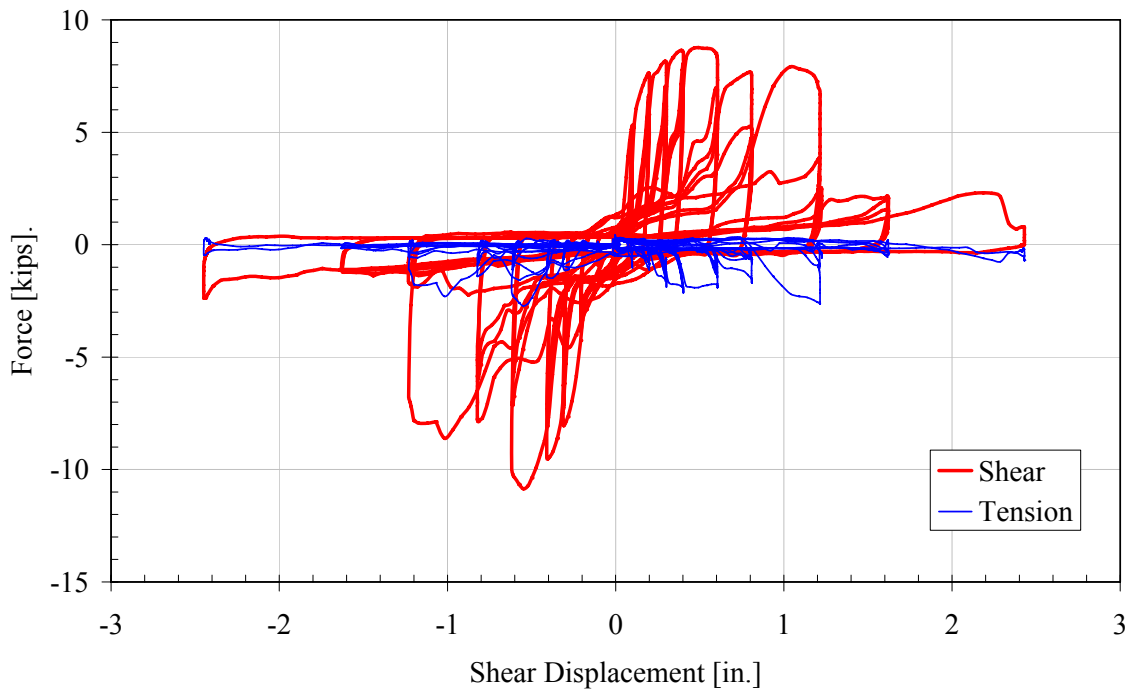


Figure 74: Cyclic combined shear/tension test CVT\_AB-4 – shear and tension load versus shear displacement

Table 26: Test Series 10 Maximum Load and Displacement			
Specimen	Max Shear (kips)	$\Delta$ @ Max Load (in)	Max Tension (kips)
CVT AB-1	11.9	0.39	3.5
CVT AB-2	12.3	0.54	4.7
CVT AB-3	11.0	0.40	2.8
CVT AB-4	10.9	0.55	2.7
<i>Average =</i>	<i>11.5</i>	<i>0.5</i>	<i>3.4</i>
<i>Standard. dev. =</i>	<i>0.71</i>	<i>0.09</i>	<i>0.92</i>

## PHASE 2 - TEST SERIES 1-A

### IN-PLANE SHEAR – ALTUS PANEL – “A” TO “B” CONNECTOR CONFIGURATION

---

The in-plane shear behavior of the connector was investigated in Test Series 1-A. In this test series, five specimens were tested. Each specimen consisted of two Altus panels 3.25 inches thick with an “A-B” connector configuration. The first specimen, MV\_AB-ALTUS-1, was tested under monotonically increasing shear load while tensile deformations were restrained. Figure 75 contains a photograph of the cracking and spalling in the top surface of the test panel at a shear load of 8.6 kips. It can be seen that there is significant deformation of the “B” connector faceplate. The load versus displacement curve is shown in Figure 76.

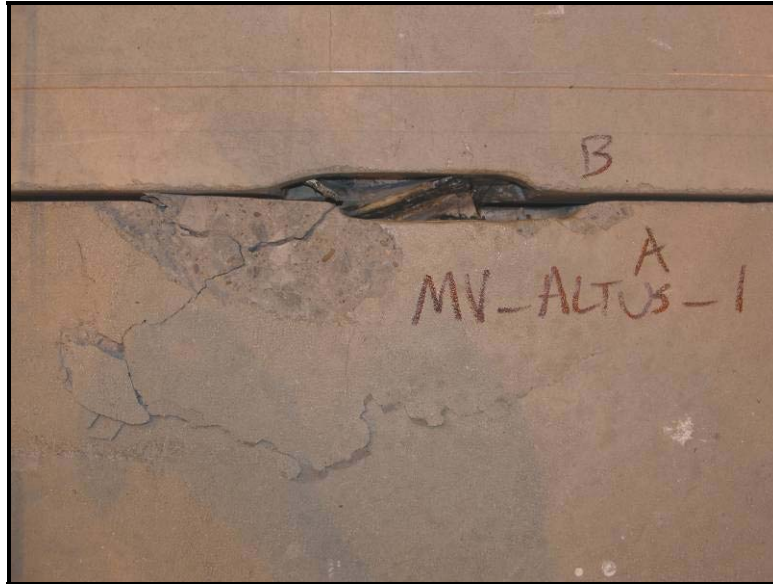


Figure 75: Specimen MV\_AB-ALTUS-1 – spalling of top surface at a shear load of 8.6 kips

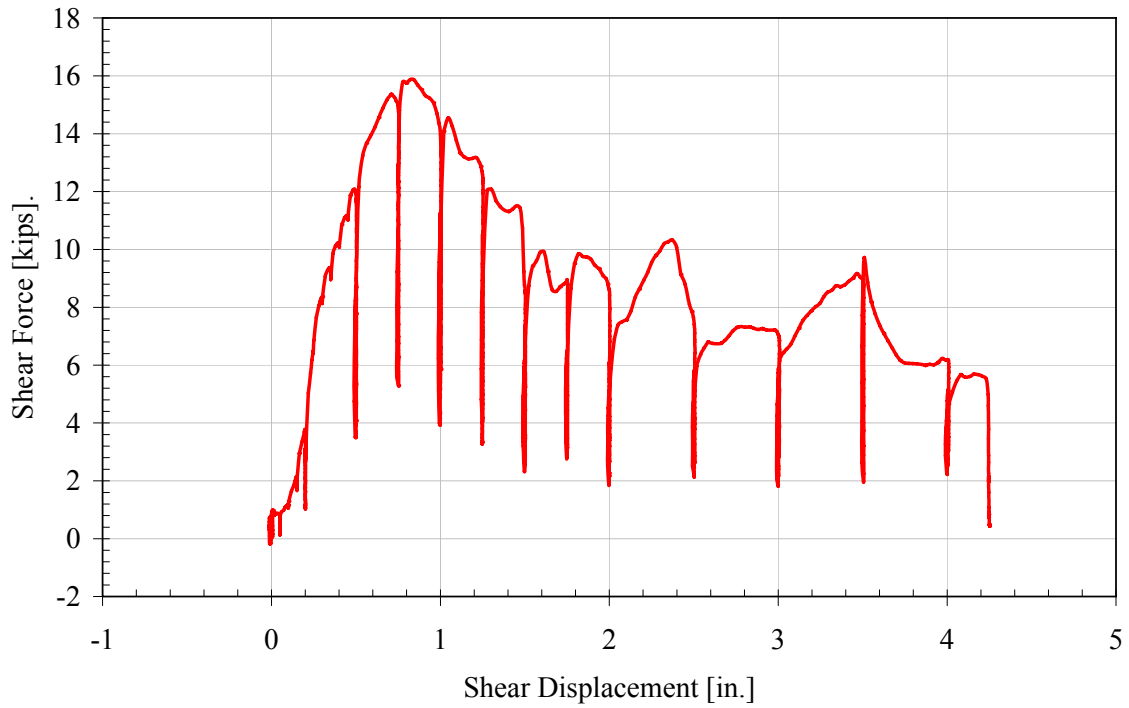


Figure 76: Monotonic shear test MV\_AB\_ALTUS-1 - shear load versus shear displacement

Four cyclic shear tests were performed (tests CV\_AB\_ALTUS-1 through CV\_AB\_ALTUS-4). The behavior of the four specimens was similar, however the post-yield behavior varied. Specimen CV\_AB\_ALTUS-1 had the lowest displacement capacity. Figure 77 shows specimen CV\_AB\_ALTUS-3 at a load of 14.0 kips (displacement of 0.6 inches). Large inelastic deformation of the “B” connector face plate is evident. This type of behavior was typical of all specimens. Figure 78 through 81 contain the load versus displacement relationship for the four specimens. Finally Table 27 contains the peak load and displacements for all specimens.



Figure 77: Specimen CV\_AB\_ATLUS-3 – deformation of “B” connector faceplate at a shear load of 14.0 kips (displacement of 0.6 inches)

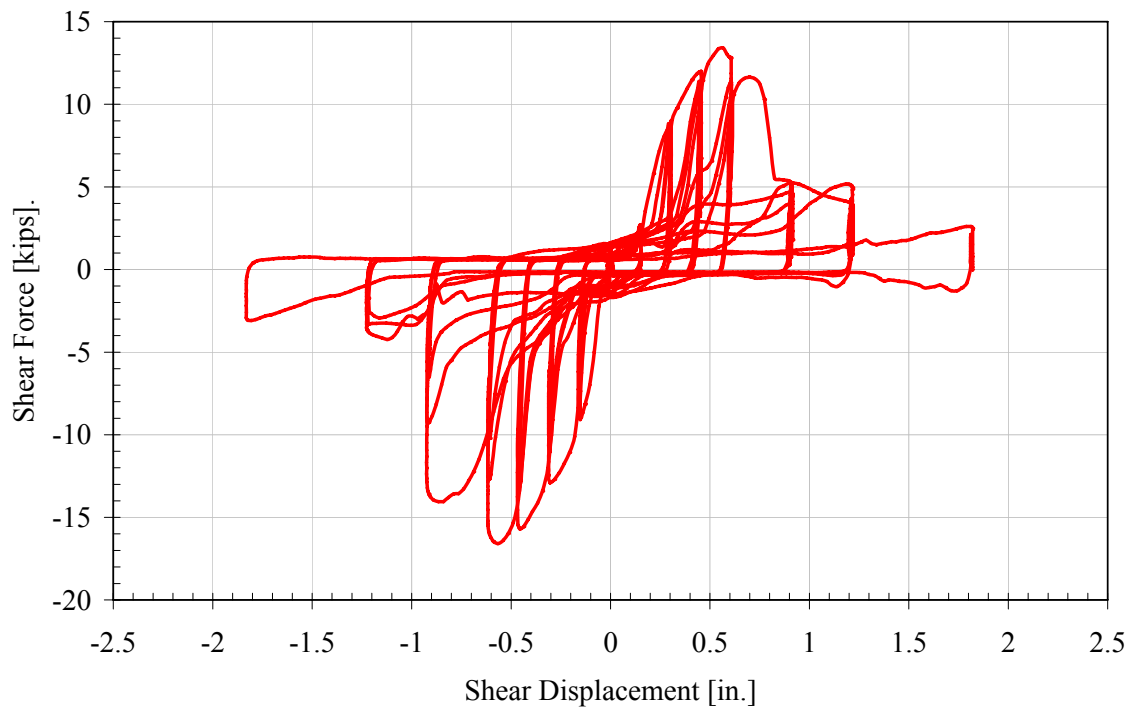


Figure 78: Cyclic shear test CV\_AB\_ALTUS-1 - shear load versus shear displacement

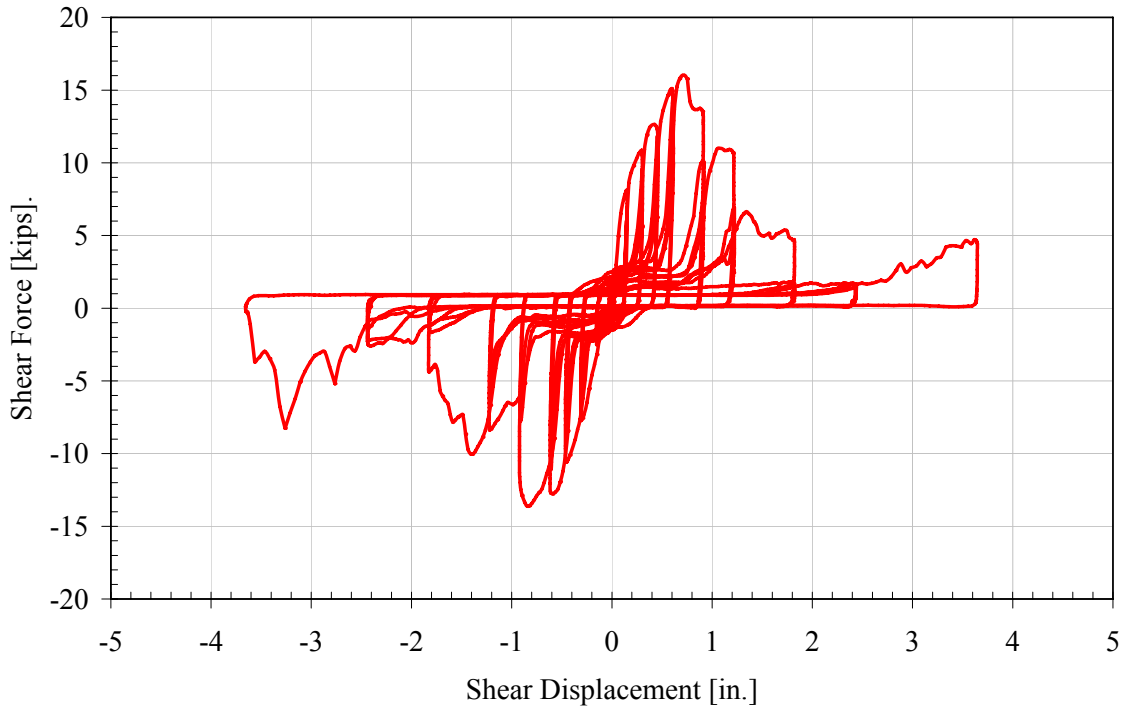


Figure 79: Cyclic shear test CV\_AB\_ALTUS-2 - shear load versus shear displacement

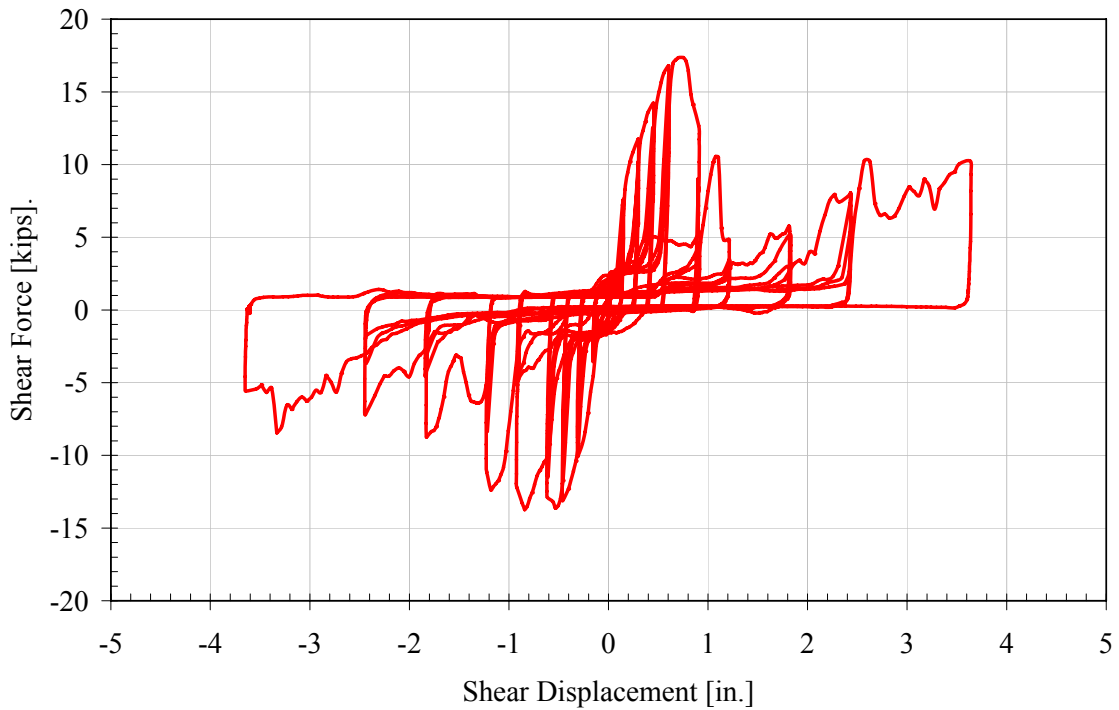


Figure 80: Cyclic shear test CV\_AB\_ALTUS-3 - shear load versus shear displacement

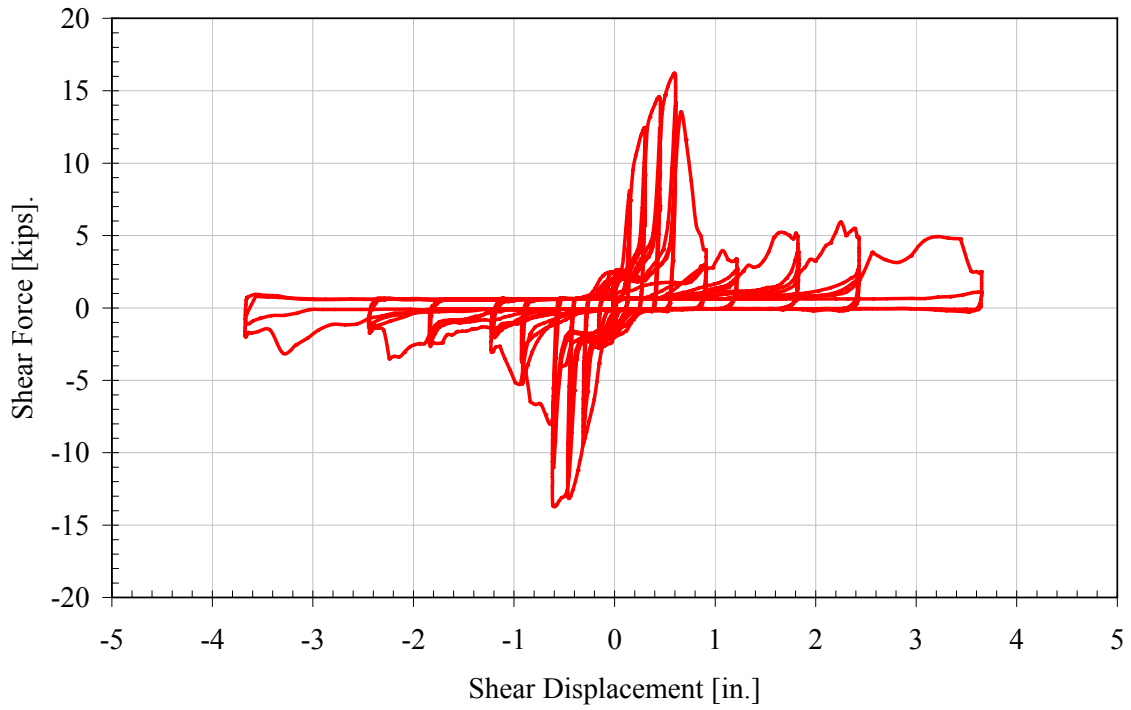


Figure 81: Cyclic shear test CV\_AB\_ALTUS-4 - shear load versus shear displacement

Table 27: Test Series 1-A Maximum Load and Displacement		
Specimen	Max Load (kips)	$\Delta$ @ Max Load (in)
MV AB ALT-1	15.9	0.82
CV AB ALT-1	16.6	0.57
CV AB ALT-2	16.0	0.70
CV AB ALT3	17.4	0.73
CV AB ALT-4	16.2	0.59
<i>Average*</i> =	<i>16.5</i>	<i>0.6</i>
<i>Standard. dev.*</i> =	<i>0.60</i>	<i>0.08</i>

*\*for cyclic tests only*



**PHASE 2 - TEST SERIES 2-A**  
**OUT-OF-PLANE SHEAR – ALTUS PANEL – “A” CONNECTOR**

During Test Series 2-A, 3.25” Altus panels were loaded out of plane, where the panel was connected to the loading fixture via an “A” connector. Five test specimens were tested under monotonically increasing out-of-plane shear. A plot containing the measured out-of-plane shear versus displacement relationship for the five panels is shown in Figure 82. As seen in the plot, the behavior of the panels is similar.

As load was increased, cracks formed on the slab upper surface, as shown in Figure 83. The load at which the first crack appeared was noted (see Table 28). The slab continued to accept increasing loads beyond the initial cracking load. As additional cracks appeared, they were marked and noted. Maximum loads for each specimen are presented in Table 28.

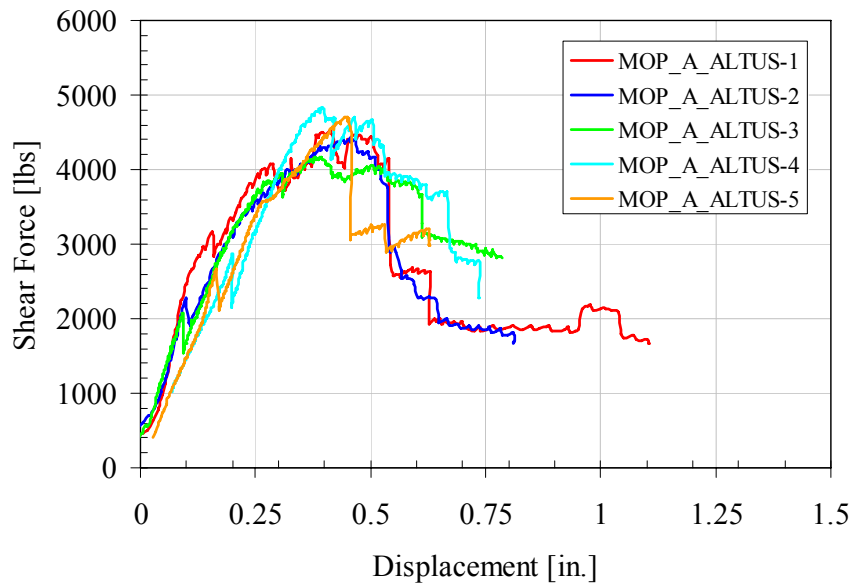


Figure 82: Test Series 2-A – Out-of-plane load versus displacement  
 Altus panel with “A” connector

Table 28: Test Series 2-A: Maximum Load and Load at First Crack			
Specimen	Max Load (lbs)	$\Delta$ @ Max Load (in)	Load at 1st Crack (lbs)
MOP_A_ALTUS-1	4,517	0.41	3,161
MOP_A_ALTUS-2	4,429	0.44	2,277
MOP_A_ALTUS-3	4,170	0.39	2,073
MOP_A_ALTUS-4	4,831	0.40	2,860
MOP_A_ALTUS-5	4,706	0.45	2,674
<i>Average =</i>	<i>4,531</i>	<i>0.42</i>	<i>2,609</i>
<i>Standard. dev. =</i>	<i>255.7</i>	<i>0.03</i>	<i>438.6</i>



Figure 83: Altus slab top surface crack patterns (near end of test)

**PHASE 2 - TEST SERIES 3-A**  
**OUT-OF-PLANE SHEAR – ALTUS PANEL – “B” CONNECTOR**

During Test Series 3-A, 3.25” Altus panels were loaded out of plane, where the panel was connected to the loading fixture via a “B” connector. Five test specimens were tested under monotonically increasing out-of-plane shear. A plot containing the measured out-of-plane shear versus displacement relationship for the five panels is shown in Figure 84. As seen in the plot, the behavior of the panels is similar.

As load was increased, cracks formed on the slab upper surface (see Figure 83). The load at which the first crack appeared was noted (see Table 29). The slab continued to accept increasing loads beyond the initial cracking load. As additional cracks appeared, they were marked and noted. Maximum loads for each specimen are presented in Table 29.

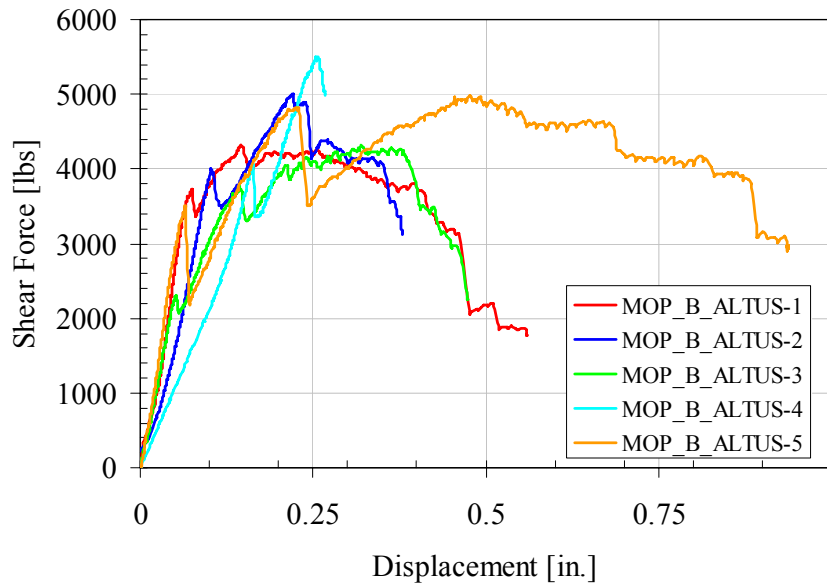


Figure 84: Test Series 3-A – Out-of-plane load versus displacement ALTUS panel with “B” connector

Specimen	Max Load (lbs)	$\Delta$ @ Max Load (in)	Load at 1st Crack (lbs)
MOP_B_ALTUS-1	4,317	0.145	3,722
MOP_B_ALTUS-2	4,999	0.220	3,999
MOP_B_ALTUS-3	4,316	0.320	2,315
MOP_B_ALTUS-4	5,506	0.257	4,057
MOP_B_ALTUS-5	4,982	0.476	3,501
<i>Average =</i>	4,824	0.28	3,519
<i>Standard. dev. =</i>	508.8	0.13	709.0

**PHASE 2 - TEST SERIES 4-A**  
**IN-PLANE TENSION – ALTUS PANEL – “B” CONNECTOR**

During Test Series 4-A, 3.25” Altus panels were loaded with in-plane tension, where the panel was connected to the loading fixture via a “B” connector. Four test specimens were tested under monotonically increasing in-plane tension. A plot containing the measured in-plane tension versus time (displacements were not measured) for the four panels is shown in Figure 85.

All specimens exhibited similar behavior. As the load increased, the B connector began to bow outwards. The bow continued until the connector plate fractured at the edge of the attachment plate weld. Figures 86 and 87 show the progression during one of the tests. Maximum loads for each specimen are presented in Table 30.

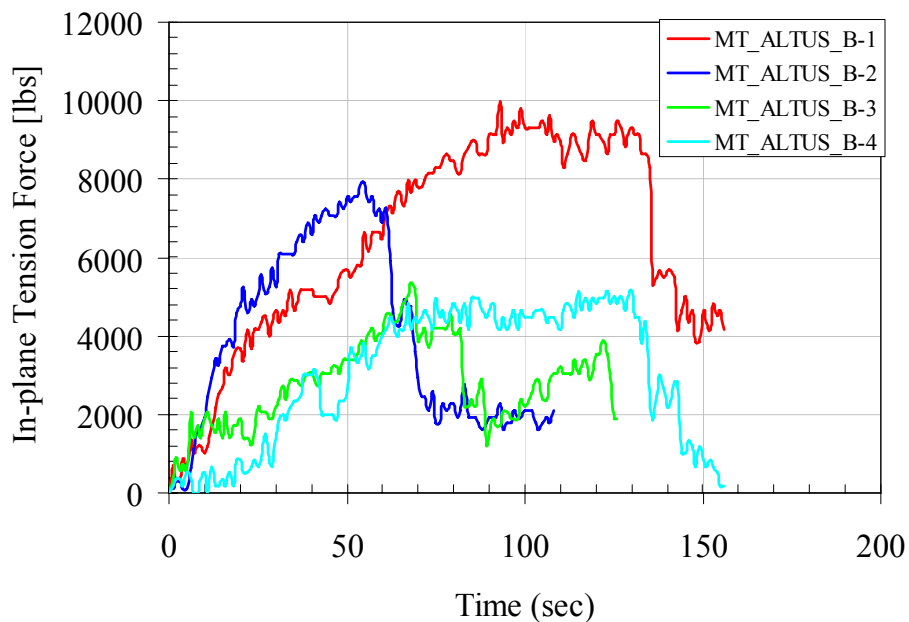


Figure 85: Test Series 4-A – In-plane tension load versus time  
 ALTUS panel with “B” connector

Table 30: Test Series 4-A: Maximum Load	
Specimen	Max Load (lbs)
MT_B_ALTUS-1	9,970
MT_B_ALTUS-2	7,900
MT_B_ALTUS-3	5,370
MT_B_ALTUS-4	5,150
<i>Average =</i>	7,090
<i>Standard. dev. =</i>	2,280



Figure 86: Bowing of connector plate



Figure 87: Connector plate fracture